Formulation and Characterization of Dispersions Loaded with Short-chain Fatty Acid

January 2017

Yohei YAMANAKA

Formulation and Characterization of Dispersions Loaded with Short-chain Fatty Acid

A Dissertation Submitted to
The Graduate School of Life and Environment Science,
the University of Tsukuba
in Partial Fulfillment of the Requirements
for the Degree of Doctor of Philosophy in Agricultural Science
(Doctoral Program in Appropriate Technology
and Sciences for Sustainable Development)

Yohei YAMANAKA

Contents

Chapter 1. Introduction……..1

1.1. Background……..2

1.1.1. Human Digestive System and Function of the Large Intestine……2

1.1.2. Short-chain Fatty Acids Utilized in the Large Intestine……..3

1.1.3. Shortage of Short-chain Fatty Acids in the Large Intestine…….3

1.2. Emulsion and Emulsification Techniques……5

1.2.1. Definition of Emulsion……5

1.2.2. Applications of Emulsions in the Food Industries……...5

1.2.3. Characterization and Stability Evaluation of Emulsions…….6

1.2.4. Emulsification Techniques……..8

1.3. Objectives and Constitution of the Thesis……11

Chapter 2. Droplet Size Measurement of Submicron W/O emulsion Using Dynamic Light Scattering……22

2.1. Introduction……23

2.2. Dynamic Light Scattering……..23

2.3. Materials and Methods……...25

2.3.1. Materials…….25

2.3.2. Preparation of Model Submicron W/O Emulsions…….25

2.3.3. Preparation of Dilute Solution……26

2.3.4. Measurement of Droplet Size of Model W/O Emulsion Using DLS…….26

2.4. Results and Discussion……...27

2.4.1. Droplet Size Distribution of Model W/O Emulsions without Dilution…..27

2.4.2. Droplet Size Distribution of Model W/O Emulsions Diluted by Each Dilution Ratio……...27

2.4.3. Correlation of Dilution Ratio, Attenuation Index and Degree of Dispersed Phase of W/O Emulsion……28

2.4.4. Discussion of General Versatility……29
2.5. Chapter Conclusion……29

Chapter 3. Formulation and Characterization of Submicron W/F and W/O Emulsions Loaded with Short-chain Fatty Acid……..43
3.1. Introduction……44
3.2. Material and Methods……45
3.2.1. Materials……45
3.2.2. Measurement of Interfacial Tension and Calculation of Molecular Area…46
3.2.3. Preparation of W/F and W/O Emulsions Loaded with Short-chain Fatty Acid……46
3.2.4. Droplet Size Measurement of W/F and W/O Emulsions……47
3.2.5. Physical Stability of W/F and W/O Emulsions……..48
3.3. Results and Discussion……..48
3.3.1. Interfacial Tension Between Milli-Q Water and Soybean Oil Containing TGCR……48
3.3.2. Droplet Size Distribution and Average Droplet Size of W/F and W/O emulsion……49
3.3.3. Storage Stability of W/F and W/O Emulsion……51
3.3.4. Stability for the Phase Conversion of W/F and W/O Emulsion……52
3.4. Chapter Conclusion……...52

Chapter 4. Formulation of W/O/W Emulsions Loaded with Short-chain Fatty Acid and Their Stability Improvement by Layer-by-Layer Deposition Using Dietary Fibers……..60
4.1. Introduction……61
4.2. Material and Methods……63
4.2.1. Materials……63

4.2.2. Preparation of W/O/W Emulsion Loaded with Short-chain Fatty Acid…...64
4.2.3. Coating of W/O/W Emulsions Droplets by Layer-by-Layer Deposition Using Dietary Fibers……..65
4.2.4. Characterization of W/O/W Emulsions……...66
4.2.5. Storage Stability of W/O/W emulsion Coated with Layer-by-Layer Deposition…….67
4.3. Results and Discussion……..68
4.3.1. Interfacial Tension Between Modified Lecithin Solution and Soybean Oil…….68
4.3.2. Characterization of Primary W/O/W Emulsions……68
4.3.3. Characterization of W/O/W Emulsions Stabilized Coated by Layer-by-Layer Deposition……..69
4.3.4. Physical Stability of W/O/W Emulsions Loaded with Short-chain Fatty Acid……..71
4.4. Chapter Conclusion……72

Chapter 5. Formulation and Evaluation of Hydrogels Loaded with Short-chain Fatty Acid……..85
5.1. Introduction……86
5.2. Materials and Methods……...88
5.2.1. Materials……88
5.2.2. Preparation of Agar and ι-Carrageenan Gels Including Methylene Blue…88
5.2.3. Analytical Curve Making of Methylene Blue…….88
5.2.4. Evaluation of Degree of Syneresis and Release of Methylene Blue……89
5.2.5. Preparation and Evaluation of Gel Beads Loaded with Short-chain Fatty Acid……..90
5.3. Results and Discussion……...90
5.3.1. Degree of Syneresis…….90
5.3.2. Release of Methylene Blue with Syneresis…….91

5.3.3. Release of Methylene Blue to the Water……92
5.3.4. Evaluation of Gel Beads Loaded with Short-chain Fatty Acid……93
5.4. Chapter Conclusion……94

Chapter 6. General Conclusions……106
6.1. Introduction……107
6.2. Summary of Each Chapter……107
6.2.1. Chapter 1……...107
6.2.2. Chapter 2……...107
6.2.3. Chapter 3……...108
6.2.4. Chapter 4……...108
6.2.5. Chapter 5……...109
6.3. General Conclusions……...109
6.4. Perspectives……110

References……..112
Acknowledgements……...120

Nomenclature

A	molecular area
ΔA	interfacial area between dispersed phase and continuous phase
A_m	absorbance of methylene blue
D	diffusion coefficient
$d_{3.2}$	the sauter mean diameter
d_i	droplet diameter
d_p	the droplet diameter
E_{min}	minimum amount of energy
g	the gravitational acceleration
$G(\tau)$	the autocorrelation function
k	the Boltzmann's constant
$l(t)$	scattering intensity in any time (t)
n_0	refractive index of solvent
N_A	Avogadro's number
n_i	number of droplets
q	scattering vector
R	gas constant
$R_{Quantity}$	release of inner components with sysneresis
R_{ratio}	degree of release of inner component with syneresis
T	absolute temperature
S	degree of syneresis
Vs	the terminal creaming/sedimentation velocity
W_0	initial weight fraction of agar gel
W_d	weight fraction of dispersed phase
W_{M0}	initial weight fraction of methylene blue
W_t	amount of syneresis
X	appropriate dilution degree

Greek symbols

γ	interfacial tension
$\Gamma_{a.c}$	attenuation constant
Γ_e	the absorption at the saturated interface expression
η_c	the continuous phase viscosity
λ_0	wavelength of the laser beam
ρ_c	the continuous phase density
ρ_d	the dispersed phase density
τ	the amount of change of the time

Chapter 1

Introduction

1.1 Background

1.1.1 Human Digestive System and Function of the Large Intestine

The organs of the human body have various physiological function. The brain has an important role in controlling our life activities including body actions and, feelings. The heart is the pump which sends oxygen-rich fresh blood to the whole human body. In the lungs, the blood intakes oxygen and exhausts carbon dioxide. Human life activities are thus realized based on the function of many organs.

In the human body, there are organs called the digestive system consisting of mouth, esophagus, stomach, small intestine, large intestine, and anus. The human digestive system is in charge of intake, digesting, and excretion of the food (Guerra. 2012). Figure 1.1 schematically depicts the human digestive system with digestion conditions in each organ. The foods ingested are chewed in the mouth, and the bolus which is a mixture of disintegrated food particles and saliva is swallowed and subsequently reaches the stomach. The bolus in the stomach is digested in the presence of the strongly acidic digestive juice secreted from the upper part of the gastric wall and the peristalsis generated in the lower part of the gastric wall. The digesta fasted from the pylorus are further chemically digested in the presence of pancreatic juice and bile, and then the digested nutrients are absorbed in the small intestine. The large intestine mainly absorbs the moisture, and its functions will be further stated later. Finally, excrements are exhausted from the anus.

Main functions of the large intestine are fermentation of dietary fibers and absorption of moisture and salt (Bogart, 2011). The digestive juice secreted in the large intestine does not have digestive enzyme, it takes a role of protection of the intestinal wall. Microbiota fermentation of the digesta fasted from the small intestine produces short-chain fatty acid and gases (e.g., methane) (Sato, 2009).

1.1.2 Short-chain Fatty Acids Utilized in the Large Intestine

Tissue in the large intestine uses short-chain fatty acid as energy source (Cummings *et al.,* 1995). Microbiota produces 300 to 400 mmol/day of short-chain fatty acids (Pituch *et al.,* 2013).

Short-chain fatty acids are generally water-soluble fatty acids with a carbon number lower than 6. Short-chain fatty acids include acetic acid, propionic acid, butyric, pentanoic acid, and caproic acid (Macfarlane, 1995). Figure 1.2 schematically depict the chemical structure of short-chain fatty acids.

The nutrients embedded in foods can be utilized in the organs after digestion and adsorption, which is necessary for the human life activities. The nutritious absorbed were transported to the organs through blood vessels. Butyric acid is used as important energy source for intestinal epithelial cells (Sakata & Ichikawa, 1997); propionic acid and acetic are metabolized in liver and muscle (Hara, 2002). Butyric acid could cause disorder of the large intestine environments (e.g. diarrhea and constipation) and more serious illnesses.

1.1.3 Shortage of Short-chain Fatty Acids in the Large Intestine

An investigation reported that around half of Japanese (43 % for man; 65 % for woman) have awareness of the disorder for the large intestine (Ministry of Health, 2010). This disorder is usually caused by shortage of dietary fibers. As mentioned above, microbiota produces short-chain fatty acids by utilizing dietary fiber. Shortage of dietary fibers results in producing insufficient quantity of short-chain fatty acids in the large intestine. As mentioned previously, the disorder of the large intestine is caused by shortage short-chain fatty acid. Therefore, it is improved by taking in Short-chain fatty

acid.

Numerous food and pharmaceutical products, each containing dietary fiber or intestinal bacteria, are currently commercialized in many different countries. Typical example include the dairy products including a lactic acid bacterium, *Bacilli bifidus* such as yogurts and the supplements fortified a dietary fiber. However, these bacterium produce lactic acid or acetic acid and simply reduce pH of large intestine, do not produce the short-chain fatty acids as the energy source of the large intestine (Morishita, 2000).

There are several bacterial species which can provide butyric acid, such as *Clostridium spp.* or *Eubacterium spp.*. The butyrate quantity that they can produce per day is 1-10 mmol/L (Pituch et al., 2013). Moreover it is suggested that quantity of production of the short-chain fatty acid is not constant by individual difference (years, gender, physical condition, and enteral environment). It is desired that short-chain fatty acids can be directly delivered to the large intestine. The few kinds of product which contained a short chain fatty acid exists, but it is on the basis of supplements and expensive. This product includes a short-chain fatty acid, but is not added for the purpose of the intake of the short-chain fatty acid (website of Shirokiya Co., Ltd. HP). Development of the food which we can take in with a daily meal is demanded. However development food and pharmaceutical products containing short-chain fatty acids are preferable, as unpleasant a smell and taste should remain in the oral cavity for a long time. A possible solution for this problems is to develop food grade dispersions containing nano/microscale particles/droplets. As these food-grade dispersions do not require chewing, residence time in the oral cavity may be sufficiently short. It should be mentioned that unchewable food-grade dispersions could also be applicable to different life stages from young children to elderly persons. It is desired that the large intestine

becomes able to take in a short-chain fatty acid efficiently by developing such a food.

1.2 Emulsion and Emulsification Techniques

1.2.1 Definition of Emulsion

In general, emulsion is defined as the dispersion of two immiscible fluids (usually oil and water) into one another as small spherical particles. Typical types of to emulsions include oil-in-water (O/W) emulsion, water-in-oil (W/O) emulsion, oil-in-water-in-oil (O/W/O) emulsion, and water-in-oil-in-water (W/O/W) emulsion. Especially, O/W/O and W/O/W emulsion are called multiple emulsions. O/W/O and W/O/W emulsion has oil or water droplets within larger water or oil droplets, and which are themselves dispersed in oil or water continuous phase (McClements, 2004). Figure 1.3 shows a schematic drawing of the above-mentioned emulsions.

1.2.2 Applications of Emulsions in the Food Industries

There are a wide variety of applications of emulsions in the food industries. O/W food emulsions include milk, mayonnaise, cream, beverages, soups, dressings, and sauces. W/O food emulsions include margarine and butter, while they have a narrower variety of applications than O/W emulsion. Multiple emulsions can be used to control the release of certain ingredients, to reduce the total fat content of food emulsions-based food, or to isolate one ingredient from another ingredient that it might normally interact with. Multiple emulsions are likely to find increasing usage in the food industries because of their potential advantages over O/W and W/O emulsions. Nevertheless, researchers are still trying to develop multiple emulsions that can be economically produced using food-grade ingredients (MaClements, 2004).

1.2.3 Characterization and Stability Evaluation of Emulsions

There are important properties of food emulsions, such as droplet size and droplet size distribution, appearance, texture, and flavor. Among them, droplet size and droplet size distribution are known as one of the most important property.

1.2.3.1 Droplets Size and Droplet Size Distribution

Droplet size primarily affects emulsion appearance. Emulsions generally have a whitish color, since emulsion droplets reflect diffusely for light. However, when droplet diameter is under 100 nm, emulsion color becomes opaque or transparent. An O/W emulsion containing small droplets are reported suppress bitterness (Nakaya *et al.*, 2006). Droplet size distribution also affects many physical, chemical and biological properties of emulsions. Polydisperse emulsions with a wide droplets size distribution are easier to coalesce than monodisperse emulsions with a narrow droplet size distribution (Saito *et al.*, 2006). Components encapsulated in smaller droplets are more quickly released from their surface, which is attributed to the larger total surface area of droplets. Smaller droplets sizes also can inhibit bacteria growth because of insufficient space inside the droplets.

1.2.3.2 Effect of Droplet Size on Emulsion Stability

Each emulsion is terminally separated into water and oil phases within a finite time. This phase separation is caused by some factors; e.g., creaming, sedimentation, flocculation, and coalescence (see Fig. 1.4).

Creaming and sedimentation are driven by the density difference between dispersed and

continuous phases. Oil droplets dispersed in an O/W emulsion usually float up to the surface, which is called creaming. In contrast, aqueous droplets dispersed in a W/O emulsion tend to settle down the bottom surface, which is called sedimentation. The terminal creaming (or sedimentation) velosity obeys the Stokes' law

$$V_S = \frac{{d_p}^2(\rho_d - \rho_c)g}{18\eta_c} \quad (1\text{-}1)$$

where *V*s is the terminal creaming (or sedimentation) velocity, d_p is the droplet diameter, ρ_d is the dispersed-phase density, ρ_f is the continuous-phase density, g is the gravitational acceleration, and η_c is the continuous-phase viscosity. This equation shows that smaller droplets are harder to perform creaming (or sedimentation). Submicron droplets can perform a Brownian motion, sufficiently preventing creaming (or sedimentation).

Flocculation/aggregation and coalescence are also major mechanisms of droplet instability. The emulsion droplets that are thermodynamically unstable tend to reduce their total surface area in order to make the energy level of the emulsion system lower. Flocculation/aggregation and coalescence of the droplets increase their terminal creaming (or sedimentation) velocity, which can be explained by Eq. 1-1. d_p in this equation becomes apparently greater due to the size of flocs/aggregates. As stated above, droplet size is one of the most important factors of emulsion stability.

1.2.3.3 Stability Improvement of the Emulsions

Emulsion stability has been received a great deal of attention to the food industries, because of an important parameter affecting quality and shelf-life of emulsions. The food emulsions produced on an industrial scale are adequately controlled in terms of quality and major properties.

There are some approaches useful for improving emulsion stability. The first

approach is to prepare droplets with smaller sizes. The second approach is to prepare monodisperse emulsions with a narrower droplet size distribution (Mason et al., 1996). The third approach is to appropriately select emulsifier(s). Emulsifier consists of hydrophilic and hydrophobic groups in a single molecule. Emulsifier molecules preferably adsorb to the droplet surface, reducing the interfacial tension (Shima, 1998). It is also effective to electrostatically charge the droplet surface, since the positively charged droplets repel each other. Therefore, the contact between droplets becomes hard to happen, and emulsion is stabilized (Nishinari, 2007).

1.2.4 Emulsification Techniques

Emulsification applies external forces to an emulsion system, as emulsion is a thermodynamically unstable system. The energy efficiency in the emulsification is provided in the following equation

$$E_{\min} = \gamma \Delta A \tag{1-2}$$

where $E_{\min}$ is the minimum amount of energy needed to increase the interfacial area between the oil and water phases, γ is interfacial tension, and ΔA is interfacial area between dispersed phase and continuous phase. Increasing of interfacial area means preparation of smaller droplets emulsions. This equation shows that if interfacial tension decreases, there is little energy of the emulsification. It also is important that giving a system energy efficiently.

Various emulsification devices have been developed so far. Major emulsification techniques and their fundamental characteristics are summarized in Table 1.1 (Nishinari, 2007; McClements, 2004).

1.2.4.1 Mechanical Emulsification Techniques

Rotor-stator homogenization (Fig. 1.5a) is one of the most commonly used emulsification methods. This technique breaks down larger droplets into smaller ones in the presence of mechanical stirring and/or shearing. This technique can produce emulsions with typical sizes of 1 to 30 μm at different production scales of 0.1 to 100 L/h, depending on the device size. However, this technique loses most of the energy input into the emulsion system, resulting in its temperature elevation after emulsification.

High-pressure homogenization is normally used to prepare submicron emulsions. High-pressure homogenizers can be roughly categorized into the high-presser valve homogenizer (Fig. 1.5b) and the microfluidizer (Fig. 1.5c). The high-presser valve homogenizer pushes coarse emulsion out of the narrow slit with a high internal pressure. The pressure applied during high-pressure homogenization is around 10 to 150 MPa. The energy efficiency of high-pressure homogenization is low, and decreasing the slit size increases the energy input required to form an emulsion, thereby increasing manufacturing costs. The cross-sectional size of the slit is approximately 15-300 μm. Micro fluidizer gives shearing force by High pressure to sample in a chamber, and lets samples collide at high speed. High pressure homogenization can prepare emulsions which have under 1 μm scale droplets. This technique can produce emulsions with typical sizes of 0.05 to 2 μm at different production scales of 1 to 10000 L/h.

Ultrasonic emulsification technique can emulsify using an ultrasonic (Fig. 1.5d). It includes an electrical vibration method and a mechanical vibration method. Both technique emulsifies by causing cavitation. Diameter of droplets of emulsion which prepared by ultrasonic emulsification is around 1-30 μm, and production volume is 1-1000 L/h. are ideal for preparing small volumes of emulsion, which is an important

consideration in research laboratories because the chemicals used are often expensive. Ultrasonic emulsification generally is ideal for preparing small volumes of emulsion, and suitable for lability scale operation.

1.2.4.2 Advanced Emulsification Techniques

Membrane emulsification (Fig. 1.6a) is technique to let emulsify disperse phase through membrane to continuous phase. It can prepare the monodisperse emulsion in comparison with mechanical emulsification. Droplets scale and coefficient variation of emulsion provided by membrane emulsification is 0.3-100 μm and 10-30 %, and production volume is 0.1-100 L/h. Energy loss of membrane emulsification is few, and it can prevent of the heat of samples. Membrane emulsification can control of the droplets diameter, and provide W/O/W and O/W/O emulsion relatively easily.

Microfludic emulsification device can prepared droplets is a method of emulsification that manufactures the monodisperse emulsion using a cross junction, the combined two phases flow is often forced through a small orifice (Fig. 1.6b). T or Y junctions show simplest microfiluidic structure for producing bubbles and droplets in junction. In the microfluidic flow focusing device (MFFD), the dispersed and continuous phase are forced to flow through a small orifice located downstream of the three channels. And continuous phase has a pressure and shear stress that force the dispersed phase into a narrow thread, which breaks inside or downstream of the orifice. Those techniques can produce emulsions with typical sizes of 5 to 30 μm at different production scales of 0.0003 to 0.3 L/h, (Vladisavljević *et al.,* 2012; Kobayashi et al., 2012).

Microchannel (MC) emulsification (Fig. 1.7; Kobayashi and Nakajima, 2004) is a method of emulsification that manufactures the monodisperse emulsion using MCs made

on a silicon substrate. MC emulsification has two kinds of the grooved MC array and the straight-through MC array. MC emulsification makes emulsion droplet by forcing disperse phase through continuous phase through MC, like a Membrane emulsification. Droplets size which provided by MC emulsification is 1-200 μm (Kawakatu, *et al.,* 1997; Kobayashi *et al.,* 2005; 2007; 2010), and coefficient variation shows under 10 %. The droplets amount of production of general MC emulsification is around 100 mL/h, however MC emulsification which can produce liter scales every hour is developed. In MC emulsification, the manufacture of a functional microcapsule and the compound emulsion is expected.

1.3 Objectives and Constitution of the Thesis

Li and co-workers (2009) prepared O/W emulsion loaded with tributyrin. the purpose of their study is examining the possibility of mixing tributyrin with long-chain triglycerides (corn oil) to reduce the tendency for Ostwald ripening, delivery systems using a cell culture model to demonstrate their potential efficacy at preventing colon cancer, however they have not prepared emulsion systems in consideration of influence of the digestion in stomach and the small intestine.

The main objectives of this research are formulation of dispersions loaded with short-chain fatty acid using each emulsification techniques, dietary fivers, and hydrogels to increase storage physical stability and digestion stability. Especially, droplets size distribution and storage physical stability in an evaluation of the dispersions were focused. Storage physical stability is important factor of food industry, it greatly affects it in expiry date of the food. This study can greatly contribute to development of the food by examining the storage physical stability of dispersions, and contribute to improvement

about the digestion stability by using solid fat, dietary fiber, and gel.

The outline of this thesis is presented in Fig. 1.8. This thesis starts from general introduction that overviews the human large intestine and its functions, short-chain fatty acids, emulsions and their important properties and stability, and emulsification techniques (Chapter 1).

In this study, dynamic light scattering (DLS) was used for measuring the droplet diameter of submicron W/O emulsions (Chapter 2). The emulsion samples have to be diluted before the DLS measurements; however, the clear attenuant standard does not exist. Therefore, the equation that could calculate appropriate dilution ratio is proposed in this chapter.

The main part of the thesis is composed of three parts (Chapters 3 to 5). The first part is preparation of W/O and water-in-fat (W/F) emulsions loaded with a short-chain fatty acid by using high-pressure homogenization (Chapter 3). Physical and storage stabilities of these emulsions are evaluated in this chapter. The second part is formulation of W/O/W emulsions loaded with a short-chain fatty acid as well as characterization and stability evaluation of W/O/W emulsions coated by dietary fibers using layer-by-layer deposition (Chapter 4). The third part is to prepare hydrogel beads containing a short-chain fatty acid based on agar and ι-carrageenan gel (Chapter 5), and evaluated characterization of sysneresis of these gels.

Finally, the findings reported in the thesis are concluded, and perspectives are described (Chapter 6).

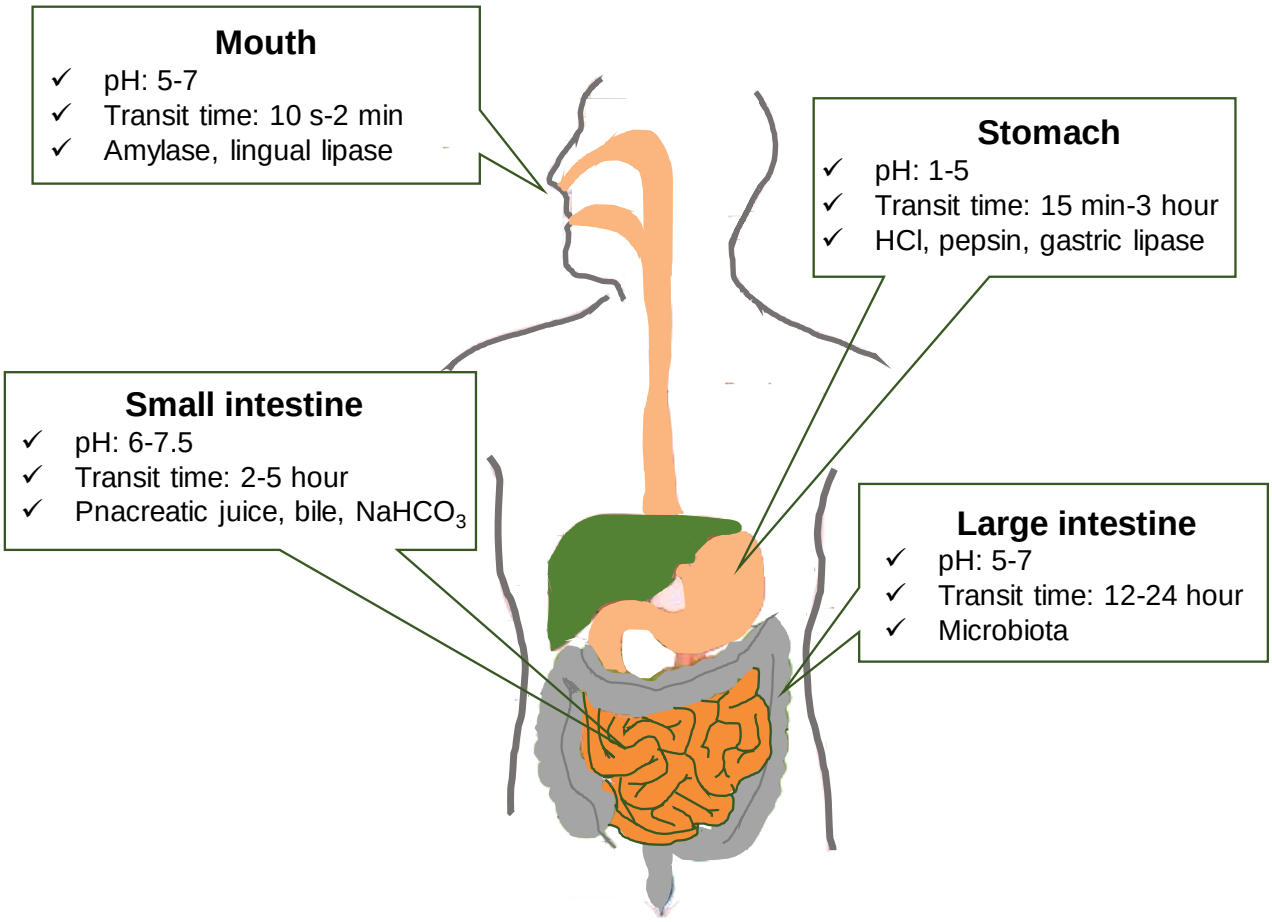

Fig.1.1. Schematic drawing of the digestive system in the human body. The information about each organ is quoted from Guerra *et al.* (2012).

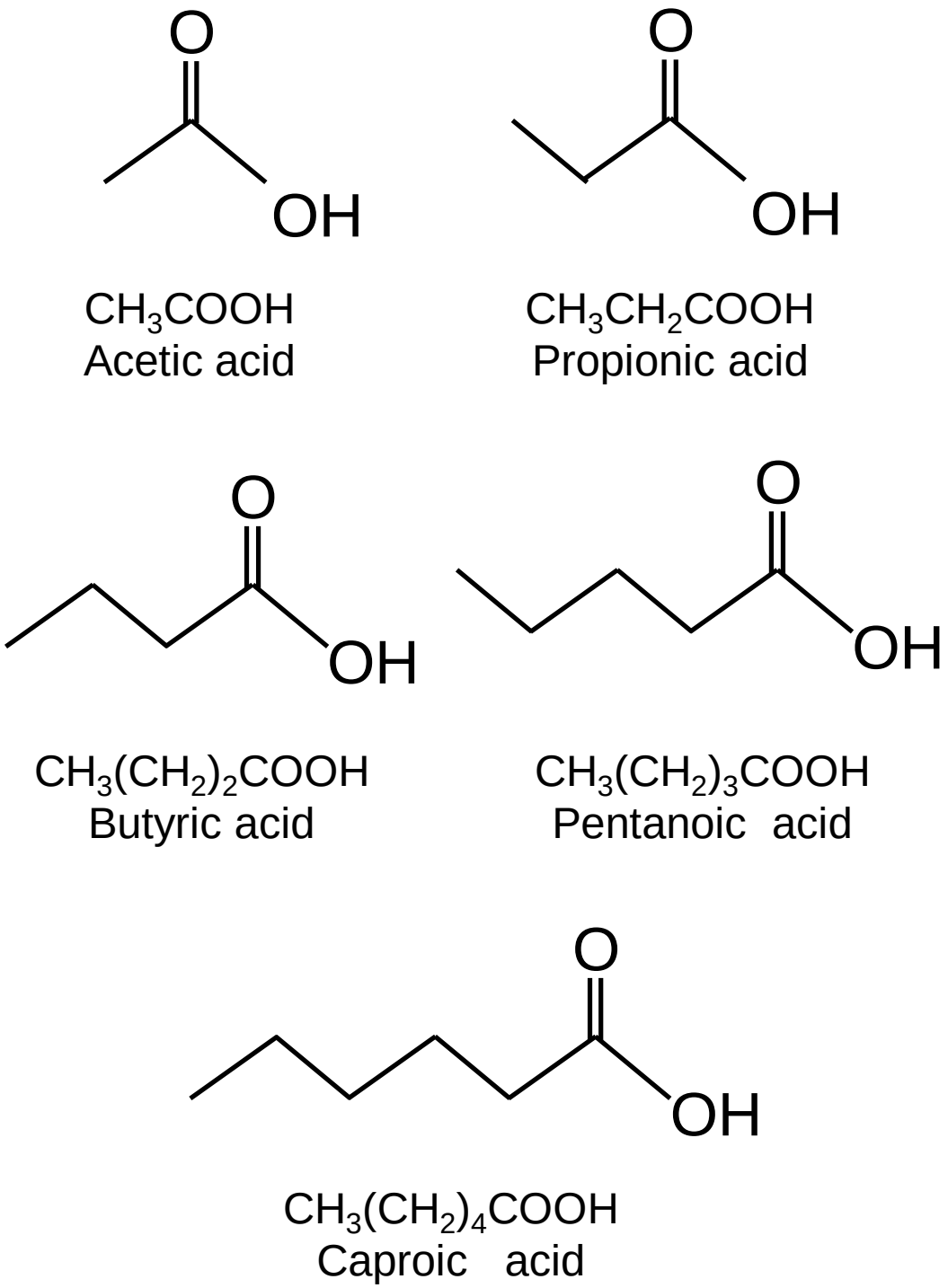

Fig.1.2. Chemical sturcture of short-chain fatty acids.

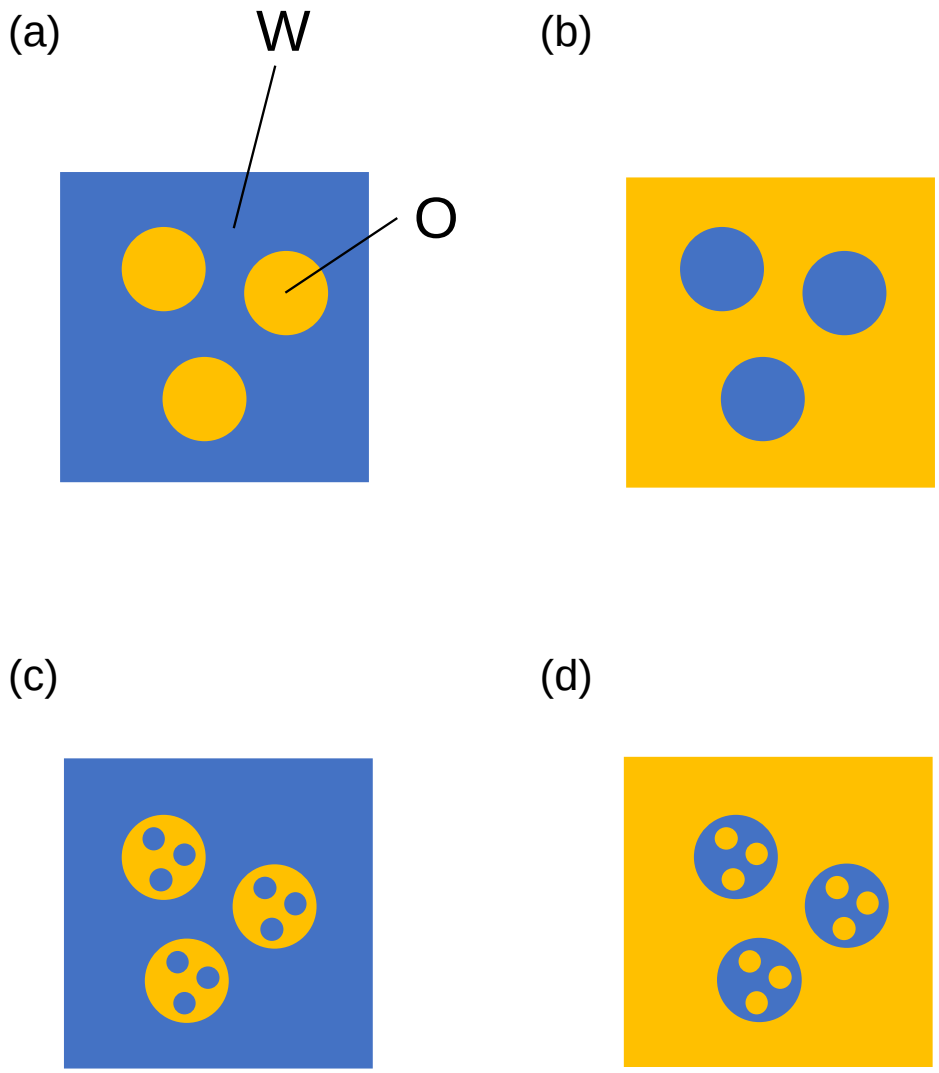

Fig.1.3. Schematics drawing of emulsion types. (a) O/W emulsion. (b) W/O emulsion. (c) W/O/W emulsion. (d) O/W/O emulsion.

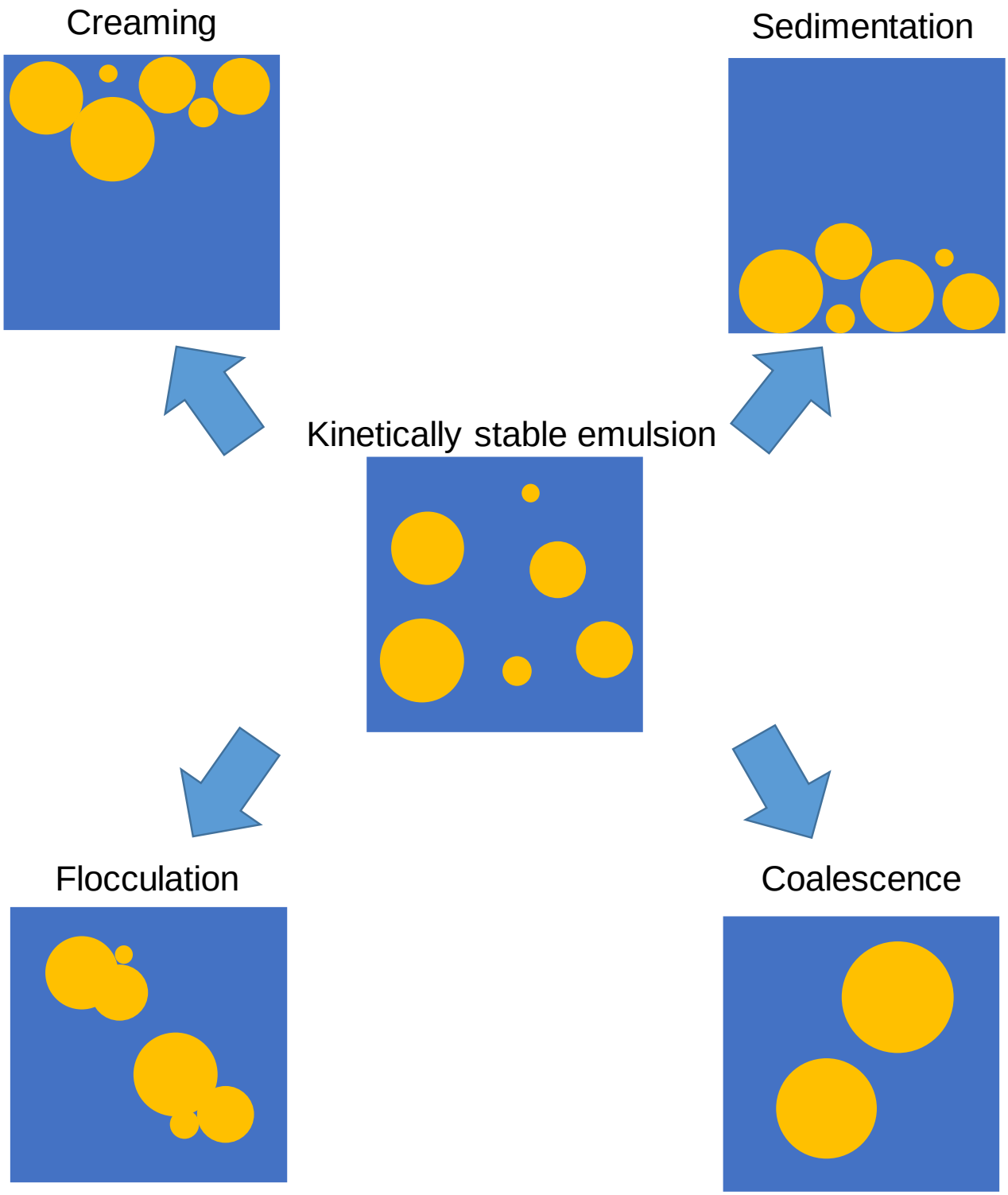

Fig.1.4. Schematics drawing of emulsion instability.

Table.1.1. Characteristics of major emulsification techniques. The information about each emulsification techniques are quoted from Nishinari *et al.* (2007), McClements *et al.* (2004).

Method	**Droplets diameter (μm)**	**Coefficient variation (%)**	**Production volume (L/h)**
Rotor-stator homogenization)	1-30	>30	0.1-100
High-pressure homogenization	0.05-2	>20	1-10000
Ultrasonic emulsification	1-30	>30	1-1000
Microfluidic device	5-30	3-10	0.0003-0.3
Membrane emulsification	0.3-100	10-30	0.1-100
Microchannel emulsification	1-200	3-10	0.001-1

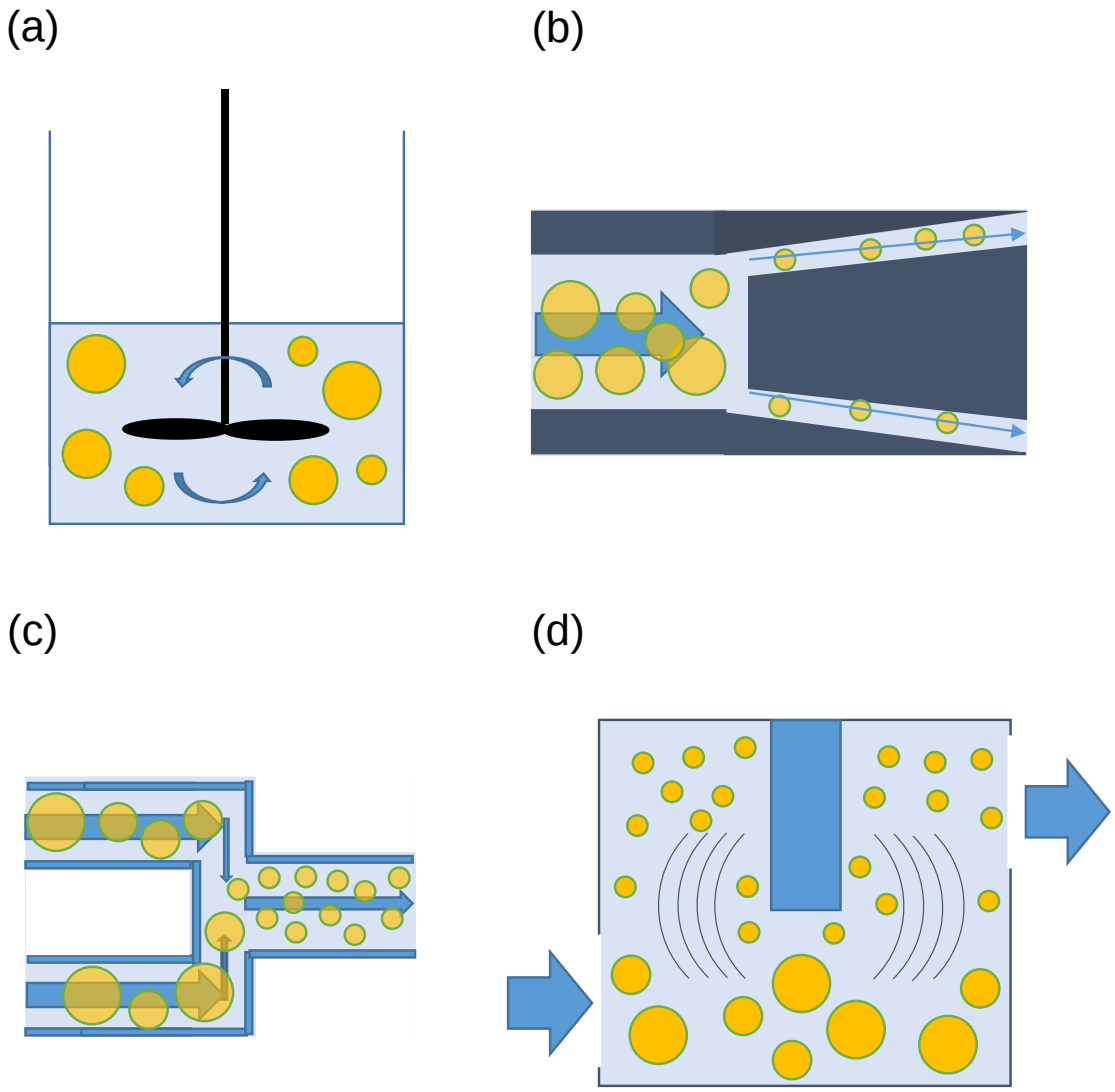

Fig.1.5. The mechanical emulsification methods. (a) Rotor-stator homogenization, (b) High-presser valve homogenizer, (c) Microfluidizer, (d) Ultrasonic emulsification.

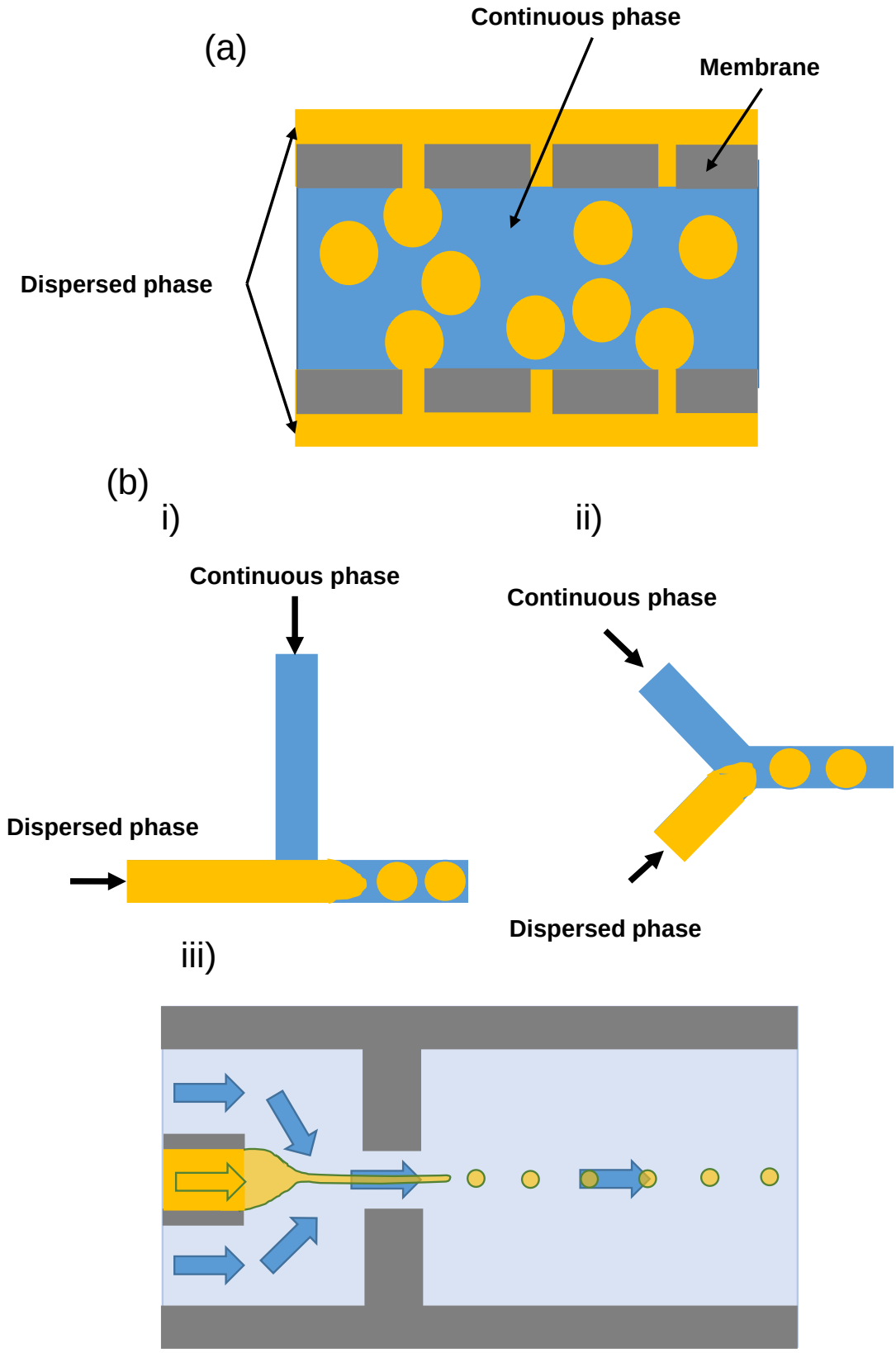

Fig.1.6. Schematic drawing of the membrane emulsification (a), T-junction (b,i), Y-junction (b,ii), and microfludic flow focusing device (b,iii).

(a)

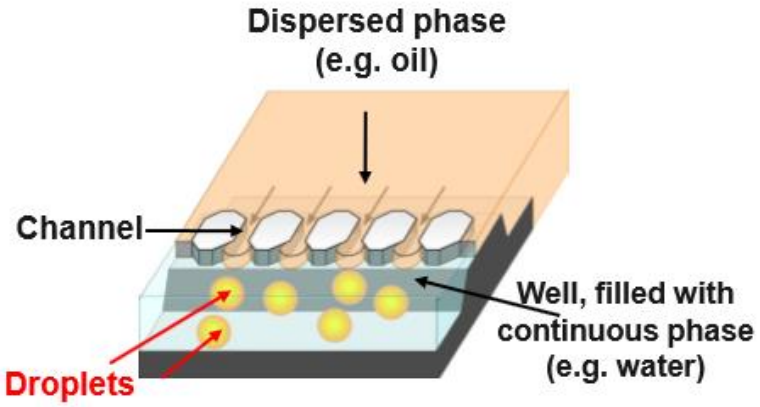

(b)

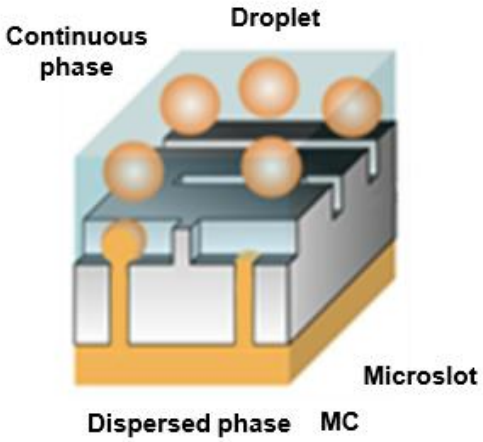

Fig.1.7. Schematic drawings of droplet generation via part of a grooved microchannel (MC) array (a) and part of a straight-through MC array (b); (Kobayashi and Nakajima, 2004).

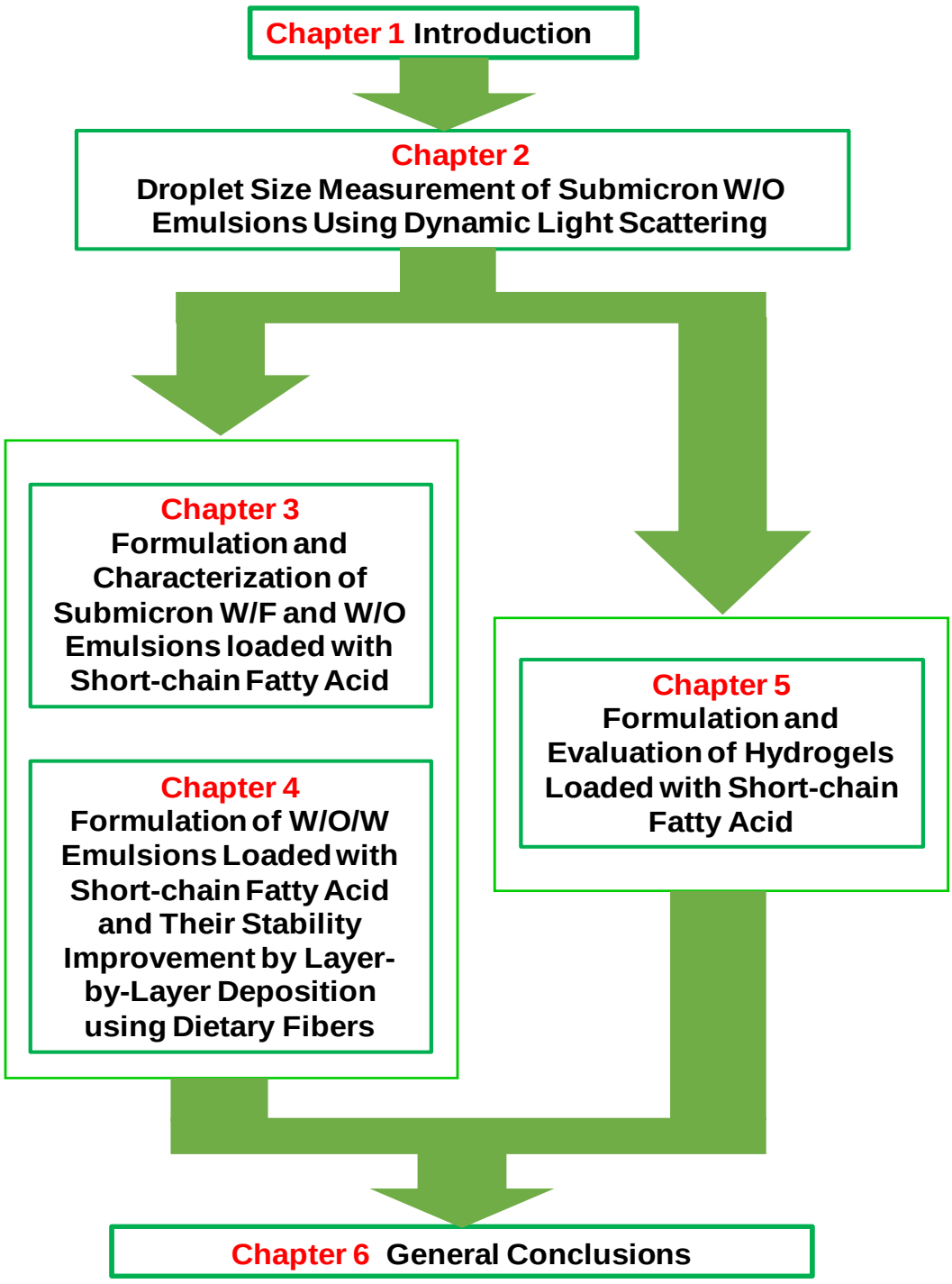

Fig.1.8. General structure of this thesis.

Chapter 2

Droplet Size Measurement of Submicron W/O Emulsion Using Dynamic Light Scattering

2.1. Introduction

Droplet size distribution is an important parameter for evaluating the stability of food emulsions. Droplet size greatly affects texture, feeling to the throat, and flavor. The measurement of an accurate droplet size distribution is an essential factor.

Different methods for measurement of droplets size distribution have been developed, and it is necessary to choose an appropriate method, according to the droplet size range. There are Dynamic Light Scattering (DLS), Laser diffractometry, Centrifugal sedimentation method, image analysis, and Field-flow fractionation (FFF) method in representative methods of droplets size distribution measurement. These methods are shown on the Table 2.1. DLS is used for the measurement of the submicron scale droplets. The range of the particle diameter that DLS can measure is around 0.001-10 μm. However, in the systems which has high weight fraction dispersed phase, DLS cannot measure exactly by multiple scattering. As a solution of this problem, diluting a sample is general. But, choice of the diluting solution and/or dilution ratio for the disperse phase density depend on reasonableness of each research organization, and there is not a clear index (Kato, 2007; Otsuka Electronic Co., Ltd. HP.; Beckman Coulter, Inc. HP.; Malvern Instruments Ltd. HP.)

The purpose of this chapter is suggestion of dilution ratio for the density of disperse phase in case of the measurement of the droplets size distribution of W/O emulsion using DLS.

2.2. Dynamic Light Scattering

In the dispersion, submicron scale droplets and/or particles perform Brownian motion, the movement is slow so that a particle is big and fast so that a particle is small (Koiwa,

et. al, 2009). Difference of movement of Brownian motion is observed as difference of diffusion speed of the particles, therefore droplets size can measured by Diffusion coefficient.

Particles under Brownian motion receive a laser beam, scattered light from laser beam received particles was obtained fluctuation depending on speed of the Brownian motion (Fig. 2.1). The autocorrelation function ($G(\tau)$) is expressed as correlation about scattering intensity ($I(t+\tau)$) after the τ time on the basis of scattering intensity ($I(t)$) in any time (t).

$$G(\tau) = \frac{\langle I(t) \cdot I(t+\tau) \rangle}{\langle I(t) \rangle^2} \quad (2\text{-}1)$$

< > is average of those factor.

The autocorrelation function depends on only τ, and it is not influenced at start of measurement time (t). In the autocorrelation function, when τ is small, particles shows little movement. However, when τ is large, position of the particle becomes uncertain and Correlation becomes hard to be confirmed. Therefore, $G(\tau)$ shows exponential decrement curve. When a particle is small; of the correlation time become short, and a particle is large; of the correlation time become long.

From a provided autocorrelation function, Diffusion coefficient is calculated.

In the monodispersion systems, Autocorrelation function can be calculated as

$$G(\tau) = exp(-\Gamma\tau) \quad (2\text{-}2)$$

$$ln\big(G(\tau)\big) = -\Gamma\tau \quad (2\text{-}3)$$

The $\Gamma_{a.c}$ is attenuation constant, diffusion coefficient (D) is difined

$$\Gamma_{a.c} = q^2 D \quad (2\text{-}4)$$

$$q = \frac{4\Pi n_0}{\lambda_0} sin(\theta/2) \quad (2\text{-}5)$$

where q is scattering vector n_0 is refractive index of solvent, λ_0 is wavelength of the laser beam.

In the polydispersion systems, autocorrelation function cannot be defined by (2-2). It can be similar to (2-2) by second series expansion an exponent in τ.

$$ln\big(G(\tau)\big) = -\Gamma\tau + \frac{1}{2!}\mu_0\tau^2 \quad (2\text{-}6)$$

Particle size (d) is calculated by diffusion coefficient and Einstein-Stokes low

$$d = \frac{kT}{3\pi\eta_0 D} \quad (2\text{-}7)$$

where k is Boltzmann's constant, T is absolute temperature, and η_0 is viscosity of continuous phase (Malvern Instruments Ltd.).

2.3. Materials and Methods

2.3.1. Materials

Sodium chloride, refined soybean oil, hexane, and chloroform were purchased from Wako Pure Chemical Industries, Ltd. (Osaka, Japan). MCT (Medium-Chain Triglyceride) oil was provided by Taiyo Kagaku Co., Ltd. (Yokkaichi, Japan). Tetra glycerin condensation ricinoleate (TGCR, HLB<1) was provided by Sakamoto Yakuhin Kogyo Co., Ltd. (Osaka, Japan).

2.3.2 Preparation of Model Submicron W/O Emulsions

In this chapter, model of measurement of particle size using DLS was used submicron W/O emulsion.

Dispersed phase of W/O emulsion was 1 wt% of sodium chloride solution, and continuous phase was 5 wt% of TGCR containing soybean oil or MCT oil. W/O

emulsions were prepared by dispersing a dispersed phase (1, 5, 10 or 20 wt%) into a continuous phase (99, 95, 90 or 80 wt%) by rotor-stator homogenization (PolytronPT-3100, Kinematica Co., Ltd., Luzern, Switzerland) at 10000 rpm for 5 min, followed by high-pressure homogenization (NanoVater200, Yoshida Kikai Co., Ltd., Nagoya, Japan) at 100 MPa for one pass. W/O emulsions were prepared at room temperature (25 ^{o}C)

2.3.3 Preparation of Dilute Solution

A mixture of hexane and chloroform was used to dilute W/O emulsions. Diluting solution was prepared by mixing 60 vol% of hexane and 40 vol% of chloroform. Two hundred mL of the diluted solution was then saturated with 50 mL of Milli-Q water while stirring for 30 min, to prevent elution of the inner water phase droplets into the diluted solution. The diluted solution after water saturation was separated from the excess Milli-Q water using centrifugation (HP-25, Beckman Coulter, Inc., Brea, USA) at 1000 rpm for 30 min.

This solution has a density valueclose to that of water. Table 2.2 shows density values of hexane and chloroform solution, as well asfor water (measurement by DA-130N, Kyoto Electronics Manufacturing Co., Ltd. Kyoto, Japan).

2.3.4. Measurement of Droplets Size of Model W/O Emulsion Using DLS

n this study, Zetasizer Nano ZS (Malvern Co., Ltd., Worcestershire, UK) was used for measurement of droplets size, based on DLS technique. In Zetasizer Nano ZS, viscosity and refractive index of continuous phase are necessary for the measurement. In this chapter, each model W/O emulsions were diluted 5, 10, 50, 100, 500 times by diluting solution. The viscosity (Cannon-Fenske, Shibata science technology LTD. Soka, Japan)

and refractive index (Pal-RI, ATAGO Co., Ltd. Shibaura, Japan) of the dispersed phase upon dilution were also measured. Table 2.3 shows viscosity and refractive index value of continuous phase of model W/O emulsions. As a measurement condition, operation temperature was around 25 ^{o}C (Room temperature), and droplets size distributions were measured 3 times for each sample.

The volume droplet size distribution which was provided by the measurement was as a results of droplet size distribution.

2.4. Results and Discussions

2.4.1. Droplets Size Distribution of Model W/O Emulsions without Dilution

Figure 2.2 shows droplets size distribution of each model W/O emulsion without dilution. It demonstrates that droplets size distribution cannot identify reproducibility with increase of degree of dispersed phase. Those results indicates that laser beam may do multiple scattering by high degree of dispersed phase, and dilution need was suggested.

2.4.2. Droplet Size Distribution of Model W/O Emulsions Diluted by Each Dilution Ratio

Figure 2.3 demonstrates droplets size distribution of model W/O emulsions diluted by each dilution ratio. In addition, droplets size distribution without diluting in the figure is average of droplets size distributions which were showed by Fig. 2.2.

Droplets size distribution of those W/O emulsions changed with increase of dilution ratio. As for this, laser beam becomes hard to do multiple scattering. Those droplets size distributions have dilution ratio which shows reproducibility, in the 1 wt% of dispersed phase system is 5 and 10 times dilution, 5 wt% of dispersed phase system is 50

times dilution, 10 wt% of dispersed phase system is 100 times dilution, and 20 wt% of dispersed phase system is 500 times dilution. Figure 2.4 shows the attenuation index for each dilution ratio. Those results indicates that attenuation index of dilution ratio which has reproducibility is around 7.

2.4.3. Correlation of Dilution Ratio, Attenuation Index and Degree of Dispersed Phase of W/O Emulsion

It was suggested that attenuation index which is 7 may provide results which has high reproducibility (2.4.2.). Figuer 2.5 show correlation of dilution ratio and the attenuation index. An approximate curves were drawn each degree of dispersed phase, and approximate curve equation was provided. The dilution rratio that an attenuation index became 7 was calculated by an approximate curve equation (Table 2.4). Each dilution ratio are 10.7 (1 wt% of dispersed phase), 60.7 (5 wt%), 106 (10 wt%), 324 (20 wt%). Fig 2.6 shows correlation of dilution ratio from Table 2.4 and degree of dispersed phase of W/O emulsion. The approximate curve equation was provided in Eq. (2-8):

$$X = 10 W_d^{1.13} \tag{2-8}$$

where X is the appropriate dilution ratio, and W_d is the degree of dispersed phase of W/O emulsion. This equation can calculate appropriate dilution ratio each degree of dispersed phase of W/O emulsion. Table 2.4 demonstrates that appropriate dilution ratio each degree of dispersed phase calculated by Eq. (2-8). Droplets size distribution which were diluted by (2-8) had high reproducibility (Fig 2.7).

Table 2.4 indicates the weight fraction of dispersed phase after dilution. It shows that weight fraction of dispersed phase of W/O emulsion after dilution is around 0.1 wt%. This result indicates the weight fraction of dispersed phase is 0.1 wt% when attenuation

index becomes 7.

2.4.4. Discussion of General Versatility

As a discussion, this equation which can be used for another systems or not was inspected. In comparison, W/O emulsions is which MCT was used as a continuous phase were used. Figure 2.8 shows droplets size distribution of each model W/O emulsions using MCT without dilution. Those droplets size distributions did not has reproducibility in the high weight fraction of dispersed phase. However, in using equation, Reproducibility was confirmed in a particle size distribution (Fig. 2.9). Those results indicated that droplets size distribution of W/O emulsions which have high weight fraction of dispersed phase can be measured by using equation. DLS can measure droplets distribution exactly by input of an appropriate value and dilution, regardless of W/O emulsion systems.

2.5. Chapter Conclusion

The findings obtained in Chapter 2 shows appropriate dilution ratio index when measurement of droplets distribution of W/O emulsion. The dilution ratio index can be calculated using by equation (2-8).

In this thesis, this dilution ratio index is used for measurement of droplets size distribution of submicron scale W/O emulsion.

Table 2.1. Characteristics of each particle size distribution measuring equipment. The information about each organ is quoted from Kato (2007).

Method	Measuring range (μm)	Merits	Drawbacks
Dynamic Light Scattering	0.001-10	Measuring submicron scale droplets	Cannot measure in the high-dispersed phase systems
Laser Diffractometry	0.015-3000	The measurement of a wide range is possible	Droplets size will be measured larger in polydispersion
Centrifugal Sedimentation Method	0.01-300	Cheap and handy	Cannot measure by temperature change
Image Analysis	0.001-	The measurement of a wide range is possible	The measurement range depends on microscope
Field-Flow Fractionation Method	0.01-1	Measuring submicron scale droplets	Low versatility

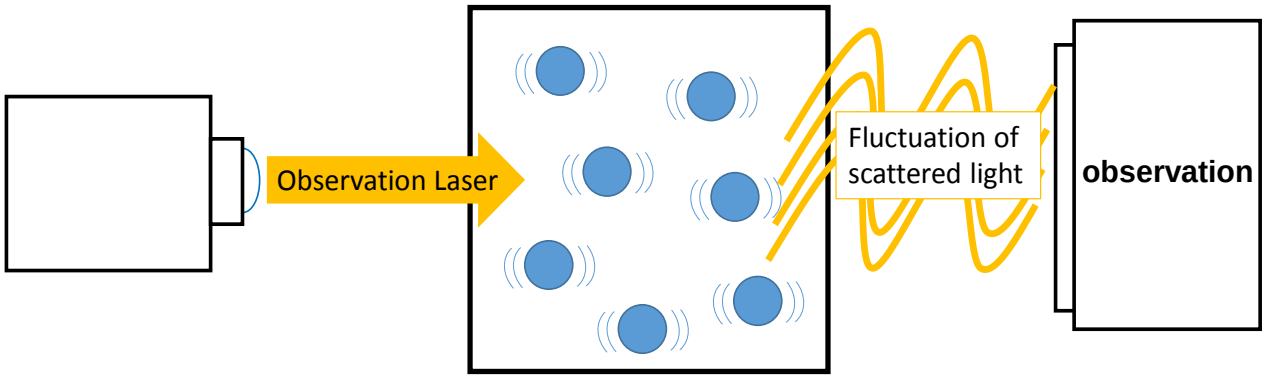

Fig.2.1. Principle of the dynamic light scattering.

Table 2.2. Density of hexane and chloroform solution and water.

	Density (kg/m^3, 25 ℃)
Hexane : Chloroform = 50 : 50 (v/v)	1159
Hexane : Chloroform = 55 : 45 (v/v)	1021
Hexane : Chloroform = 60 : 40 (v/v)	979
Pure water	997

Table 2.3. Viscosity and refractive index of continuous phase of model W/O emulsions.

	Continuous phase of W/O emulsion diluted by hexane-chloroform solution					
	5 times	10 times	50 times	100 times	500 times	Without dilution
Viscosity (mPa/s, 25 ℃)	0.962	0.673	0.490	0.480	0.478	60.7
Refractive index (-, ℃)	1.417	1.408	1.402	1.400	1.400	1.474

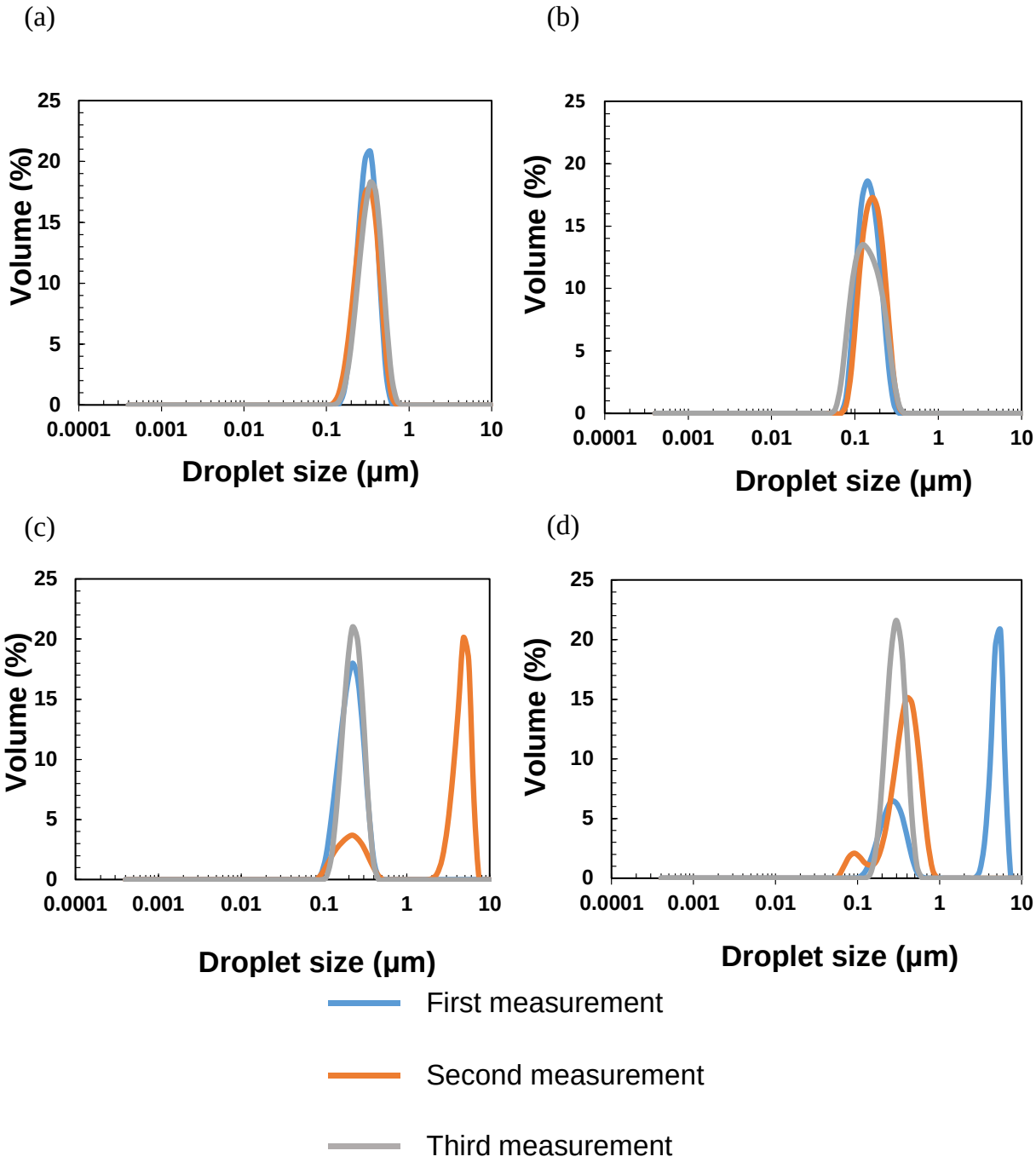

Fig.2.2. Droplet size distribution of model W/O emulsions with out dilution.
(a) : 1 wt% of dispersed phase system
(b) : 5 wt% of dispersed phase system
(c) : 10 wt% of dispersed phase system
(d) : 20 wt% of dispersed phase system

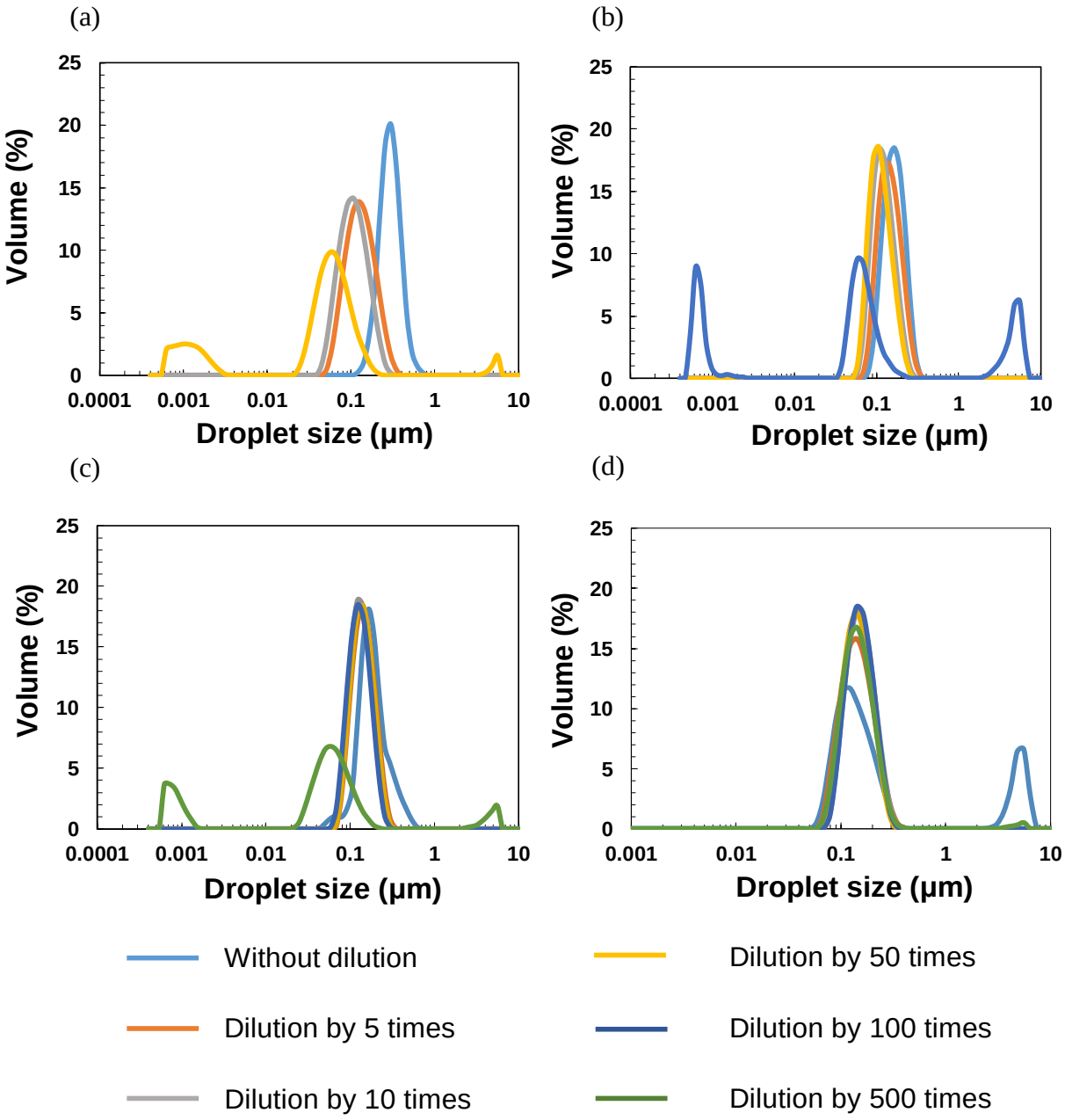

Fig.2.3. Droplet size distribution of model W/O emulsions with each dilution.
(a) : 1 wt% of dispersed phase system
(b) : 5 wt% of dispersed phase system
(c) : 10 wt% of dispersed phase system
(d) : 20 wt% of dispersed phase system

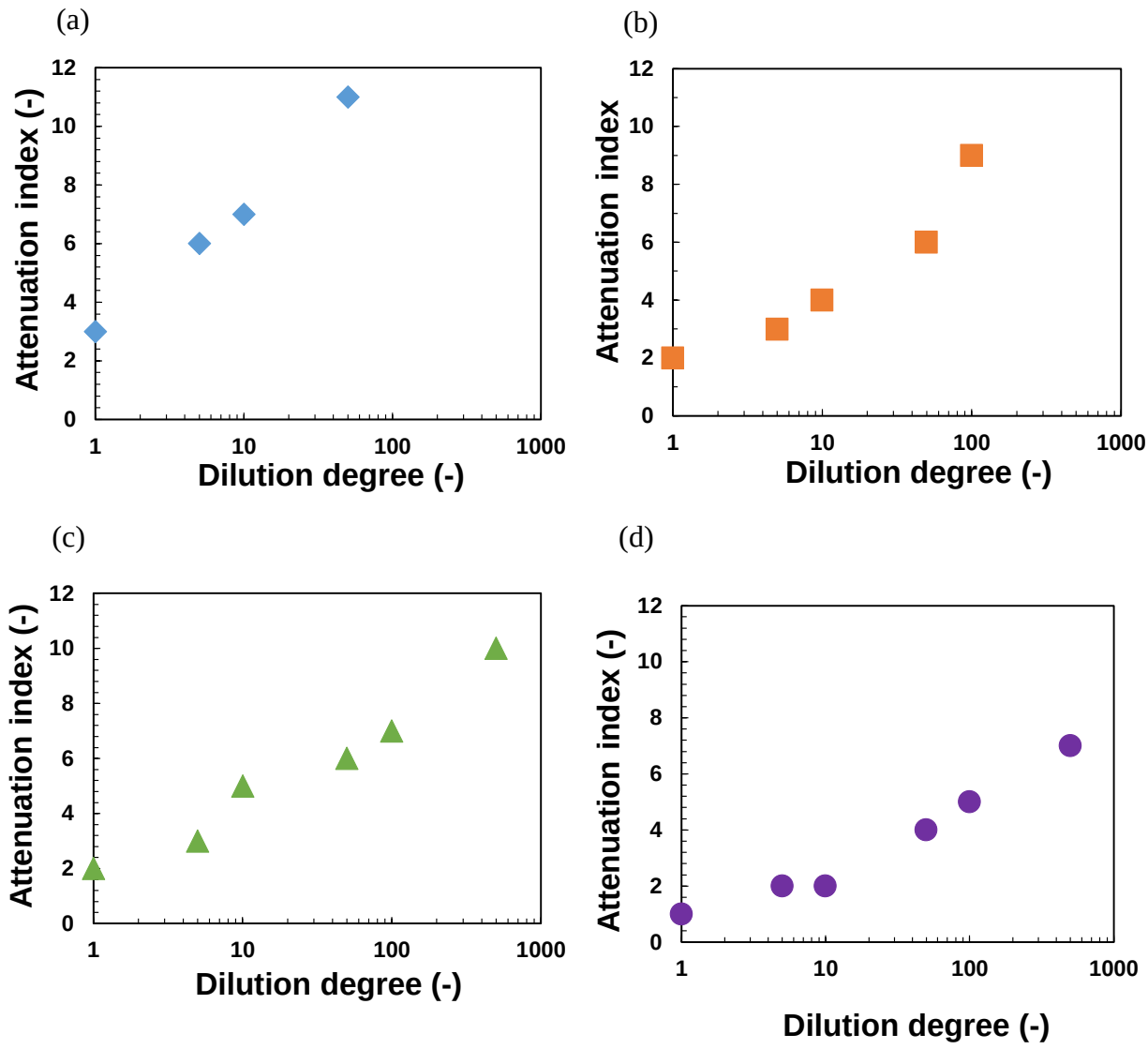

Fig.2.4. Attenuation index of each dilution degree.
(a) : 1 wt% of dispersed phase system
(b) : 5 wt% of dispersed phase system
(c) : 10 wt% of dispersed phase system
(d) : 20 wt% of dispersed phase system

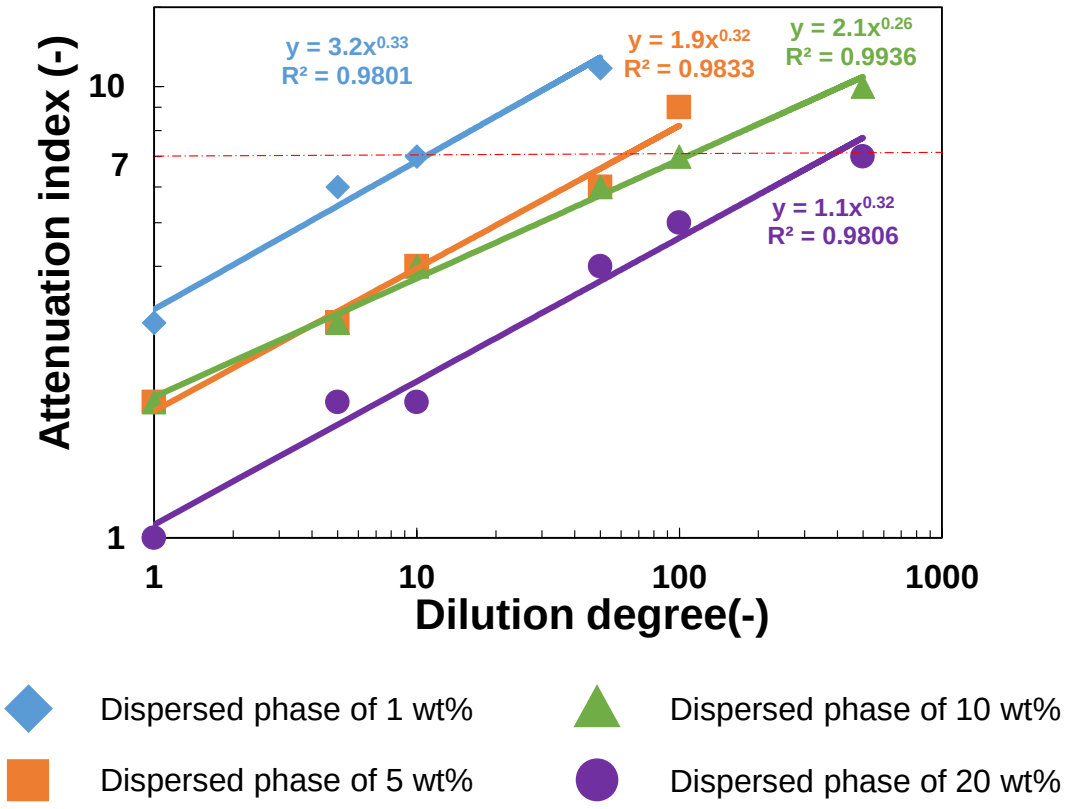

Fig.2.5. Correlation of attenuation index and dilution degree.

Table 2.4. Appropriate dilution degree each degree of dispersed phase and weight fraction of dispersed phase after dilution.

	Initial weight fraction of dispersed phase			
	1 wt%	5 wt%	10 wt%	20 wt%
Dilution ratio	10.7	60.7	106	324
Appropriate dilution ratio	10.0	62.2	137	300
Weight fraction of dispersed phase after dilution (wt%)	9.35×10^{-2}	8.23×10^{-2}	9.43×10^{-2}	6.17×10^{-2}

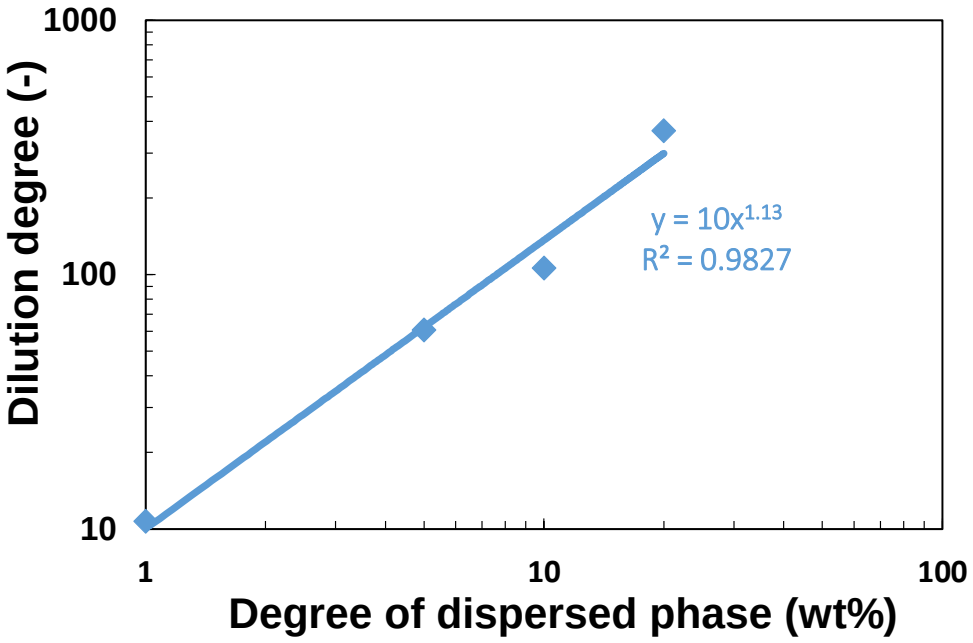

Fig. 2.6 : Correlation of weight fraction of dispersed phase and dilution degree from Table 2.4.

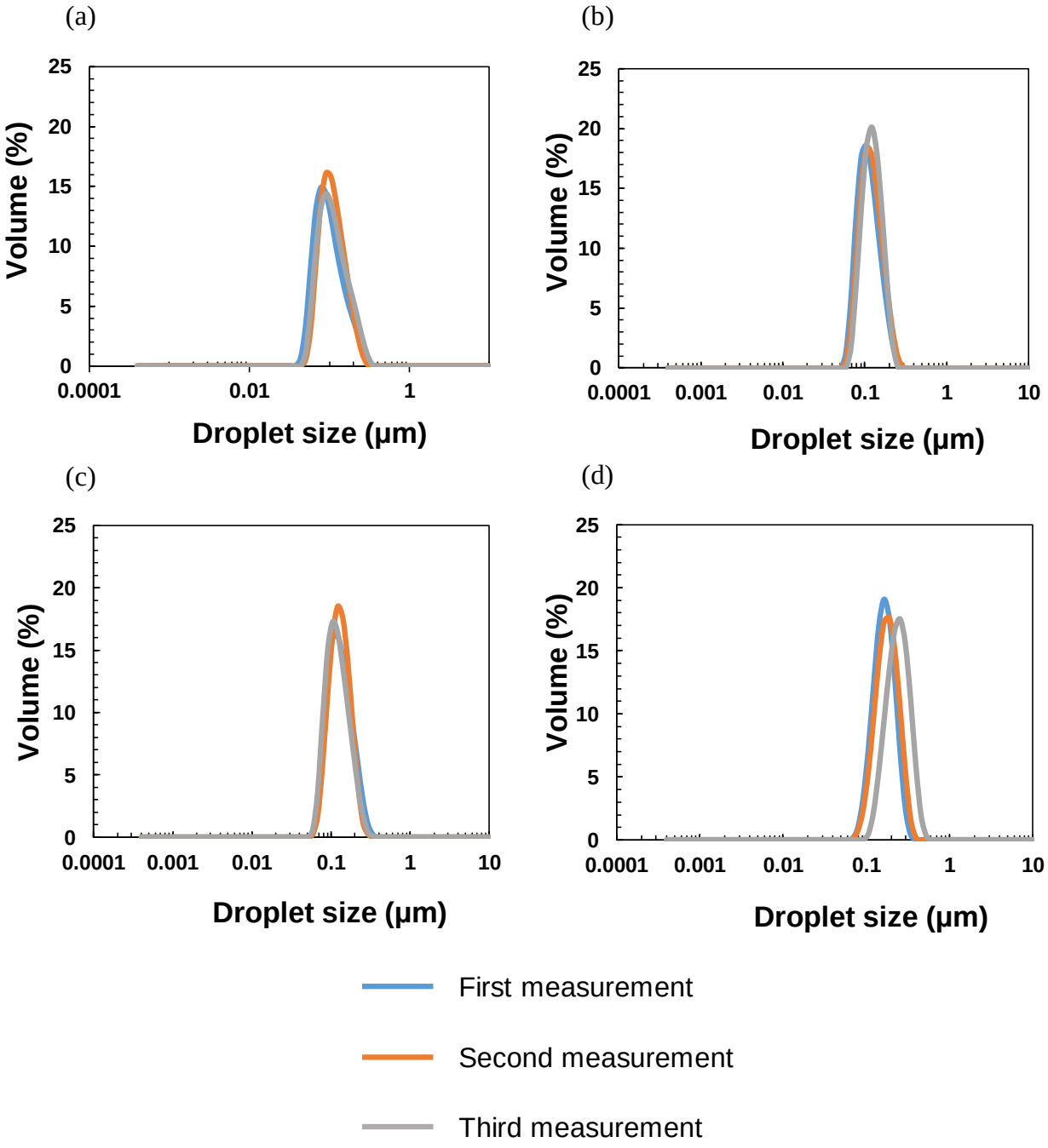

Fig.2.7 Droplet size distribution of model W/O emulsions with appropriate dilution degree.
(a) : 1 wt% of dispersed phase system
(b) : 5 wt% of dispersed phase system
(c) : 10 wt% of dispersed phase system
(d) : 20 wt% of dispersed phase system

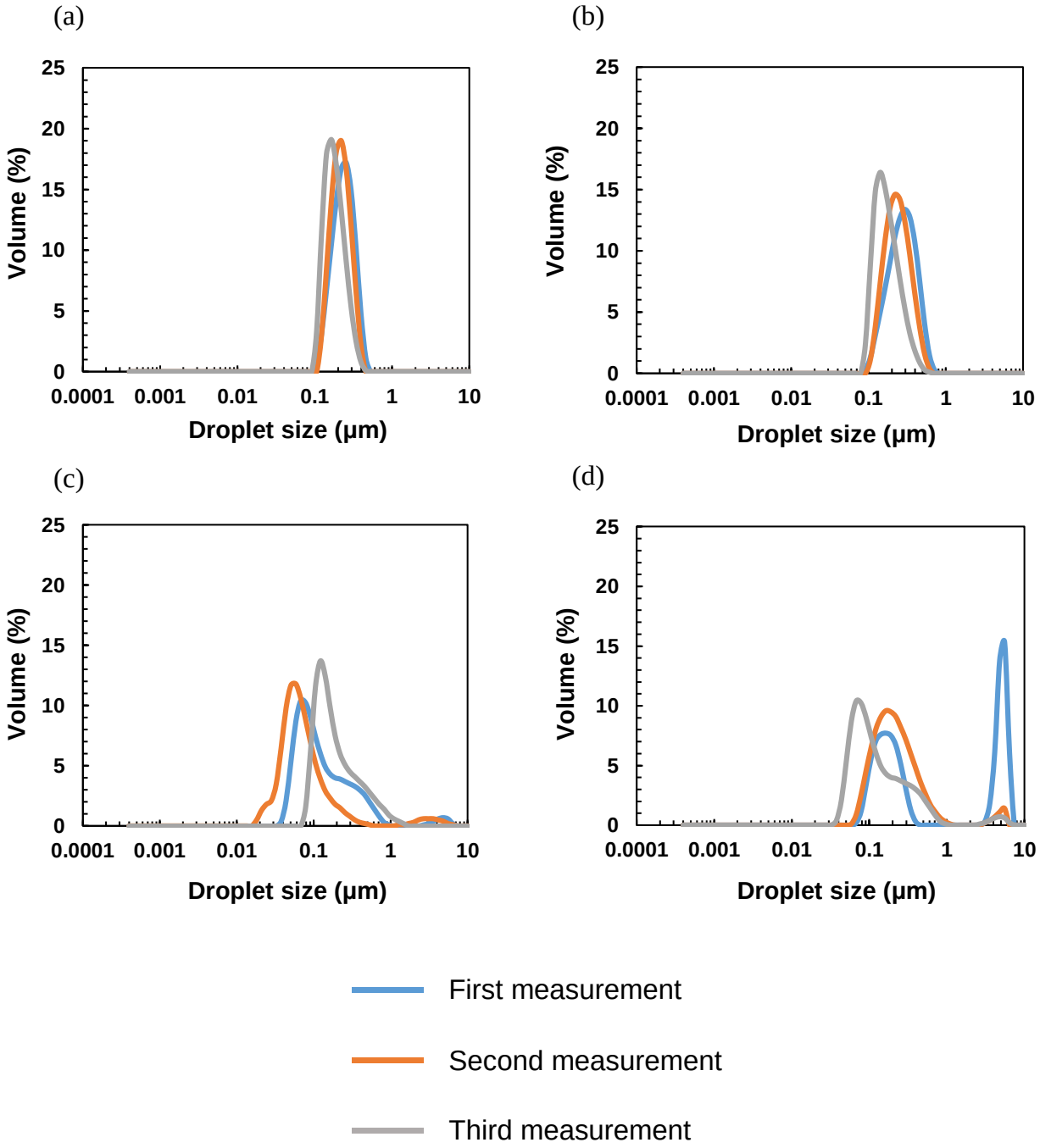

Fig.2.8. Droplet size distribution of model W/O emulsions using MCT as a continuous phase with out dilution.
(a) : 1 wt% of dispersed phase system
(b) : 5 wt% of dispersed phase system
(c) : 10 wt% of dispersed phase system
(d) : 20 wt% of dispersed phase system

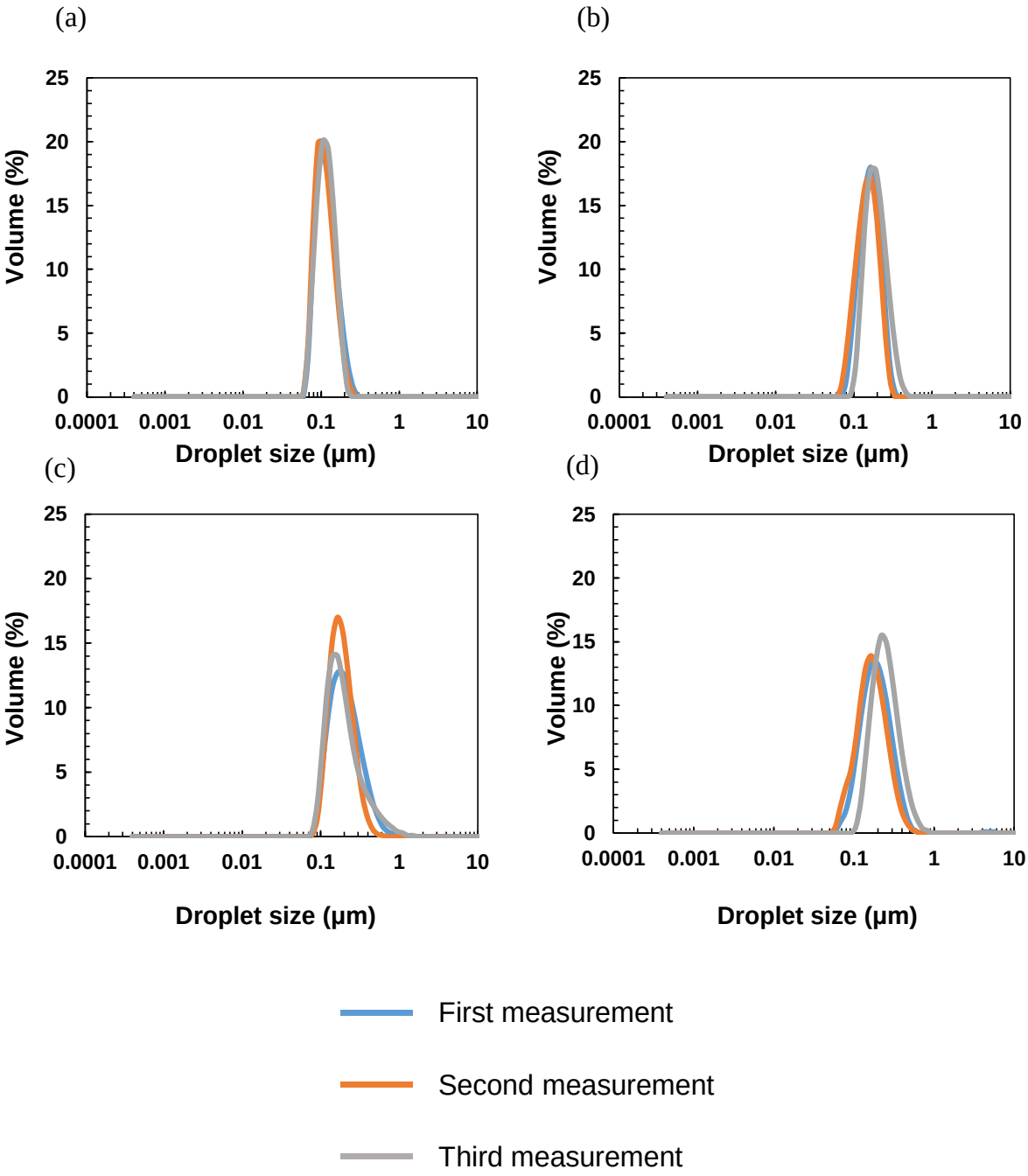

Fig.2.9. Droplet size distribution of model W/O emulsions using MCT as a continuous phase with appropriate dilution degree.
(a) : 1 wt% of dispersed phase system
(b) : 5 wt% of dispersed phase system
(c) : 10 wt% of dispersed phase system
(d) : 20 wt% of dispersed phase system

Chapter 3

Formulation and Characterization of Submicron W/F and W/O Emulsions Loaded with Short-chain Fatty Acid

3.1. Introduction

Short-chain fatty acids are important energy sources for the human body (Cummings *et al.*, 1995). The shortage of short-chain fatty acids at the large bowel lumen could cause constipation or diarrhea. Short-chain fatty acid s prevent colon carcinogenesis (Hamer *et al.*, 2008) and help maintain the colonic lumen environment (Greer & O'Keefe, 2011). Short-chain fatty acid s produced in the proximal colon are utilized as energy sources in the large bowel (Cummings *et al.*, 1995). 300 to 400 mmol/day of short-chain fatty acid s are produced by intestinal bacteria (Pituch *et al.*, 2013). Direct delivery of short-chain fatty acid s to the large bowel could improve the enteral environment. Li and co-workers formulated oil-in-water (O/W) emulsions loaded with tributyrin as the carrier of butyric acid (Li *et al.*, 2009). Tributyrin of hydrophobic nature has major characteristics that differ from those of hydrophilic short-chain fatty acid s.

An emulsion is a dispersion consisting of two immiscible phases (e.g., oil and water), with droplets dispersed into the other continuous phase. Food-grade emulsions with typical droplet sizes of 0.1 to 100 μm are generally produced using mechanical emulsification devices (McClements, 2004; Clausse *et al.*, 2005). These emulsions loaded with functional components have received much attention in the food industries (McClements & Li, 2010). Hydrophobic functional components can be encapsulated in O/W emulsions, while hydrophilic functional components can be encapsulated in water-in-oil (W/O) and water-in-oil-in-water (W/O/W) emulsions.

Emulsions containing emulsifiers/stabilizers are thermodynamically unstable systems, indicating their stability within a finite period of time. Emulsion stability is a dominant factor affecting important properties and quality of food-grade emulsions (McClements, 2004). Emulsions that do not contain emulsifiers/stabilizers tend to cause phase

separation quickly. Emulsion stability is also greatly influenced by the droplet size of emulsions. For instance, according to Stokes' law, the sedimentation velocity of W/O emulsions is proportional to the square of the droplet size. Sedimentation is quite suppressed in submicron W/O emulsions with droplets <1 μm; the use of a viscous continuous oil phase slows their creaming/sedimentation. Moreover, submicron emulsions usually have better stability against coalescence (Kobayashi *et al.*, 2005). Emulsion stability can be further improved using a solid fat as the continuous phase: the formulation of water-in-fat (W/F) emulsions.

This study sought to formulate submicron W/O and W/F emulsions as potential carriers of short-chain fatty acid s to the large bowel using a liquid oil and a solid fat as the continuous phase, and to evaluate their physical stability in terms of coalescence stability. Butyric acid was used as the model of short-chain fatty acid in this study.

3.2. Material and Methods

3.2.1. Materials

Butyric acid was purchased from Sigma-Aldrich Co. (St. Louis, USA). Chloroform, hexane, and refined soybean oil were purchased from Wako Pure Chemical Industries, Ltd. (Osaka, Japan). Palm stearin with a melting point of 54.2 ^{o}C was provided by ADEKA Co., Ltd. (Tokyo, Japan). Its major fatty acid components include palmitic acid (63.2%) and oleic acid (29.7%). Tetra glycerin condensation ricinoleate (TGCR, HLB<1) was provided by Sakamoto Yakuhin Kogyo Co., Ltd. (Osaka, Japan).

3.2.2. Measurement of Interfacial Tension and Calculation of Molecular Area

Interfacial tension between Milli-Q water and soybean oil containing TGCR was measured at 25 ºC using an interfacial tension meter (PD-W, Kyowa Interface Science Co., Ltd., Niiza, Japan) with a pendant drop method. The tip of the 22G stainless-steel needle connected to a 1 mL glass syringe filled with the inner water phase was dipped in the oil phase filled in a 24 × 24 × 30 -mm glass cube cell. Interfacial tension was calculated based on the shape of droplets, each expanding from the needle tip.

The molecular area of TGCR can be obtained from equation

$$A = \frac{10^{16}}{N_A \Gamma} \tag{3-1}$$

where A is molecular area, N_A is Avogadro's number and, Γ_e is the absorption at the saturated interface expressed in mol/cm^2, Γ_e can be calculated according the Gibbs equation

$$\Gamma_e = \frac{-(d\gamma/d\log C)}{2.303RT} \tag{3-2}$$

where (dγ/dlogC) is the slope of linear portion of the graph before the critical micelle concentration. (Lucas, 2010)

3.2.3. Preparation of W/F and W/O emulsions Loaded with Short-chain Fatty Acid

A palm stearin solution (70 ºC) containing 5 wt% TGCR was used as the continuous phase of the W/F emulsion. A soybean oil solution containing 5 wt% TGCR was used as the continuous phase of the W/O emulsion. A water solution containing butyric acid as the dispersed phase of the W/F or W/O emulsion was prepared by dissolving 5 wt% butyric acid in Milli-Q water. The W/F and W/O emulsions were prepared by dispersing a dispersed phase (1, 5, 10, or 20 wt%) into a continuous phase (99, 95, 90, or 80 wt%)

by rotor-stator homogenization (Polytron PT-3100, Kinematica Co., Ltd., Luzern, Switzerland) at 10000 rpm for 5 min, followed by high-pressure homogenization (NanoVater200, Yoshida Kikai Co., Ltd., Nagoya, Japan) at 100 MPa for one pass. The W/F emulsions were prepared at room temperature (25 ^{o}C), and the W/O emulsions were prepared at 70 ^{o}C.

3.2.4. Droplet Size Measurement of W/F and W/O Emulsions

An organic solution for diluting the W/F or W/O emulsion was initially prepared by mixing 40 vol% chloroform and 60 vol% hexane. 200 mL of this organic solution was then saturated with 50 mL Milli-Q water while stirring for 30 min, to prevent elution of the aqueous droplets into the water-saturated organic solution. This water-saturated organic solution was separated from the excess Milli-Q water by centrifugation (HP-25, Beckman Coulter, Inc., Brea, USA) at 1000 rpm for 30 min.

The droplet size distribution of the resulting W/F and W/O emulsions was measured using dynamic light scattering (DLS) (ZetasizerNano ZS, Malvern Co., Ltd., Worcestershire, UK). The W/F and W/O emulsions were diluted 60 times using water-saturated organic solution. Average droplet size was expressed as the Sauter mean diameter ($d_{3,2}$) defined as

$$d_{3,2} = \frac{\sum n_i d_i^{\,3}}{\sum n_i d_i^{\,2}} \tag{3-3}$$

where d_i is droplet diameter and n_i is number of droplets. Here, $d_{3,2}$ was manually calculated based on the obtained droplet size data. The $d_{3,2}$ was calculated from the droplets number and droplets diameter, using number droplet distribution obtained from the dynamic light scattering.

3.2.5. Physical Stability of W/F and W/O Emulsions

The resulting W/F and W/O emulsions were stored for four weeks at 25 °C. The droplet size of these emulsion samples was measured every week. W/F emulsions were melted at 70 °C before droplet size measurement. For storage evaluation, four W/F emulsion samples were prepared, since each emulsion sample was used for the droplet size measurement only at a specific week.

W/F emulsions were also subjected to a maximum of four melting-solidification cycles. Their average droplet size and droplet size distribution were measured after each melting-solidification cycle. All measurement was performed within two days.

3.3. Results and Discussion

3.3.1. Interfacial Tension Between Milli-Q Water and Soybean Oil Containing TGCR

Figure. 3.1a shows interfacial tension between Milli-Q water and soybean oil contining TGCR. Interfacial tension suddenly decreased by around 1 wt% of TGCR concentration, Afterwards, it gentry decreased. As a result, the critical micellar concentration of the TGCR was 1 wt%.

The approximate curve between interfacial tension and Ln TGCR concentration is showed by Fig. 3.1b. The approximate curve equation was

$$y = -4.049x - 5.7655 \quad (3\text{-}4)$$

The coefficient of determination of approximate curve (R^2) is 0.9518, and it showed the value that was almost 1. From approximate curve equation, $d\gamma/d\ln C$ is -4.049, and the surface excess concentration (Γ_e) was 7.1×10^{-7} mol/m^2. The molecular area of

TGCR was 233.9 $Å^2$. About the validity of the molecular area of TGCR, Souilem calculated the molecular occupation area of oleuropein (Souilem, 2014). Molecular weight of oleuropein is 540.5 g/mol, and molecular area is 240 $Å^2$. Oleuropein has the molecular weight that is near to TGCR, TGCR may have a molecular area that is near to oleuropein。

3.3.2. Droplet Size Distribution and Average Droplet Size of W/F and W/O Emulsions

All the freshly prepared W/F emulsions lost their fluidity after cooling to room temperature. Figure. 3.2a indicates the droplet size distribution of the freshly prepared W/F emulsions at different weight fractions of the dispersed phase (W_d) of 1 to 20 wt%. The W/F emulsion at the lowest W_d (1 wt%) had a monomodal droplet size distribution with a narrow peak at 0.4 μm. The W/F emulsion at a W_d of 5 wt% also had a narrow primary peak between 0.4 and 0.5 μm but had a small second peak at 5 μm. The aqueous droplets in these W/F emulsions were on a submicron scale, except for those of the second peak at a W_d of 5 wt%. The W/F emulsions at a high W_d (10 and 20 wt%) had broad droplet size distributions; many of the resulting droplets were larger than 1 μm. Fig. 2.2b presents the droplet size distribution of the freshly prepared W/O emulsions. Monomodal, narrow droplet size distributions were observed for the W/O emulsions at a W_d of 1 and 5 wt%. The aqueous droplets in these W/O emulsions were smaller than 1μm. The W/O emulsions at a W_d of 10 and 20 wt% had a narrow main peak that shifted to the larger side and a second peak at 5 μm. It is noteworthy that no phase separation was observed in any of the freshly prepared W/F and W/O emulsions. As indicated in Fig. 3.1c, the $d_{3,2}$ of the freshly prepared emulsions increased with increasing W_d for W/F

and W/O emulsions. Their $d_{3,2}$ values were smaller than 0.5 μm at a W_d of 1 to 10 wt%, while the aqueous droplets larger than 1 μm which cannot be negligible at a W_d of 10 wt% (Fig. 3.2a).

The results presented in Fig.3.2 indicate that the use of high-pressure homogenization formulated submicron W/F and W/O emulsions loaded with short-chain fatty acid at a W_d of 1 and 5 wt%. In contrast, the W/F emulsions at a W_d of 10 and 20 wt% had broad droplet size distributions (Fig. 3.2a), which can be explained as follows. As one of the hypotheses, TGCR was short for total surface area of the emulsion droplets. In this study, W/F emulsions were prepared in high temperature, it is suggested that interfacial tension and viscosity are lower than W/O emulsion systems. Therefore, the droplets which was smaller than W/O emulsion was made. In this case, Unlike W_d of 1 and 5 wt%, there becomes a great deal of number of droplets in W_d of 10 and 20 wt%, and TGCR was short for total surface area of the emulsion droplets. Therefore, the coalescence of the droplets occurred just after preparation. The molecular area of TGCR was 233.9 $Å^2$. Except CMC, the area of the molecules which can adhere to the droplet interface is 3.97×10^{17} $Å^2$ (3.97×10^2 m^2). On the other hand, when diameter of droplets is defined 0.4 μm, total surface area of W_d of 10 wt% is around 70 m^2. Accordingly, TGCR was quantity enough, this hypothesis should be rejected.

As other factors of coalescence of the droplets occurred, W/F emulsion should be polydispersion than W/O emulsion systems, because there are small droplets by decrease of the interfacial tension by the high temperature. In general, as for the emulsion droplets, union is easy to occur in high temperature and polydispersion condition (Saito *et al.*, 2006). This tendency occurred conspicuously in W_d of 10 and 20 wt%, We assume that the broad droplet size distributions were obtained because of the balance

between droplet formation and coalescence.

3.3.3. Storage Stability of W/F and W/O Emulsions

Figure 3.3 indicates the variation of the droplet size distributions of W/F and W/O emulsions prepared at W_d of 1 and 5 wt% during four weeks of storage. At W_d of 1 wt%, their monomodal, narrow droplet size distribution remained after four weeks of storage (Figs. 3.3a,i and 3.3b,i). The W/F emulsion prepared at W_d of 5 wt% maintained the primary peak, while the secondary peak gradually became higher (Fig. 3.3a,ii). Palm stearin consists mainly of tripalmitin (Tsung, 2002); thus, the droplets dispersed in the W/F emulsion did not move freely and coalesce. In contrast, the primary peak for the W/O emulsion prepared at W_d of 5 wt% shifted toward the larger side during storage (Fig. 3.3b,ii). Figure 3 indicates the variation of $d_{3,2}$ of the W/F and W/O emulsions prepared at W_d of 1 and 5 wt% during storage. The $d_{3,2}$ for W/F emulsions was almost constant after four weeks, regardless of W_d. The $d_{3,2}$ for W/O emulsion increased slightly at W_d of 1 wt% but increased remarkably even after 1 week. It should be noted that a steep increase and/or phase separation was observed for the W/F and W/O emulsions prepared at high W_d of 10 and 20 wt% during four weeks of storage, strongly indicating that they were less stable.

A difference in variation of the $d_{3,2}$ of W/F and W/O emulsions was observed at W_d of 5 wt% (Fig. 3.4). The main difference between W/F and W/O emulsions was the phase condition of the continuous oil phase, due to the composition difference of fatty acid residues between palm stearin and soybean oil. The continuous phase in the W/F emulsions crystallized under storage conditions. Motion of the aqueous droplets was restricted in the continuous phase during storage, leading to unchanged $d_{3,2}$ values. The

continuous phase in the W/O emulsions maintained its liquid state under storage conditions. Aqueous droplets are capable of randomly moving and easily coming into contact with neighboring droplets, which may increase the frequency of coalescence and the $d_{3,2}$ data plotted in Fig. 3.4b.

3.3.4. Stability for the Phase Conversion of W/F and W/O Emulsions

Figure 3.5 illustrates the effect of the melting-solidification cycle on variation of the droplet size distribution and $d_{3,2}$ of the W/F emulsions prepared at W_d of 1 and 5 wt%. W/F emulsions at a W_d of 1wt% basically maintained their monomodal, narrow droplet size distribution and $d_{3,2}$ value after four melting-solidification cycles (Figs. 3.5a, c). For the W/F emulsions at W_d of 5 wt%, both primary and secondary peaks remained, and the $d_{3,2}$ value hardly varied during the four melting-solidification cycles (Figs. 3.5b, c). The $d_{3.2}$ of these W/F emulsions ranged from 0.35 to 0.45 μm during the four melting-solidification cycles. These results suggest high stability of W/F emulsions loaded with butyric acid against melting and solidification of the continuous phase. The W/F emulsions at W_d of 5 wt% had high stability against both storage and melting-solidification cycles.

3.4. Chapter Conclusion

In this study, submicron W/F and W/O emulsions loaded with short-chain fatty acids were stably prepared using high-pressure homogenization. Our results demonstrate that submicron W/F and W/O emulsions can be prepared at W_d up to 5 wt%. At W_d of 5 wt%, the W/F emulsions had higher storage stability than that of the W/O emulsions, due to the difference in the physical state of the continuous phase. Further investigations are needed

to clarify the performance of W/F emulsions loaded with short-chain fatty acids as carriers of short-chain fatty acids to the large intestine (e.g., release profile of short-chain fatty acids during storage and their *in vitro* digestibility).

(a)

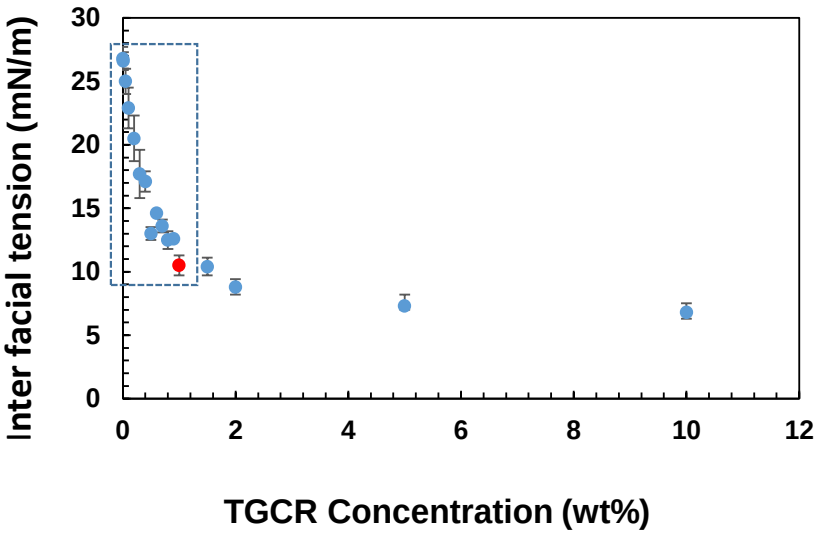

(b)

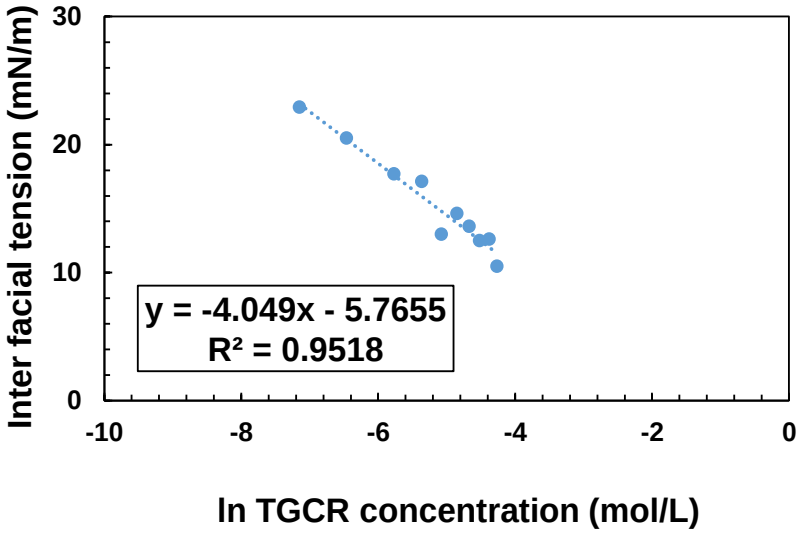

Fig.3.1. (a) Variations of interfacial tension between Milli-Q water and soybean oil containing TGCR . (b) The data plotted in the dashed rectangle.

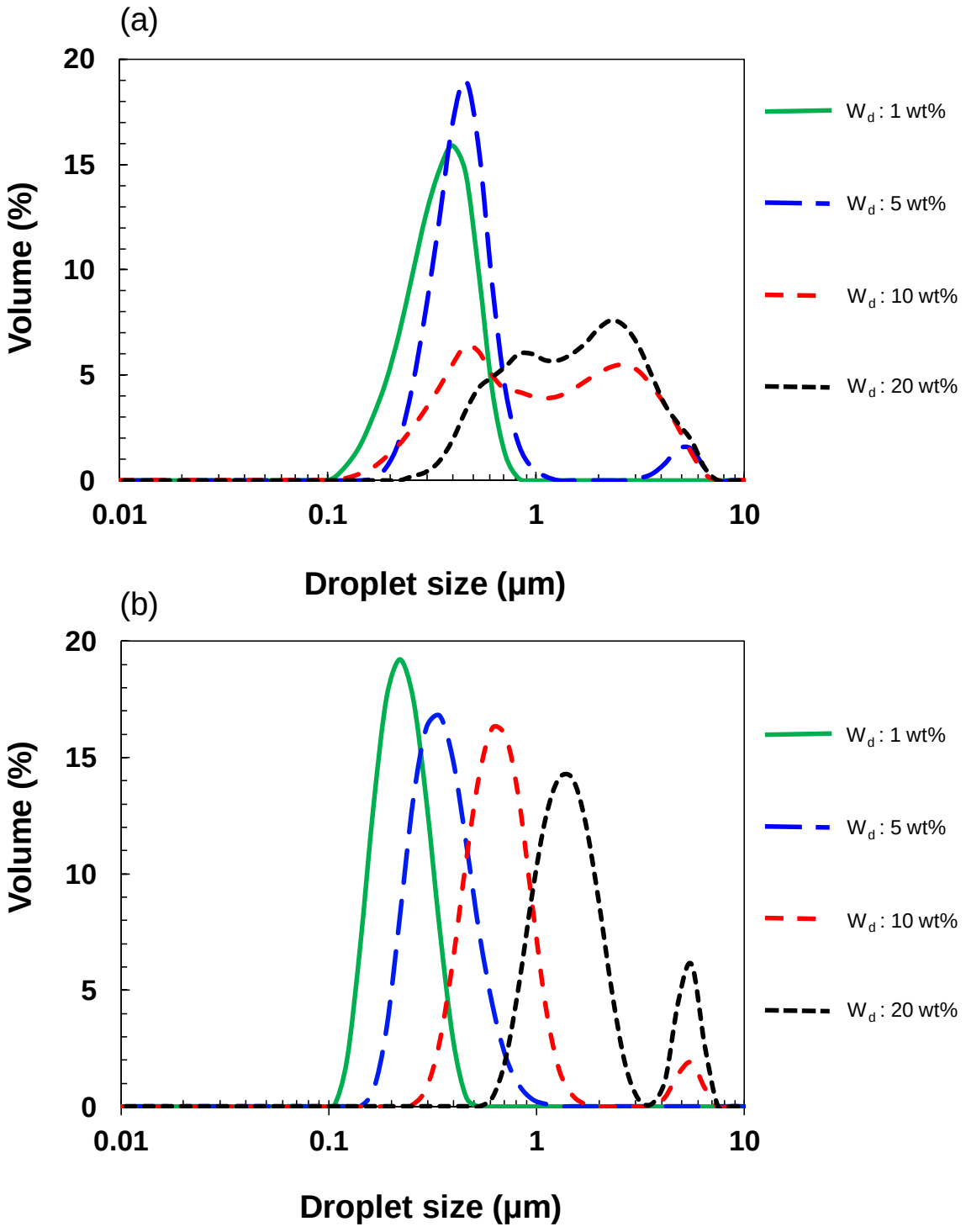

Fig.3.2. Droplet size distributions of (a) W/F emulsions and (b) W/O emulsions just after formulation. (c) Effect of weight fraction of the dispersed phase (W_d) of the Sauter mean diameter ($d_{3,2}$) on the resulting W/F and W/O emulsions.

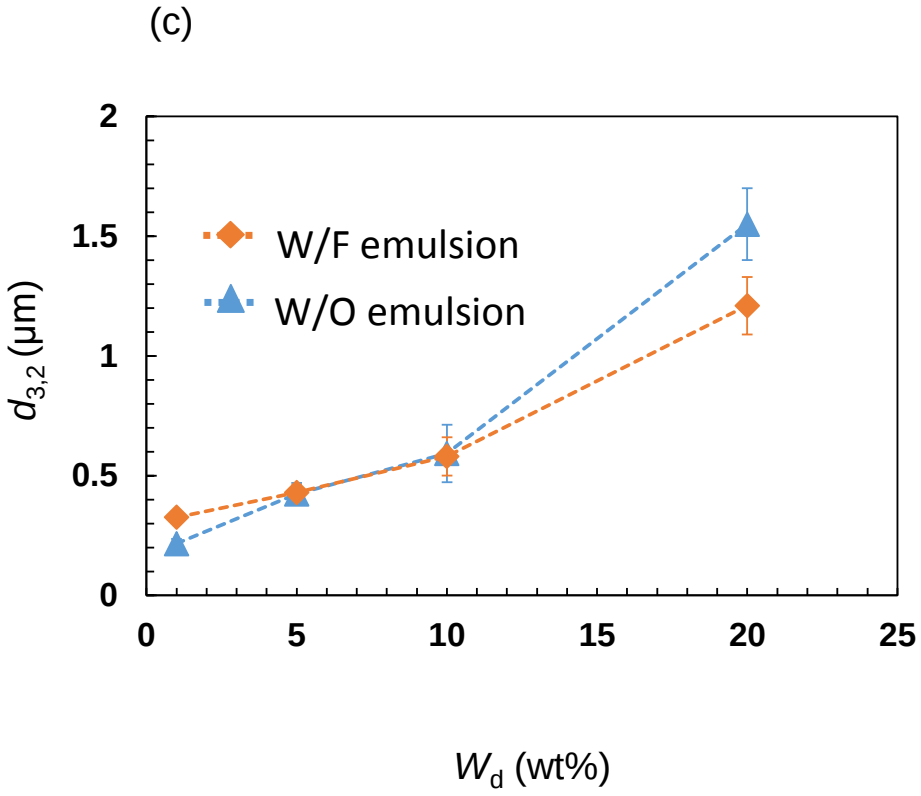

Fig.3.2. (continue) Droplet size distributions of (a) W/F emulsions and (b) W/O emulsions just after formulation. (c) Effect of weight fraction of the dispersed phase (W_d) of the Sauter mean diameter ($d_{3,2}$) on the resulting W/F and W/O emulsions.

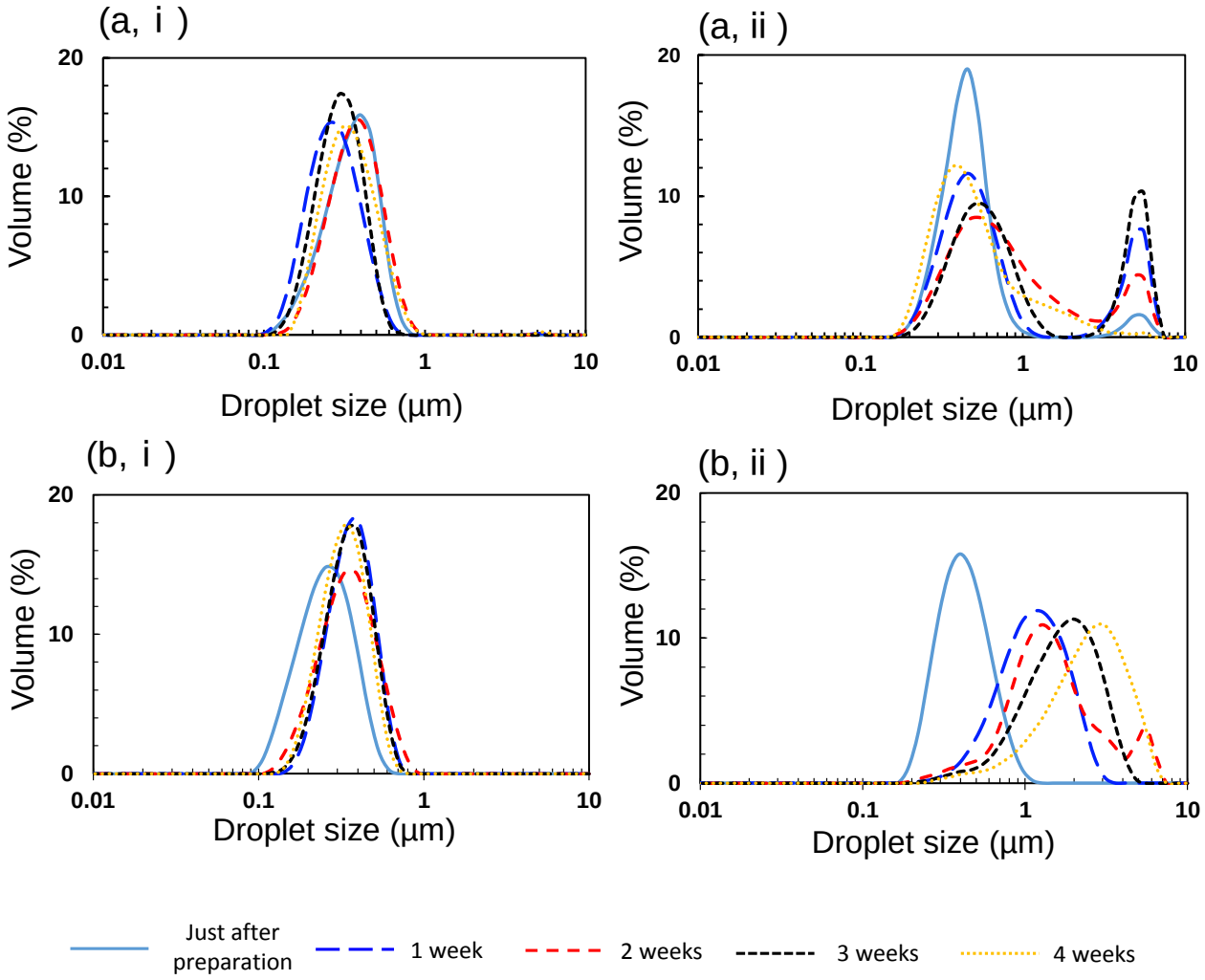

Fig.3.3. Time course of droplet size distributions of (a) W/F emulsions and (b) W/O emulsions. (i) W_d: 1wt%; (ii) W_d: 5wt%.

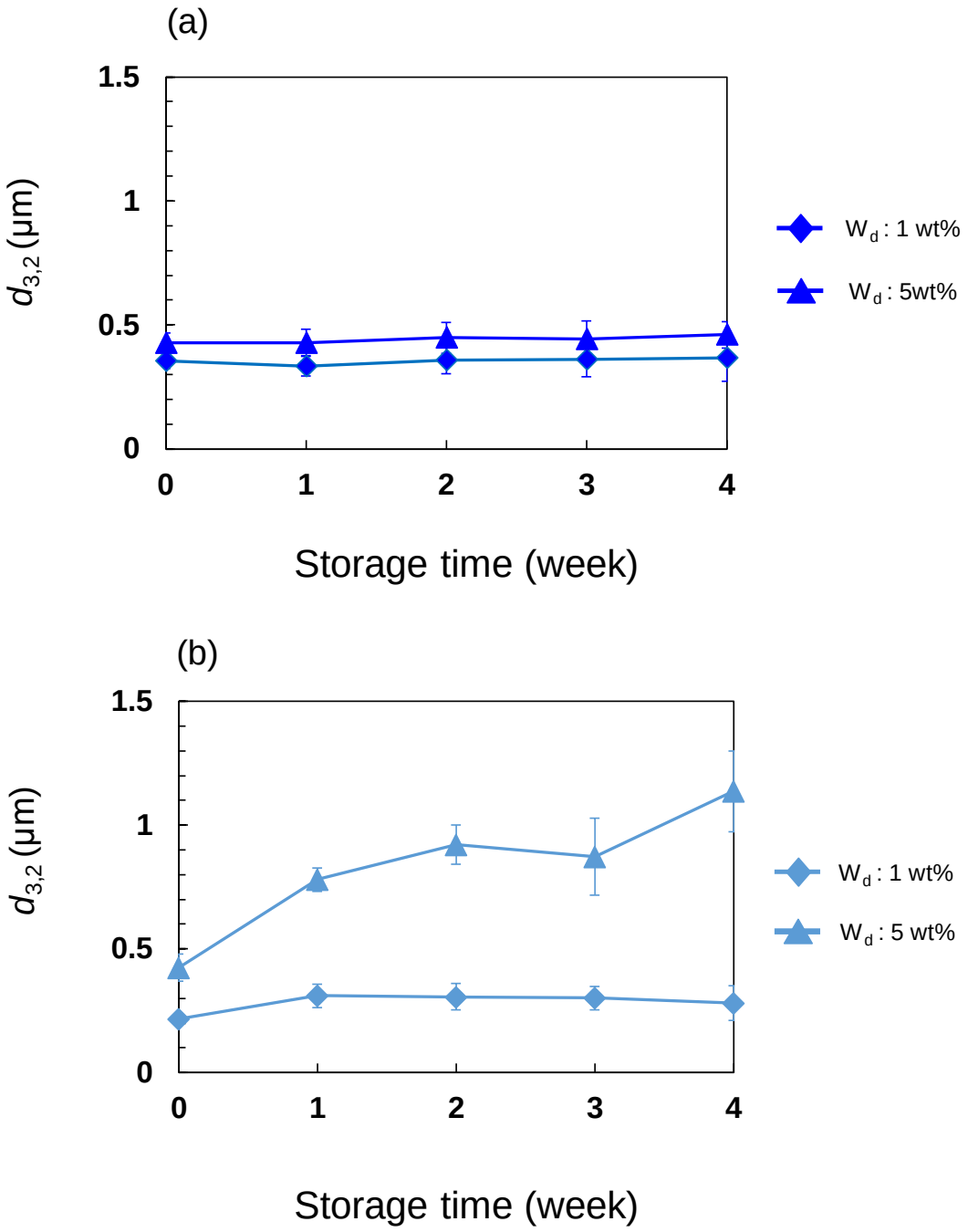

Fig.3.4. Time course of the Sauter mean diameter ($d_{3,2}$) of the resulting W/F (a) and W/O (b) emulsions.

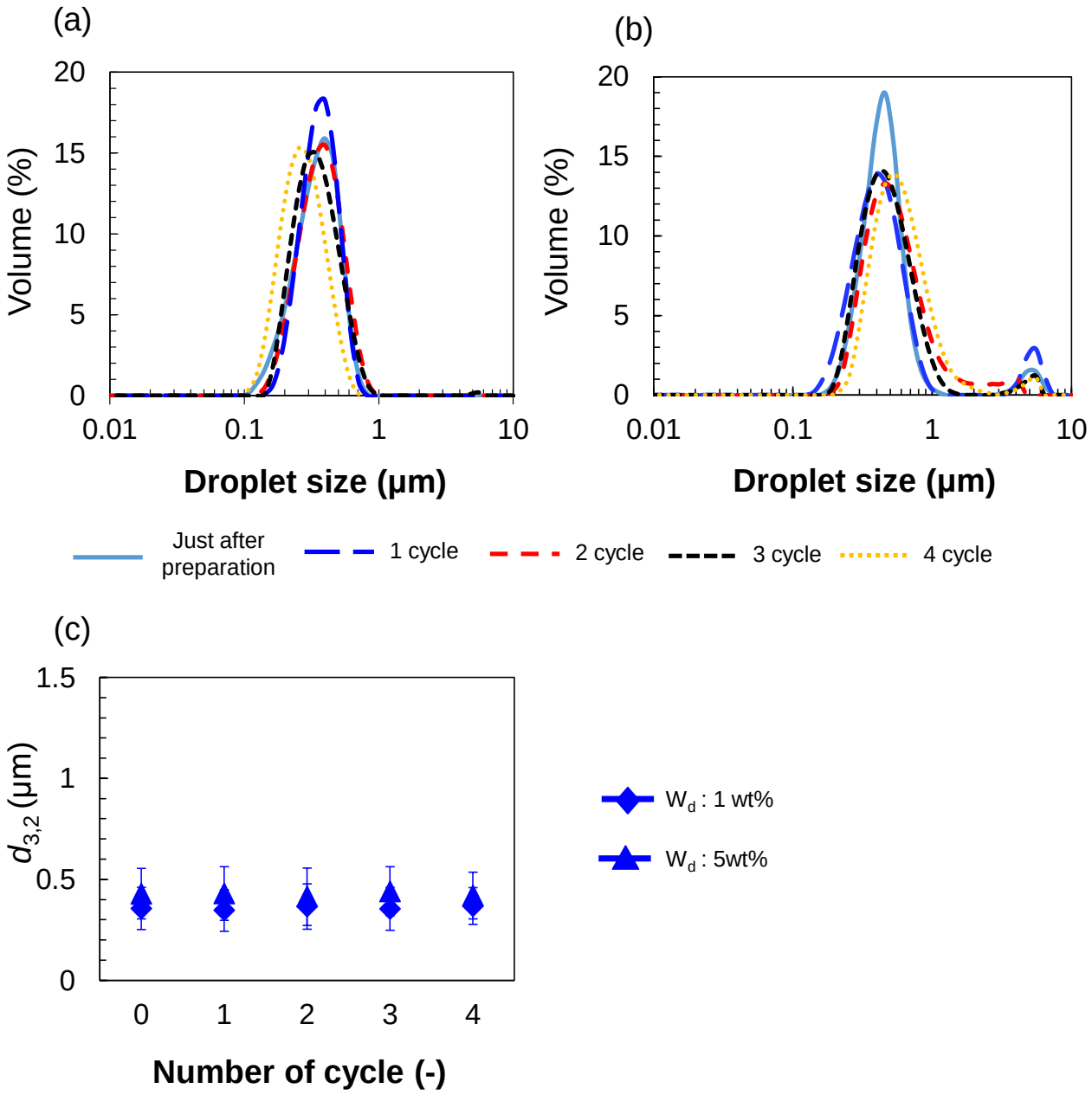

Fig.3.5. Variation of droplet size distributions of the resulting W/F emulsions at weight fraction of the dispersed phase (W_d) of (a) 1wt% and (b) 5wt% during melting-solidification cycles. (c) Effect of the number of the melting-solidification cycles on the Sauter mean diameter ($d_{3,2}$) of the resulting W/F emulsions.

Chapter 4

Formulation of W/O/W Emulsions Loaded with Short-chain Fatty Acid and Their Stability Improvement by Layer-by-Layer Deposition Using Dietary Fibers

4.1. Introduction

In general, emulsion is defined as the dispersion of two immiscible fluids (e.g., oil and water) into one another as small spherical particles. The droplet size of emulsions prepared using different techniques is generally 0.1 to 100 μm (McClements, 2004; Clausse *et al.*, 2005). A rotor-stator homogenizer is frequently used in food industries to prepare nonuniform droplets of 2 to 10 μm. A high-pressure homogenizer can produce droplets having a monomodal size distribution on a submicron scale (McClements, 2004). Emulsions are a thermodynamically unstable but semi-stable systems (Okazawa & Bron, 1979). If an emulsion does not contain an emulsifier and a stabilizer, phases eventually separate. An emulsifier and a stabilizer are required to improve emulsion stability, which is greatly influenced by the viscosity and density of liquid phase and ζ-potential of droplets. Viscosity and density also influence creaming/sedimentation of the droplets, which can be expressed by Stokes' law. Droplets with high absoluteζ-potential are capable of preventing aggregation, due to electrostatic repulsion.

There is a wide variety of food emulsions. Oil-in-water (O/W) food emulsions include mayonnaise, dressing, milk, and soups. Water-in-oil (W/O) food emulsions include butter, margarine, and chocolates. Multiple emulsions, known as “emulsions of emulsions,” may be water-in-oil-in-water (W/O/W) emulsions consisting of oil droplets containing smaller droplets of an inner water phase dispersed in water phase (Aserin, 2007). Emulsions containing functional ingredients have received a great deal of attention in food industries (McClements & Li, 2010). Hydrophilic functional ingredients can be encapsulated in W/O emulsions, and hydrophobic functional ingredients can be encapsulated in O/W emulsions. W/O/W emulsions can load both

hydrophilic and hydrophobic functional ingredients (Aserin, 2007; Trentin *et al.*, 2011; Kanafusa *et al.*, 2007; Farahmand *et al.*, 2006; Lee *et al.*, 2004; Nauman *et al.*, 2013; and Nauman *et al.*, 2014).

Short-chain fatty acids are water-soluble fatty acids with a carbon number lower than 6. short-chain fatty acid is an important energy source for intestinal epithelial cells. For example, butyric acid represents a major energy supply for the large intestine. short-chain fatty acid prevent colon carcinogenesis (Hamer, Jonkers, Venema, Vanhoutvin, Troost & Brummer, 2008) and help maintain the colonic environment (Greer & O'Keefe, 2011). Large intestine utilizes short-chain fatty acid that were produced in proximal colon as its energy source (Cummings *et al.*, 1995). Several foods and supplements are rich in enteric bacteria and dietary fiber. However, the enteral environment influences the type and quantity of short-chain fatty acid (Cummings *et al.*, 1995). Therefore, delivering short-chain fatty acid directly to the large intestine effectively improves the enteral environment. Short-chain fatty acid have an unpleasant smell, so that endeavoring their oral intake. To solve this problem, Li and co-workers obtained O/W emulsion loaded with tributyrin as the carrier of butyric acid (Li *et al.*, 2009). Tributyrin is lipophilic and has major characteristics different from those of short-chain fatty acid. Since short-chain fatty acid are water-soluble, the solution containing short-chain fatty acid should be used as the inner water phase of W/O or W/O/W emulsion. W/O/W emulsion is a potential carrier of short-chain fatty acid to the large intestine, whereas the oil phase of W/O/W emulsion is digested by lipase in the stomach and small intestine (McClements, & Li, 2010). Short-chain fatty acid absorbed in the small intestine cannot reach the large intestine. Therefore, it is necessary to improve stability of these W/O/W emulsions in the gastrointestinal tract. Dietary fibers are normally not digested in the

gastrointestinal tract, since they are decomposed by enteric bacteria (Cummings, *et al.*, 1995).

Layer-by-layer deposition is one method of multicoating using electrostatic polymers to the object (Richardson, Bjornmalm, & Crauso, 2015). Dietary fibers that have electrical charge such as chitosan (CHI) and carboxymethyl cellulose (CMC) can be used for layer-by-layer deposition. W/O/W emulsion coated with dietary fiber may increase the physical stability and reach the large intestine without being digested. Layer-by-layer deposition has been applied to only O/W emulsions thus far (Bortnowska, 2015; Iwata *et al.*, 2014).

The purposes of this study are to formulate W/O/W emulsions coated with dietary fibers using layer-by-layer deposition as a potential carrier of short-chain fatty acid to the large intestine and to evaluate their physical stability in terms of coalescence stability of W/O/W emulsion droplets. Butyric acid was selected as the model short-chain fatty acid in this study.

4.2. Material and Methods

4.2.1. Materials

Modified lecithin (SLP WhiteLyso) was provided by Tsuji Oil Mills Co., Ltd. (Matsuzaka, Japan) as the emulsifier of W/O/W emulsion. The modified lecithin consists of phosphorus lipid content of consists of lysophosphatidylcholine (18-30%), phosphatidylinositol (10-20%), phosphatidylcholine (2-8%), phosphatidylethanolamine (1-7%) and phosphatidic acid (0-5%). Figure 4.2 shows chemical structure and composition of modified lecithin. In this study, molecular weight of modified lecithin was defined as molecular weight of lysophosphatidylcholine.

CHI (CHI HD; molecular weight 58 kDa; degree of deacetylation of 98%), was provided by Yaegaki Bio-industry, Inc. (Himeji, Japan). CMC was provided by Wako Pure Chemical Industries, Ltd. CHI and CMC were used as the dietary fibers for layer-by-layer deposition. Acetic acid, sodium acetate, hydrochloric acid (1 mol/L), chloroform, hexane, and sodium hydroxide (1 mol/L) were purchased from Wako Pure Chemical Industries, Ltd. Fluorescein isothiocyanate (FITC) was provided by Sigma-Aldrich Co.

4.2.2. Preparation of W/O/W Emulsions Loaded with Short-chain Fatty Acid

4.2.2.1. Solution Preparation

Modified lecithin solution was prepared as the outer water phase of W/O/W emulsion by dissolving 0.5 wt% modified lecithin in Milli-Q water. An acetate buffer solution (pH5) was prepared by solubilizing sodium acetate into acetic acid (30 mmol/L) used for diluting W/O/W emulsion samples.

4.2.2.2. Measurement of Interfacial Tension and Calculation of Molecular Area

Interfacial tension between modified lecithin solution and soybean oil was measured at 25 ^{o}C using an interfacial tension meter (PD-W, Kyowa Interface Science Co., Ltd., Niiza, Japan) with a pendant drop method. The tip of the 22G stainless-steel needle connected to a 1 mL glass syringe filled with the inner water phase was dipped in the oil phase filled in a 24×24×30-mm glass cube cell. Interfacial tension was calculated based on the shape of droplets, each expanding from the needle tip.

Calculate of molecular area of modified lecithin was performed in a procedure like chapter 3 and molecular weight of lysophosphatidylcholine was used for calculate of

molecular area as molecular weight of modified lecithin.

4.2.2.3. Preparation of W/O/W Emulsions Loaded with Short-chain Fatty Acid

The W/O/W emulsion was prepared by dispersing a 20 wt% of W/O emulsion (5 wt% of water phase containing 5 wt% butyric acid, 95 wt% of soybean oil containing 5 wt% TGCR, W/O emulsion was described in detail in Chapter 3) into an outer phase (80 wt%) that is an aqueous solution containing 0.5 wt% modified lecithin by using rotor-stator homogenization at 5000 rpm for 5 min. The pH of the W/O/W emulsion was adding 200 mL of an acetate buffer solution in 50 mL of this emulsion sample. This emulsion was defined as primary W/O/W emulsion. Figure 4.3 presents method of preparing W/O/W emulsion.

4.2.3. Coating of W/O/W Emulsions Droplets by Layer-by-Layer Deposition Using Dietary Fibers

4.2.3.1. Solution Preparation

An aqueous phase containing CHI was prepared by dissolving 1 wt% mixture of CHI powder (90 wt% pure-CHI powder and 10 wt% FITC-labeled CHI powder (Huang *et al.*, 2002)) in Milli-Q water. Hydrochloric acid (1 mol/L) was added to dissolve the CHI powder in this aqueous phase at pH 2. Afterwards, sodium hydroxide (1 mol/L) was added to adjust the pH of the CHI-containing solution to 5. The ionic strength of the CHI-containing solution (pH 5) is 1.0×10^{-5} mol/L, and that of the W/O/W emulsion mixed with CHI-containing solution is 2.9×10^{-6} mol/L. These ionic strength values may not affect the properties of the W/O/W emulsion coated with CHI. The CMC was prepared by dissolving ca. 1 wt% CMC powder in the acetate buffer solution.

4.2.3.2. Coating of W/O/W Emulsions Droplets Using Layer-by-Layer Deposition

Figure 4.4 shows method of Layer-by-layer deposition to W/O/w emulsion loaded with short-chain fatty acids.

First, 40 mL of primary W/O/W emulsion were added to 16 mL CHI solution while stirring. After 2 h, the surfaces of the W/O/W emulsion droplets of primary W/O/W emulsion were coated with CHI using electrostatic interaction between modified lecithin and CHI. The remaining CHI was then reduced by removing 30 mL of outer water phase and adding 30 mL of acetate buffer solution. This treatment was repeated three times. Next, 56 mL of the W/O/W emulsion coated with CHI was added to 4 mL of the CMC-containing solution. W/O/W emulsion coated with CHI and CMC was prepared based on previous literature (Iwata *et al.*, 2014). The procedures similar to prepare the W/O/W emulsions coated by CHI and CHI-CMC were applied to prepare those coated by CHI-CMC-CHI and CHI-CMC-CHI-CMC.

4.2.4. Characterization of W/O/W Emulsions

4.2.4.1. Determination of Average Droplet Size and Droplet Size Distribution

The droplet size distribution of W/O/W emulsions was measured using a laser diffraction particle size analyzer (LS13 320, Beckman Coulter, Inc., USA). About 1 mL of the W/O/W emulsion sample was added drop by drop to the circulation chamber initially filled with 125 mL of water.

4.2.4.2. ζ -potential Analysis

The ζ-potential of W/O/W emulsion droplets was measured using microscope electrophoresis (Zeecom, Microtec Co., Ltd., Funabashi, Japan) at a voltage of +20 mV.

W/O/W emulsion droplets move from left to right or vice versa, depending on their surface charge. The velocity and direction of 200 droplets movement were automatically measured to determine ζ-potential.

4.2.4.3. Microscopic Observation

Images of W/O/W emulsion droplets were taken using optical and fluorescence microscope with an optical microscope (DM IRM, Leica Microsystems, Wetzler, Germany). We used a fluorescence filter cube (N3), an excitation filter (BP546/12), a dichroic mirror (RKP565), and an adsorption filter (BP600/40) to filter the light generated by a mercury lamp. The wavelength of the light filtered was 546 nm. A W/O/W emulsion sample was gently shaken prior to its microscopic observation. A drop of this sample was placed on a slide glass and covered with a cover slip. W/O/W emulsion droplets coated with FITC-labeled CHI could be observed as green color circles in the fluorescence field.

4.2.5. Storage Stability of W/O/W Emulsions Coated by Layer-by-Layer Deposition

The physical stability of W/O/W emulsions was evaluated by changes of $d_{3,2}$ and RSF of resultant W/O/W emulsion droplets. W/O/W emulsions were kept for 4 weeks at 25 ^{o}C. Droplet size was measured every 2 weeks. Primary W/O/W emulsion and W/O/W emulsion coated with CMC as the outer layer were used as W/O/W emulsion samples.

4.3. Results and Discussion

4.3.1. Interfacial Tension Between Modified Lecithin Solution and Soybean Oil

Figure 4.5a shows interfacial tension between modified lecithin solution and soybean oil. Interfacial tension suddenly decreased by 0.065 wt% of modified lecithin concentration, Afterwards, it gentry decreased. As a result, the critical micellar concentration of the modified lecithin was 0.065 wt%. In this study, weight fraction of modified lecithin in the outer water phase is 0.5 wt%, it is enough to prepare W/O/W emulsion.

The approximate curve between interfacial tension and Ln modified lecithin concentration is showed by Fig. 4.5b. The approximate curve equation was

$$y = -18.082x - 109.35 \quad (4\text{-}1)$$

The coefficient of determination of approximate curve (R^2) is 0.9643, and it showed the value that was almost 1. From approximate curve equation, d γ /dlnC is -18.08, and the surface excess concentration (Γe) was 3.17×10^{-6} mol/m^2. The molecular area of modified lecithin was 52.4 Å^2. The molecular area of modified lecithin was smaller than TGCR (233.9 Å^2), molecular of modified lecithin was able to adsorb to interface between water and soybean oil more thickly. Therefore decreasing of interfacial tension of modified lecithin is more suddenly than TGCR.

4.3.2 Characterization of Primary W/O/W Emulsions

Figure 4.6a is an optical micrograph of the primary W/O/W emulsion containing submicron droplets of the inner water phase dispersed in each oil droplet. The primary W/O/W emulsion loaded with butyric acid is prepared using a rotor-stator homogenizer.

Droplet size distribution of the primary W/O/W emulsion is presented in Fig. 4.7a

The primary W/O/W emulsion had a broad droplet size distribution with the main peak at 10 μm. $d_{3,2}$ was 16.9 μm and RSF was 1.13, demonstrating the formulation of polydisperse emulsion.

As indicated in Fig. 4.7c, the ζ-potential of the W/O/W emulsion droplets stabilized using modified lecithin had a highly negative charge of -77.8 mV. These W/O/W emulsion droplets can be coated with positively charged dietary fiber.

4.3.3. Characterization of W/O/W Emulsions Stabilized Coated by Layer-by-Layer Deposition

4.3.3.1. Microscopic Observation

Figure 4.6 presents optical and fluorescence micrograph of the W/O/W emulsions before and after layer-by-layer deposition. The optical micrographs could not confirm a clear difference in the surface of the droplets between the primary W/O/W emulsion (Fig. 4.6a) and W/O/W emulsions coated with dietary fibers (Figs. 4.6b and d). The W/O/W emulsion droplets depicted in Figs. 4.6c and 4.6e are illuminated with green due to surface coating by FITC-labeled CHI.

4.3.3.2. Droplet Size Distribution and Average Droplet Size

The droplet size distribution, $d_{3,2}$, and RSF of the W/O/W emulsions at different coating stages are plotted in Figs. 4.7a and 4.5b. The values of $d_{3,2}$ were 12.1 μm for CHI single coating (CHI coating), 12.7 μm for CHI-CMC coating, 13.2 μm for CHI-CMC-CHI coating, and 15.3 μm for CHI-CMC-CHI-CMC coating. The $d_{3,2}$ of W/O/W emulsion droplets after CHI coating of W/O/W emulsion droplets was slightly smaller than that of W/O/W emulsion droplets of the primary W/O/W emulsion. Further

alternative coating using CHI and CMC led to slight and gradual increase of $d_{3,2}$ and RSF.

As excess CHI was added in the primary W/O/W emulsion, free modified lecithin and CHI molecules did not adsorb to the surface of W/O/W emulsion droplets and formed complexed microparticles smaller than W/O/W emulsion droplets. The slight decrease in $d_{3,2}$ of CHI coated W/O/W emulsion droplets may be attributed to the presence of modified lecithin and CHI complexed microparticles. Figure 4.8 indicates that particle size distribution of modified lecithin and CHI complexed microparticles (measurement by LS13 320).

In this study, free CHI and CMC molecules decreased during replacement of the outer water phase with acetate buffer. The complex microparticles were removed stepwise during replacement. This washing process is used mainly to reduce the complexed micro particles (Fig. 4.7a) and to shift the main peak toward the larger said, which causes an increase of $d_{3,2}$ of W/O/W emulsion droplets.

4.3.3.3. ζ-potential of W/O/W Emulsions Droplets

Figure 4.7c indicates variation of the ζ-potential of W/O/W emulsion droplets coated by layer-by-layer deposition using CHI and CMC. The ζ-potential values of W/O/W emulsion droplets were 38.1 mV after CHI coating, -66.4 mV after CHI-CMC coating, 47.5 mV after CHI-CMC-CHI coating, and -44.2 mV after CHI-CMC-CHI-CMC coating. The polarity of this ζ-potential changed depending on the outermost layer coating the W/O/W emulsion droplets, demonstrating that W/O/W emulsion droplets were alternately coated with CHI and CMC alternatively.

Chuah and co-workers (2009) also obtained ζ-potential of oil droplets of O/W emulsion using modified-lecithin as an emulsifier. Their ζ-potential was -80 mV,

measured using the same measuring equipment as the present study. This result indicated that the ζ-potential of droplet surface is not affected by whether or not the droplet is a multiple emulsion. Iwata and co-workers (2014) reported a monodisperse O/W emulsion coated with high polymer. Their report indicated the same tendency as the present study: ζ-potential changed for positive and negative altimetry, depending on the outermost high polymer layer.

4.3.4 Physical Stability of W/O/W Emulsions Loaded with Short-chain Fatty Acid

Figure 4.9 indicates the variation of droplet size distributions of W/O/W emulsion before and after layer-by-layer deposition. The $d_{3,2}$ of primary W/O/W emulsion remarkably increased 48.4 μm at 2 weeks and 120.8 μm after 4 weeks (Table 1). Primary W/O/W emulsion droplets increased with time (Fig. 4.9a). After 2 weeks of storage, the main peak shifted toward the larger side, and a low peak at a droplet size of 1000 μm appeared (Fig. 4.9a). After 4 weeks of storage, the main peak greatly shifted to a droplet size exceeding 100 μm. As a consequence, the primary W/O/W emulsion was not stable enough to coalescence during 4 weeks of storage. Coating with CHI and CMC improved the stability of W/O/W emulsion droplets to some extent and helped maintain their monomodal size distribution at 2 weeks (Fig. 4.9b), whereas a shoulder appeared on the larger side at 4 weeks. The $d_{3,2}$ of W/O/W emulsion droplets after CHI-CMC coating increased to 20.2 μm at 2 weeks, and to 22.5 μm at 4 weeks. The W/O/W emulsion droplets after CHI-CMC-CHI-CMC coating had monomodal droplet size distribution with little shift of the main peak even after 4 weeks of storage (Fig. 4.9c). Their $d_{3,2}$ slowly increased to 16.1 μm at 2 weeks, and to 19.5 μm at 4 weeks. These results

demonstrated that the physical stability of W/O/W emulsion droplets in terms of droplet coalescence can be greatly improved by layer-by-layer deposition using dietary fibers.

As demonstrated above, the physical stability of W/O/W emulsion loaded with short-chain fatty acid improved with layer-by-layer deposition using dietary fibers (positively charged CHI and negatively charged CMC). The W/O/W emulsion droplets having strong electrostatic charge could avoid coalescence and aggregation due to electrostatic interaction and rigid multilayers of dietary fibers that coat their surface. The stability of W/O/W emulsion improved with CHI-CMC coating, and W/O/W emulsion after CHI-CMC-CHI-CMC coating had higher stability than that after CHI-CMC coating.

4.4. Chapter Conclusion

In this study, stable W/O/W emulsions loaded with short-chain fatty acid were prepared using rotor-stator homogenization and subsequent layer-by-layer deposition using differently charged dietary fibers. The primary W/O/W emulsion had monomodal size distribution of oil droplets coating submicron droplets of an inner water phase. These W/O/W emulsion droplets had a strongly negative charge due to adsorption of modified lecithin onto their surface. Dietary fibers could coat W/O/W emulsion droplets, as confirmed by fluorescence micrography and the change of ζ-potential. The physical stability of the W/O/W emulsion loaded with short-chain fatty acid was improved with layer-by-layer deposition, depending on the number of layers that coated the W/O/W emulsion droplets. W/O/W emulsion after CHI-CMC-CHI-CMC coating had the highest physical stability and monomodal size distribution. In the future, the usefulness of W/O/W emulsion loaded with short-chain fatty acid coated by layer-by-layer deposition using dietary fiber will be clarified using *in vitro* digestion tests, and hopefully

which will be developed as a carrier of short-chain fatty acid to the large intestine.

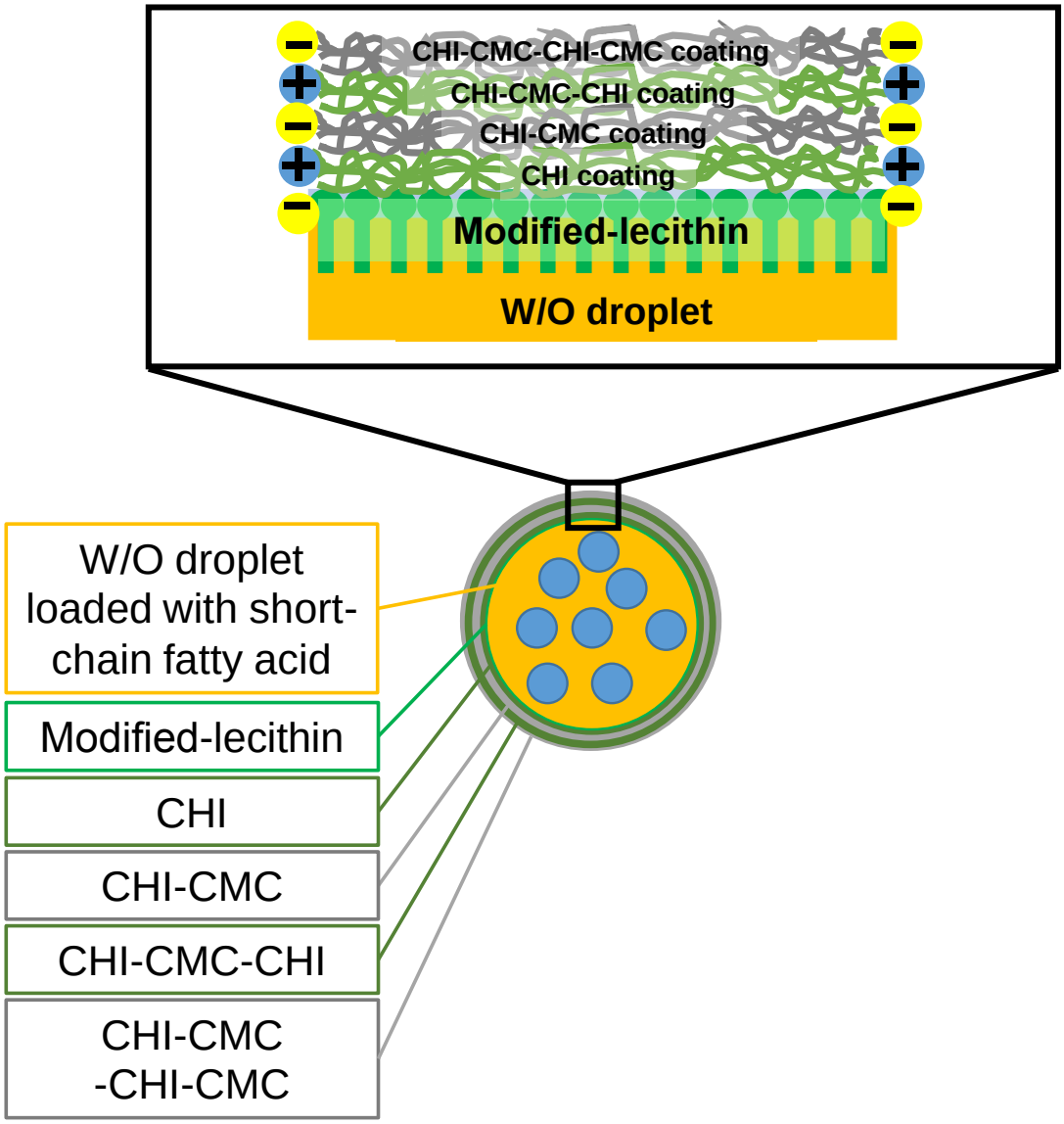

Fig.4.1. Schematic of a W/O droplet coated with chitosan (CHI) and carboxymethyl cellulose (CMC) using layer-by-layer deposition.

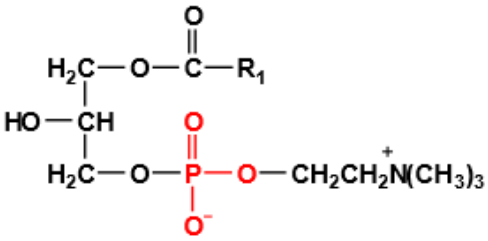

Lysophosphatidylcholine (LPC)
(18-30 %)

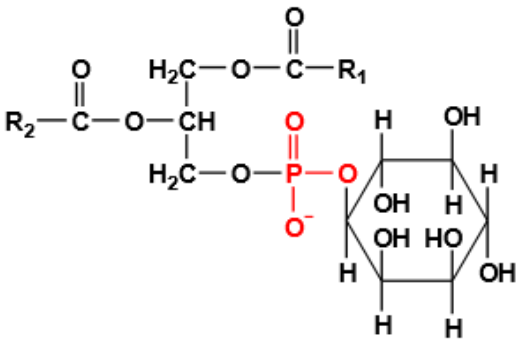

Phosphatidylinositol (PI)
(10-20 %)

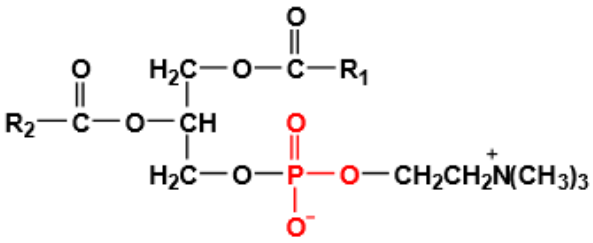

Phosphatidylcholine (PC)
(2-8 %)

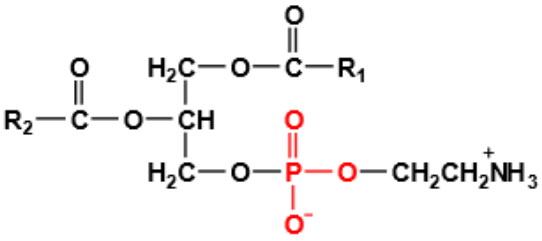

Phosphatidylethanolamine (PE)
(1-7 %)

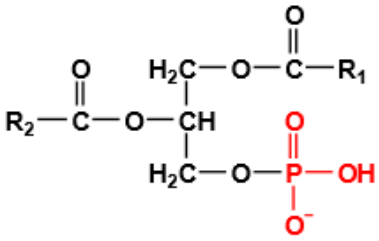

Phosphatidic Acid (PA)
(0-5 %)

Fig.4.2. Chemical structure and composition of modified lecithin.

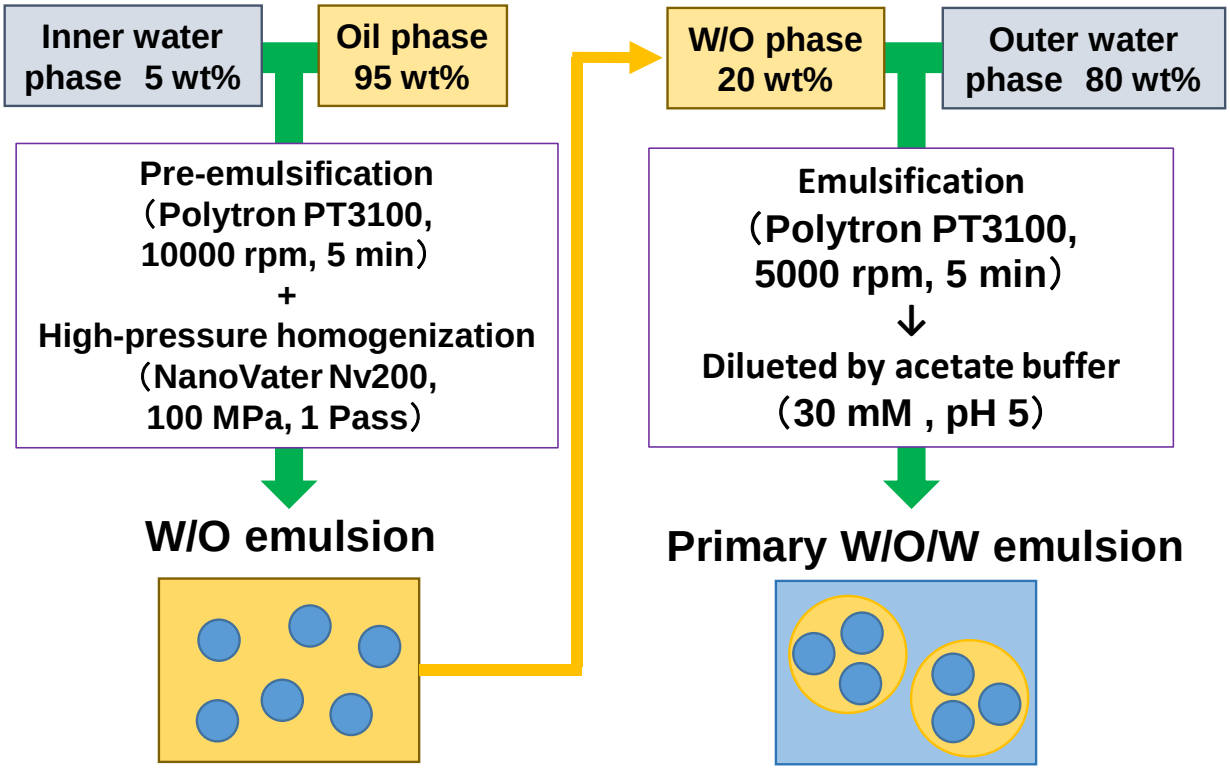

Fig.4.3. Schematic diagrams of the procedures for preparation of a primary W/O/W emulsion.

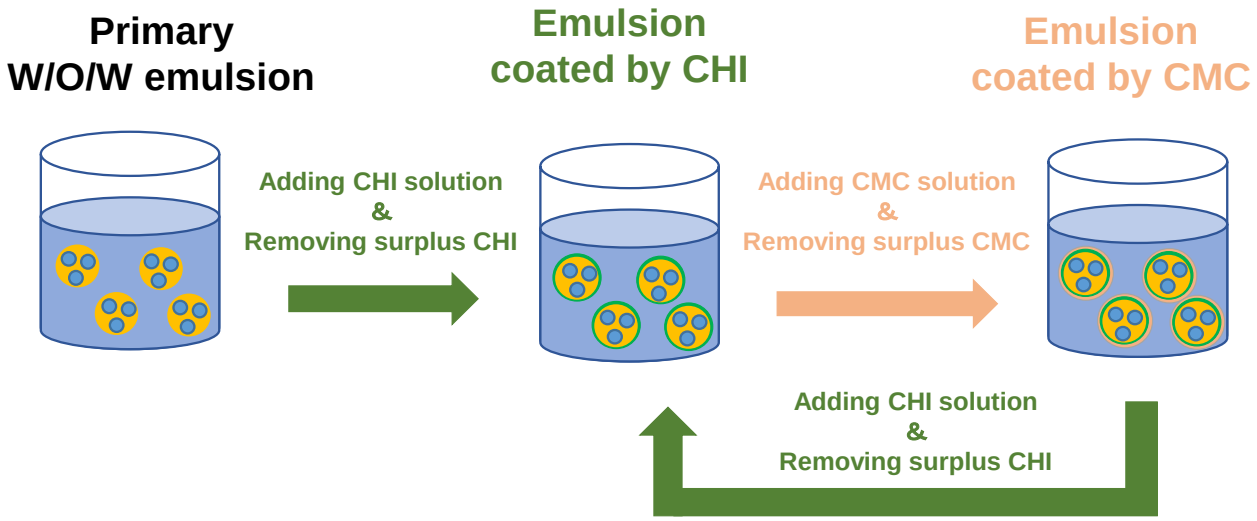

Fig.4.4. Schematic diagrams of the procedures for layer-by-layer deposition of the primary W/O/W emulsion.

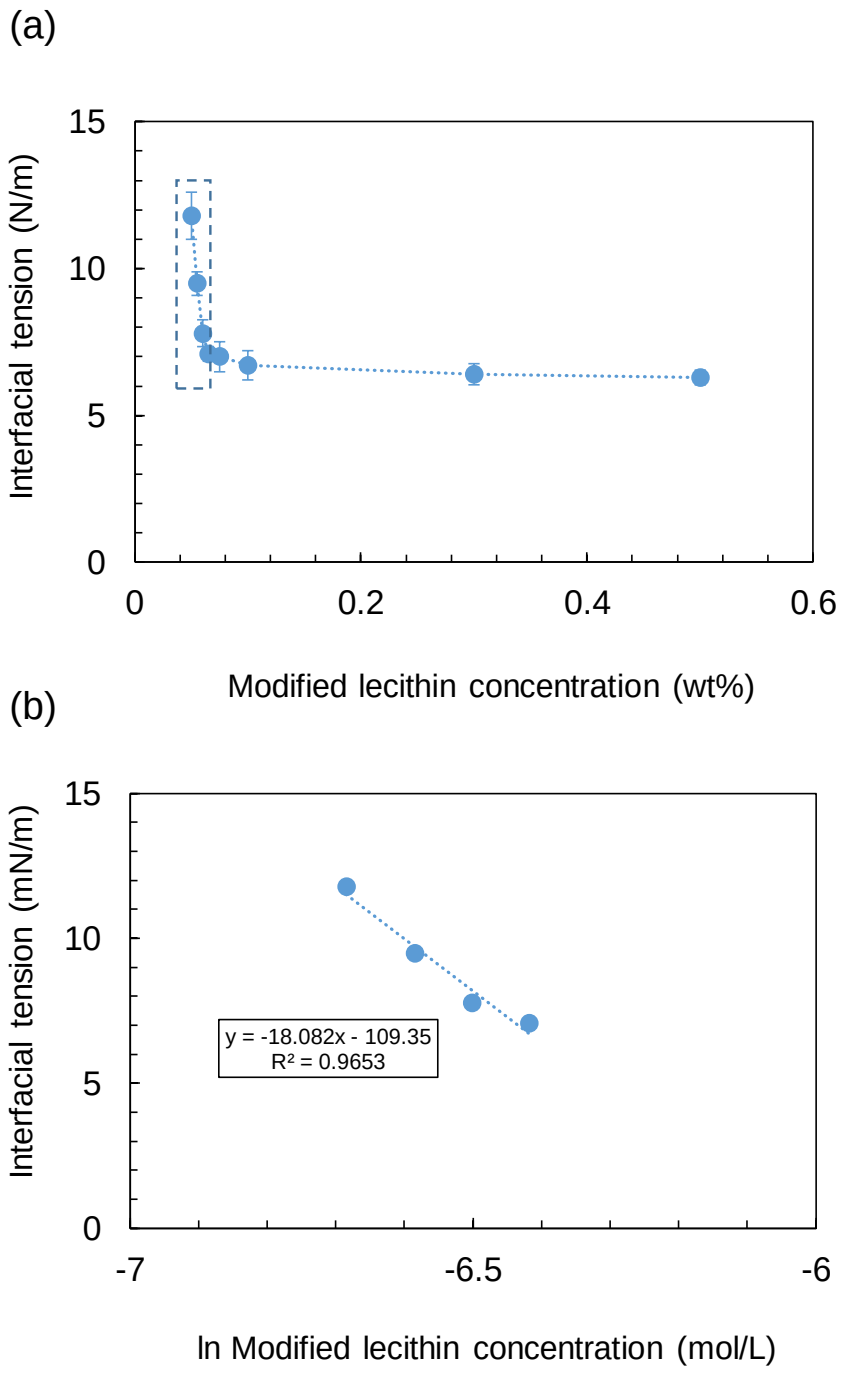

Fig.4.5. Variations of interfacial tension between soybean oil and an aqueous solution containing modified lecithin as a function of modified lecithin concentration (a). The data plotted in the dashed rectangle are fitted with equations in (b).

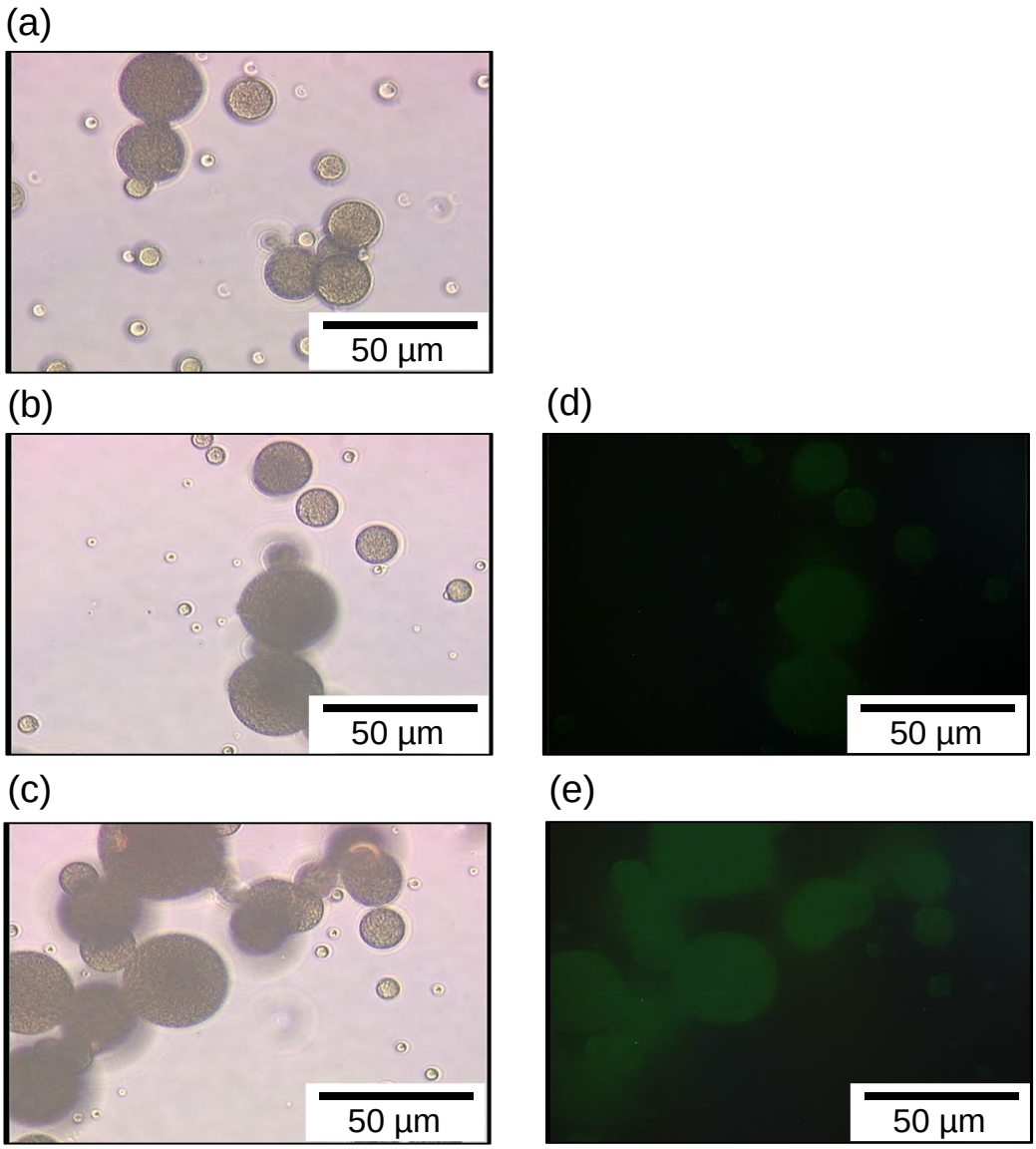

Fig.4.6. (a) Optical micrographs of primary W/O/W emulsion. (b,d) Optical micrographs and fluorescence micrographs of CHI coating. (c,e) Optical and fluorescence micrographs of CHI-CMC-CHI coating. The inner water phase contained 5 wt% butyric acid.

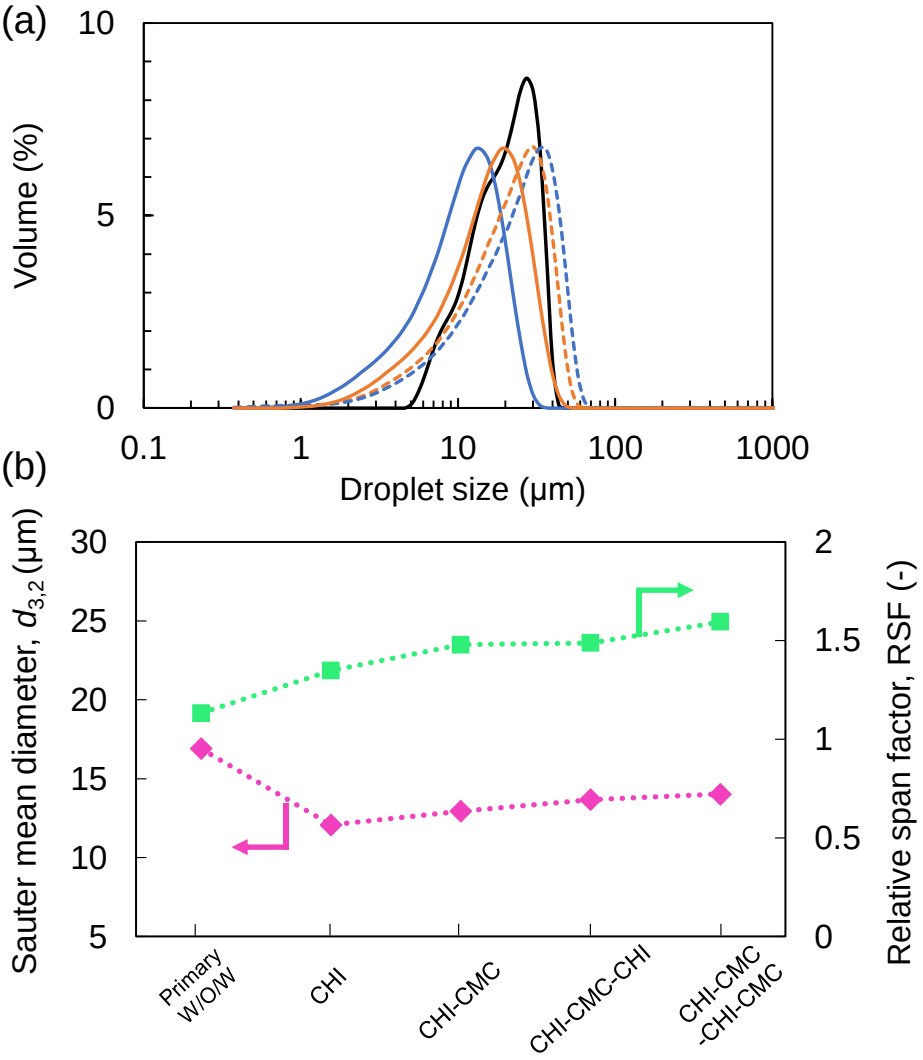

Fig.4.7. (a) Size distributions of primary W/O/W emulsion droplets (——), W/O/W emulsion droplets after CHI coating (——), W/O/W emulsion droplets after CHI-CMC coating (——), W/O/W emulsion droplets after CHI-CMC-CHI coating W/O/W emulsion droplets (- - -), and W/O/W emulsion droplets after CHI-CMC-CHI-CMC coating W/O/W emulsion droplets (------). (b,c) $d_{3,2}$ (■) and RSF (◆) of W/O/W emulsion droplets before or after with and without coating using CHI and/or CMC.

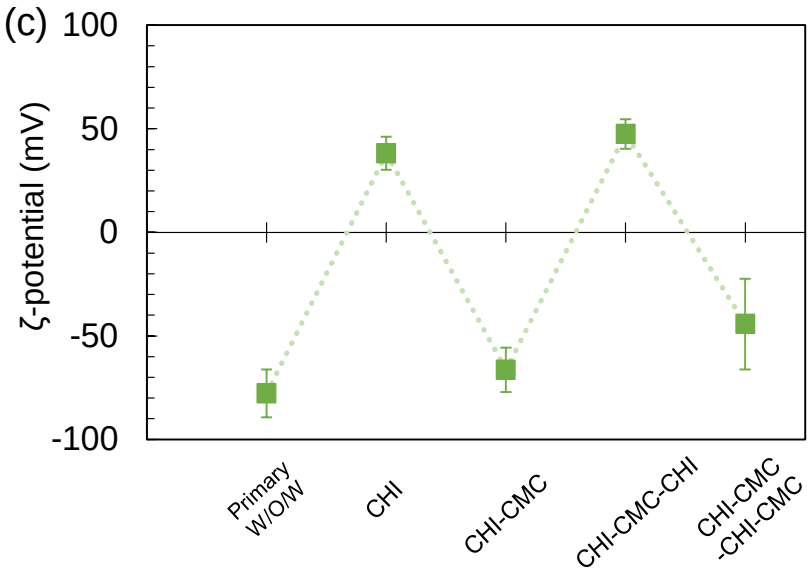

Fig.4.7. (continue) (c) ζ-potential of W/O/W emulsion droplets before or after with and without coating using CHI and/or CMC. The inner water phase contained 5 wt% butyric acid.

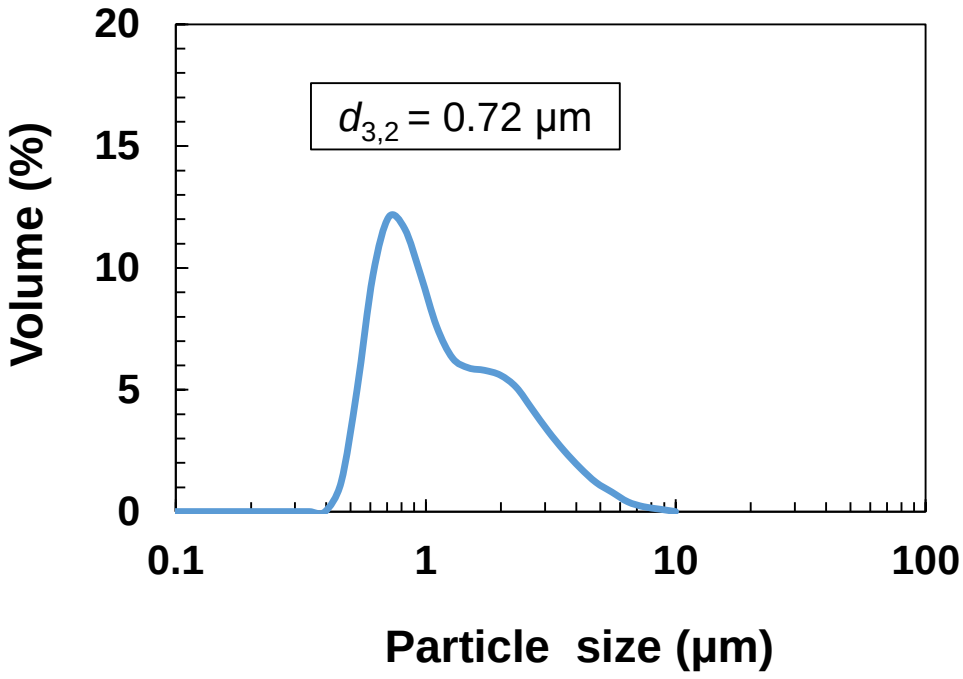

Fig.4.8. Particle size distribution of modified lecithin and CHI complexed microparticles.

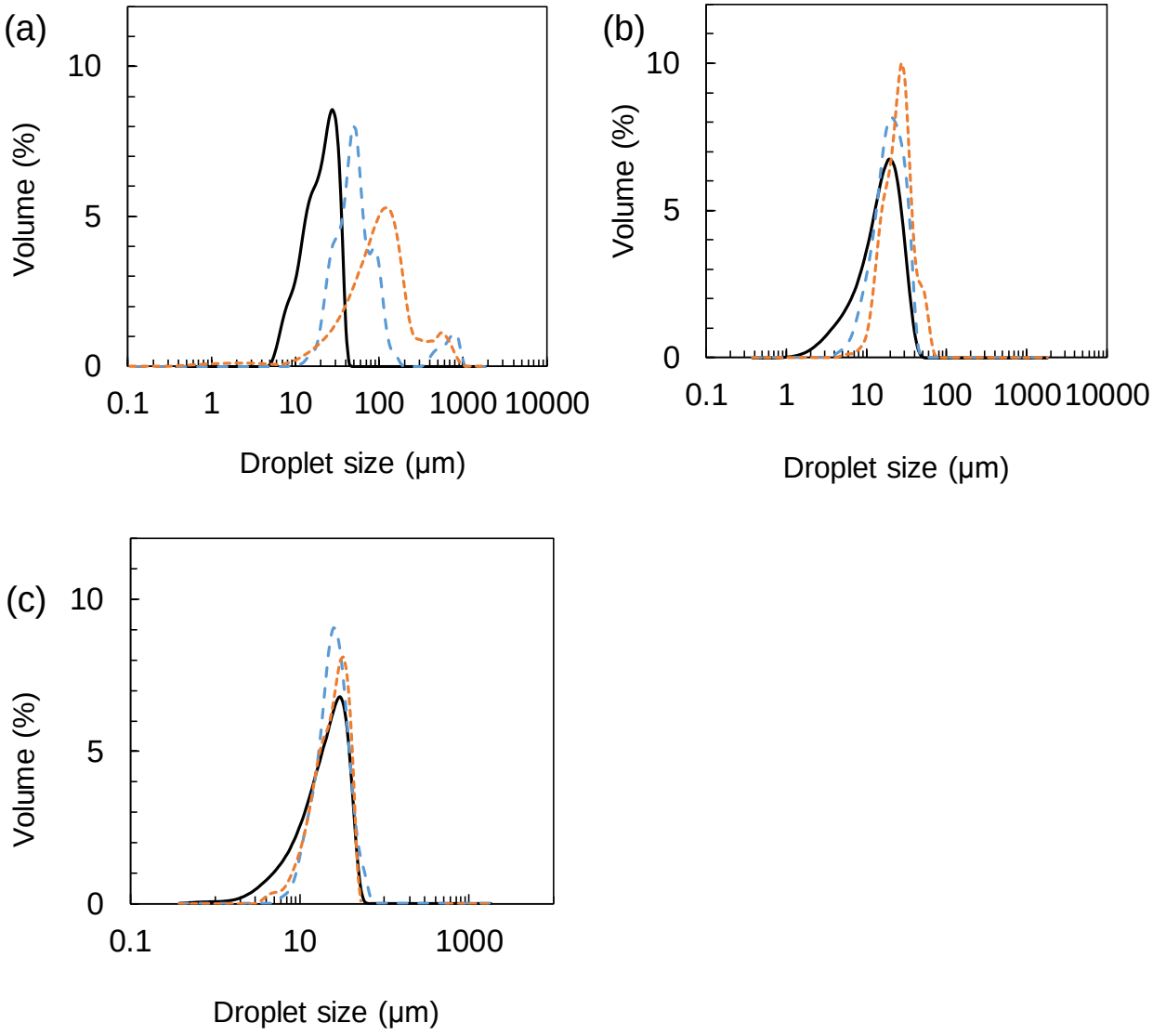

Fig. 4.9 : Time course of droplet size distributions of (a) primary W/O/W emulsions, (b) CHI-CMC coating, and (c) CHI-CMC-CHI-CMC coating. (—) denotes just after preparation. (- -) denotes after 2 weeks of storage. (---) denotes after 4 weeks of storage. The inner water phase contained 5 wt% butyric acid.

Table 4.1. The time course of $d_{3,2}$ of primary W/O/W emulsion and W/O/W emulsion coated with CHI and CMC.

	$d_{3,2}$ (μm)		
	Just after preparation	**After 2 weeks**	**After 4 weeks**
Primary W/O/W emulsion	16.9 ± 0.7	48.4 ± 2.0	120.8 ± 8.3
CHI-CMC coating	12.6 ± 1.7	20.2 ± 1.9	22.5 ± 1.8
CHI-CMC -CHI-CMC coating	15.4 ± 1.5	16.1 ± 1.6	19.5 ± 1.5

Chapter 5

Formulation and Evaluation of Hydrogels Loaded with Short-chain Fatty Acid

5.1. Introduction

Hydrogels are important materials and products in the foods industries. In Japan, we usually taste hydrogels of agar, konjac, gelatin, Tofu, and Kamaboko etc. In general, hydrogels are characterized by mechanical properties (e.g., elastic modulus and breaking strain rate), thermal properties (e.g., gelation by heating or the cooling), optical properties (elg., transparencity/opacity and colors), and (micro-)structures. Mechanical properteies are the most commonly considered to characterize hydrogels (Nishinari, 2007). Hydrogels have a high water content, and a hydrophilic short-chain fatty acid can be encapsulated in food-grade hydrogels.

Hydro maicroparticles which can be utilized in different industries. Hydro gel beads dispersion are prepared by mixing or shearing in the middle of gel forming, or breaking gel which was formed. Generally, gel particle are around few μm. Frith discovered that gelation of aqueous droplets after emulsification can prepare uniformly-sized submicron gel particles. This method has some advantages over the existing methods. First, it can control droplet size distribution by controlling emulsification condition. Second, manufacture of the various are structured by control of droplet size distribution. Third, digestion activity is improved by control of the surface area. The manufacture of the gel using the emulsification is one of the useful means to control properties of matter of the food as above. The manufacture of the gel using the emulsification is useful means to control properties of matter of the food as above.

Agar and carrageenans are manufactured from seaweeds. The hydrogels prepared are different by a kind of the seaweed (Fig. 5.1, Nishinari, 2007; Hayashi & Okazawa, 1970).

Agar hydrogels are traditionally and commonly consumed in Japan. Agar contains

polysaccharides having galactose as a basic frame (Araki, 1956). These polysaccharides are classified into agarose with high gelation strength and agaropectin with low gelation strength (Fig 5.2a). Agar hydrogels are simply and easily manufactured; they are made by adding less than 1 % of agar powder into boiling hot water and by subquently cooling off of agar hydrosols. During agar hydrogel formation by cooling, dissolved agarose and agaropectin exist as random coil molecules, changing into double-helix structure. Finally, agarose and agaropectin form the three-dimensional gel network (Fig. 5.2b).

There are three kinds of carrageenans: κ-carrageenan, ι -carrageenan and λ-carrageenan. They can be differentiated by the bond position and amount of sulfate group in carrageenan (Yamada 2001) (Fig. 5.3). κ-Carrageenan is made from kappaphycus (Solierriaceae). κ-Carrageenan hydrogel is hard but fragile; its properties are closer to agar hydrogel than ι -carrageenan and λ-carrageenan hydrogels. ι-Carrageenan made from Eucheuma (Solierriaceae) has the softness and elasticity texture. As κ-Carrageenan and ι -carrageenan have double helix structure by 3,6-anhydro bind, they form heat reversible hydrogels, and adding a cation makes stronger hydrogels. λ-Carrageenan made from Gigartina (Gigartinaceae) cannot form hydrogel, because it does not have 3,6-anhydro bind and cannot have double helix structure. ι -Carrageenan hydrogels can suppress their syneresis; therefore, they are suitable as carriers for loading with a hydrophilic short-chain fatty acid.

In this chapter, syneresis and release of inner package of agar and ι -carrageenan were evaluated. Hydrogel beads loaded with a short-chain fatty acid were also prepared using agar and ι -Carrageenan hydrogels.

5.2 Materials and Methods

5.2.1. Materials

Agar was purchased from Wako Pure Chemical Industries, Ltd. (Osaka, Japan). ι - Carrageenan was kindly provided by San-Ei Gen F.F.I., Inc. (Osaka, Japan).

Methylene blue and calcium lactate pentahydrate were also purchased from Wako Pure Chemical Industries Ltd. Methylene blue was used as the model of short-chain fatty acid. Molecular weight of methylene blue is 320 g/mol and close to short chain-fatty acids in water soluble food color. Calcium lactate pentahydrate was a cation of ι - carrageenan. Butyric acid was purchased from Sigma-Aldrich Co. (St. Louis, USA).

5.2.2. Preparation of Agar and ι - Carrageenan Hydrogels Including Methylene Blue

A 20 mg/L methylene blue aqueous solution was used as a solvent of agar or ι-carrageenan. Agar powder was dissolved in the solution at the 1, 3, and 5 wt% in 80 ^{o}C. ι-Carrageenan powder was dissolved in the solution at the 0.5, 1, and 2 wt% in 80 ^{o}C and at 1, 2.1, and 4.5 wt% calcium lactate pentahydrate as a cation. After this dissolution process, those agar solution and ι-Carrageenan solution were cooled overnight at 4 ^{o}C and completely gelated. Those gels were cut by a cube of 5mm.

5.2.3. Analytical Curve Making of Methylene Blue

In this study, absorbance of methylene blue was measured at 660 nm with Spectrophotometer (V-570, JASCO Co., Tokyo). Figure 5.4a shows spectrum of methylene blue. Its highest intensity was observed at 664 nm.

The absorbance of the methylene blue water solution was measured at different methylene

blue levels. The data were plotted and fitted by an approximate line (Fig. 5.4b). The following approximate line was given:

$$y=0.1403\,x \tag{5-1}$$

where y is absorbance of methylene blue, and x is methylene blue density. In this study, this equation was used for calculation of the amount of the methylene blue released from hydrogels.

5.2.4. Evaluation of Degree of Syneresis and Release of Methylene Blue

Degree of syneresis was measured by a centrifugation test using centrifuge (HP-25 Beckman Coulter, Inc.; Verbeken, 2006; Banerjee & Bhattacharya, 2011). Each centrifuge tube was partially filled with a hydrosol, being subsequently cooled overnight at 4 ^{o}C to complete gelation. Afterwards, the prepared hydrogels were centrifuged at 5000 rpm for 5 to 25 min. The water released during the centrifugation was separated, and its weight and absorbance were measured. The degree of syneresis is defined as

$$S = \frac{W_t}{W_0} \tag{5-2}$$

where S is the degree of syneresis, W_t is the weight of the released water, and W_0 is the initial weight of a hydrogel sample.

Regarding release of the inner component (methylene blue) to the water, 30 g of 5-mm agar hydrogel cubes were soaked in 200 g of water in the flask. Absorbance of water containing the released methylene blue was measured after 3 h of shaking at 115 strokes/min and 37 ^{o}C. Release of methylene blue from the hydrogel ($R_{Quantity}$) is defined as

$$R_{Quantity} = \frac{A_m}{0.1403} \tag{5-3}$$

where A_m is absorbance of methylene blue, and 0.1403 is the slope of the approximate

line in Fig. 5.4b. The degree of release of methylene blue ($_{Rratio}$) is also defined as

$$R_{ratio} = \frac{R_{Quantity}}{W_{M0}} \quad (5\text{-}4)$$

Where W_{M0} is the initial weight of methylene blue in the hydrogel cubes.

5.2.5. Formulation and Evaluation of Hydrogel Beads Loaded with Short-chain Fatty Acid

A W/O emulsion was prepared by dispersing an aqueous solution containing 5 wt% agar (or 2 wt% ι-carrageenan) and 5 wt% butyric acid into a soybean oil solution containing 5 wt% TGCR by rotor-stator homogenization at 5000 rpm for 5 min at 80 °C. The resulting W/O emulsion was cooled overnight at 4 °C to cause gelation of the dispersed droplets. The hydrogel beads were evaluated by measuring their particle size distribution and microscopic observation. The particle size measurement was performed with image analysis (WinRoof, Mitani Co., Fukui, Japan) using the acquired particle images. The average particle size of the resulting hydrogel beads was defined by d3,2 and span.

5.3. Results and Discussion

5.3.1. Degree of Syneresis of Hydrogelss

Figure 5.5 illustrates degree of syneresis of the prepared agar hydrogels. Synerisis of for the hydrogels containing 1 and 3 wt% agar increased with increasing centrifuge time. After centrifuging for 25 min, the degree of syneresis reached 2.36 wt% and 0.39 wt% for 1 and 3 wt% agar hydrogels, respectively. In contrast, the hydrogel containing 5 wt% agar did not cause syneresis. These results show that syneresis of the agar

hydrogels became large with increasing mechanical stress, resulting in decrease of the degree of syneresis at higher agar concentrations. Agar hydrogel has bound water that combines strongly with agarose and agaropectin. Unbound water are also combined in the gap of network structure by weak hydrogen bond (Abe, 1997); therefore, unbound water can leak due to the mechanical stress.

On the other hands, all of ι-carrageenan hydrogels did not cause syneresis (Fig. 5.6). However, at the low ι-carrageenan concentrations, a slight amount of water leaked on the surface of the ι-carrageenan hydrogels after centrifugation. ι-carrageenan has a double helix structure due to 3,6-anhydro bond; there are hydrophilic groups in outside of helix structure (Nishinari, 2007). ι-carrageenan hydrogels are, thus, superior in terms of water retention.

5.3.2. Release of Methylene Blue Associated with Syneresis

Figure 5.7a illustrates release of methylene blue associated with syneresis of the 1 wt% agar hydrogels. Release of methylene blue from these hydrogels increased with increasing the centrifuge time, having a tendency similar to their syneresis. These results indicate that release of methylene blue is caused by its syneresis. Namely, it is suggested that preventing of syneresis can reduce release of inner package.

The 3 and 5 wt% agar hydrogels and all the ι-carrageenan hydrogels could not measure the amount of the released methylene blue, because their syneresis was too small to be used for spectrophotometer measurement. However in the agar gel may have a tendency same as 1 wt% system.

5.3.3. Release of Methylene Blue from Hydrogel Cubes to the Water

Figure 5.8 shows release of methylene blue from hydrogel cubes to the water phase. Around 15.0 wt% of methylene blue was released from the 1 wt% agar hydrogel cubes. Release of methylene blue decreased with increasing the agar concetration, reaching 11.1 wt% from the 5 wt% agar hydrogel cubes. Agar hydrogel cubes can release more than 10 wt% of methylene blue as a loaded component, even by simple shaking. If an in vitro digestion in the presence of the peristalsis is conducted, it is suggested that more inner package will be released by 5.3.1.

The use of ι-carrageenan hydrogel cubes showed release of methylene blue higher than that from the agar hydrogel cubes (Fig. 5.9). The 0.5 wt% ι-carrageenan hydrogel cubes released 38.1 wt% of methylene blue after 3 h of shaking. The methylene blue released decreased with increasing the ι-carrageenan concentration. The 2 wt% ι -carrageenan hydrogel cubes released 21.4 wt% of methylene blue.

Release of methylene blue from the 1 wt% agar hydrogel cubes was about half of that from 1 wt% ι-carrageenan hydrogel cubes. The ι-carrageenan hydrogel cubes are negatively charged. In this study, positively charged calcium lactate was added to make crosslinked structures between the gaps inside the hydrogel, and it is added a glut to ι-carrageenan solution. As a consequence, ι-carrageenan hydrogels may have positive electric charge. Methylene blue also has positive electrostatic charge due to the presence of sulfur. Methylene blue molecules loaded in the ι-carrageenan hydrogel cubes may be readily released into the surrounding water phase by electrostatic repulsion. As agar hydrogels are not electrostatically charged, methylene blue loaded in the agar hydrogel cubes may not be released into the water phase. These results suggest that the electrostatic charge of the hydrogels is a factor affecting the release behavior of methylene

blue from the hydrogel cubes. It should be mentioned that short-chain fatty acids have a negative charge due to the presence of a carboxylic acid group. ι-carrageenan hydrogel cubes could retain short-chain fatty acids when they are soaked in water.

5.3.4. Evaluation of Hydrogel Microbeads Loaded with Short-chain Fatty Acid

Optical micrographs of the resultant hydrogel microbeads are depicted in Fig. 5.9a (agar) and Fig. 5.10a (ι-carrageenan). Micron-scale hydrogel microbeads were dispersed in the continuous oil phase, demonstrating that hydrogel beads loaded with a short-chain fatty acid are obtained. However, their droplets size was dependent on the type of the polysaccharides used. Figures 5.9b and 5.10b indicate the droplet size distributions of the prepared hydrogel microbeads. The agar hydrogel microbeads had a single and broad droplets size distribution (Fig. 5.9b); their $d_{3,2}$ and span were 3.75 μm and 0.733, respectively. ι-carrageenan hydrogel microbeads also had a single and broad droplet size distribution; their $d_{3,2}$ and span 7.57 μm and 0.985, respectively. The $d_{3,2}$ for the ι-carrageenan hydrogel microbeads exceeded about twice that for the agar hydrogel microbeads. The ι-carrageenan aqueous solution is positively charged, and its viscosity might be higher than the agar aqueous solution. The difference in their viscosity is considered to affect the size of the resulting hydrogel microbeads.

The preceding results show that the dispersions containing hydrogel microbeads loaded with a short-chain fatty acid were successfully prepared by rotor-stator emulsification. It is suggested that inner component will be released in large quantities to the water by results of 5.3.3. If those gel beads are used career of short-chain fatty acid to large intestine, improvement of controlling sustained release of the inner package is necessary for those gel beads.

5.4. Chapter Conclusion

In this chapter, release of compound loaded in the agar and ι-carrageenan hydrogels was investigated. The agar and ι-carrageenan hydrogel microbeads loaded with short-chain fatty acid were also prepared. A large portion of methylent blue was released by syneresis of the agar hydrogels. In contrast, synerisis was not observed from the ι-arrageenan hydrogels. The amount of the methylene blue released from the hydrobel cubes into water was less than the results obtained using the ι-carrageenan hydrogels. The hydrogel microbeads loaded with a short-chain fatty acid were prepared by high-temperature emulsification and subsequent cooling in the refrigerator. Controlled release of loaded components from hydrogel microbeads have to be improved as microcareers of a short-chain fatty acid to the large intestine.

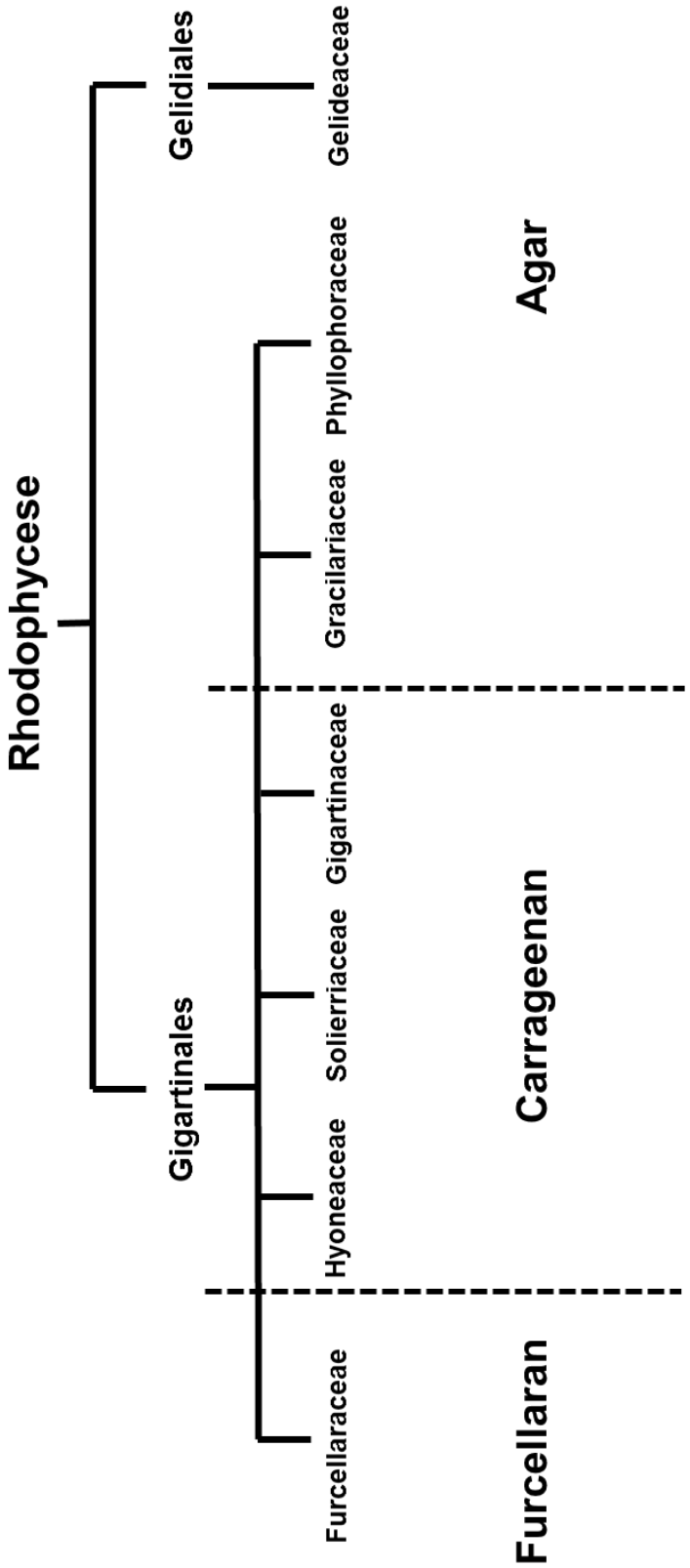

Fig.5.1. Seaweed materials and polysaccharides.

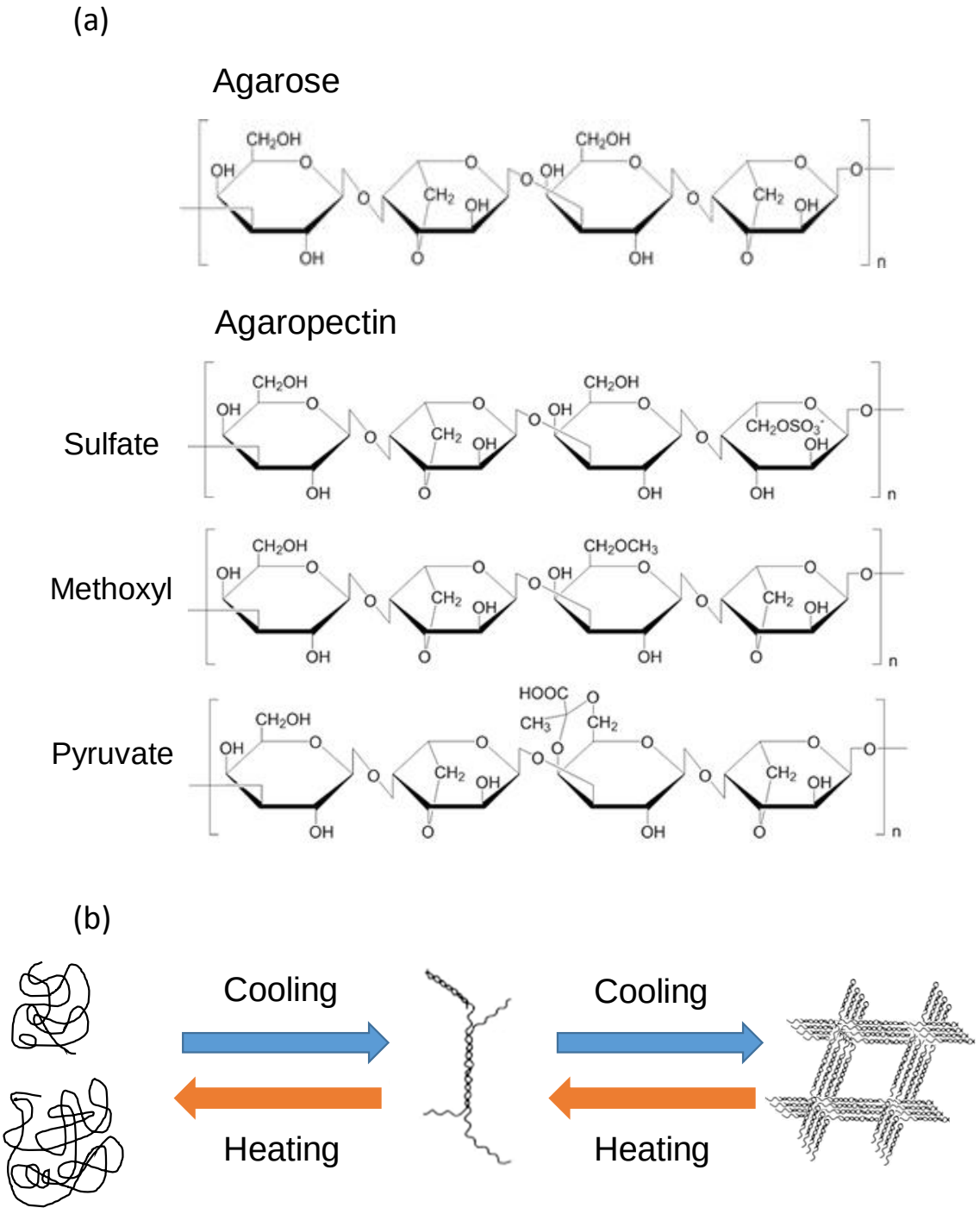

Fig.5.2. (a) Chemical structure of agarose and agaropectin
(b) Changes in the molecular structure of agar gel

κ-carrageenan

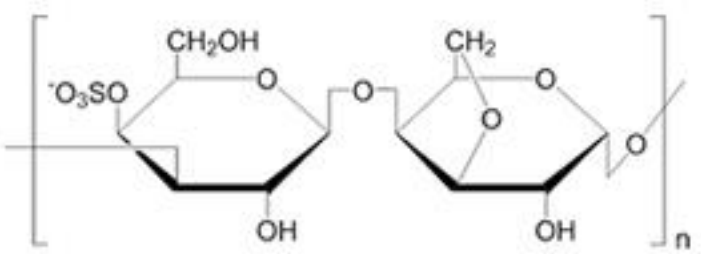

λ-carrageenan

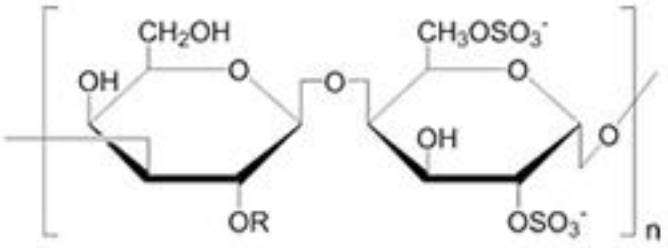

ι-carrageenan

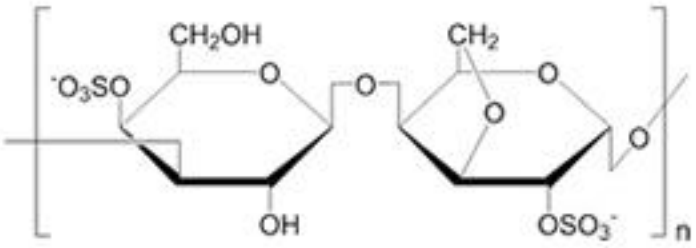

Fig.5.3. Chemical structure of carrageenan.

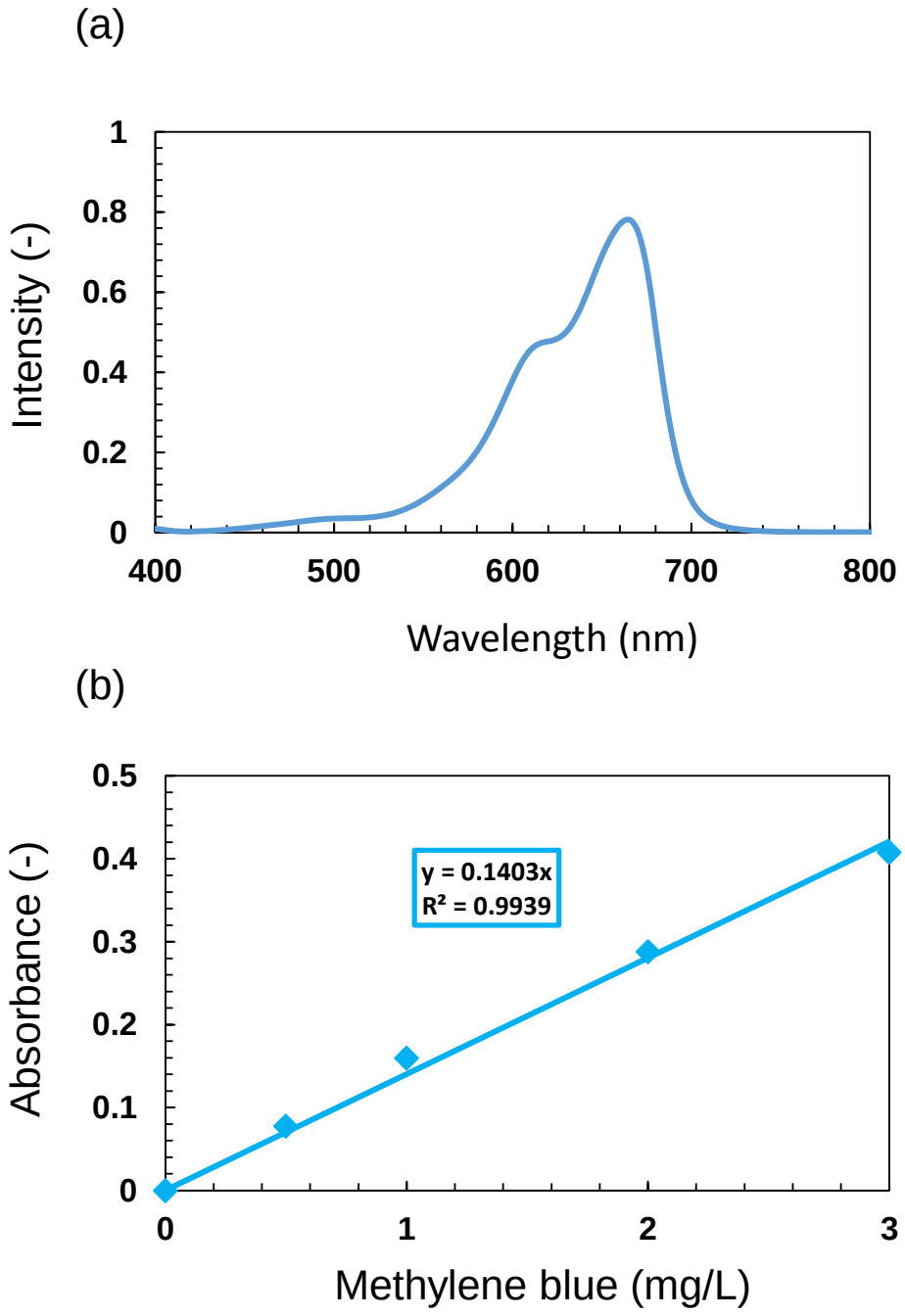

Fig.5.4. (a) Spectrum of methylene blue. (b) Analytical curve of methylene blue.

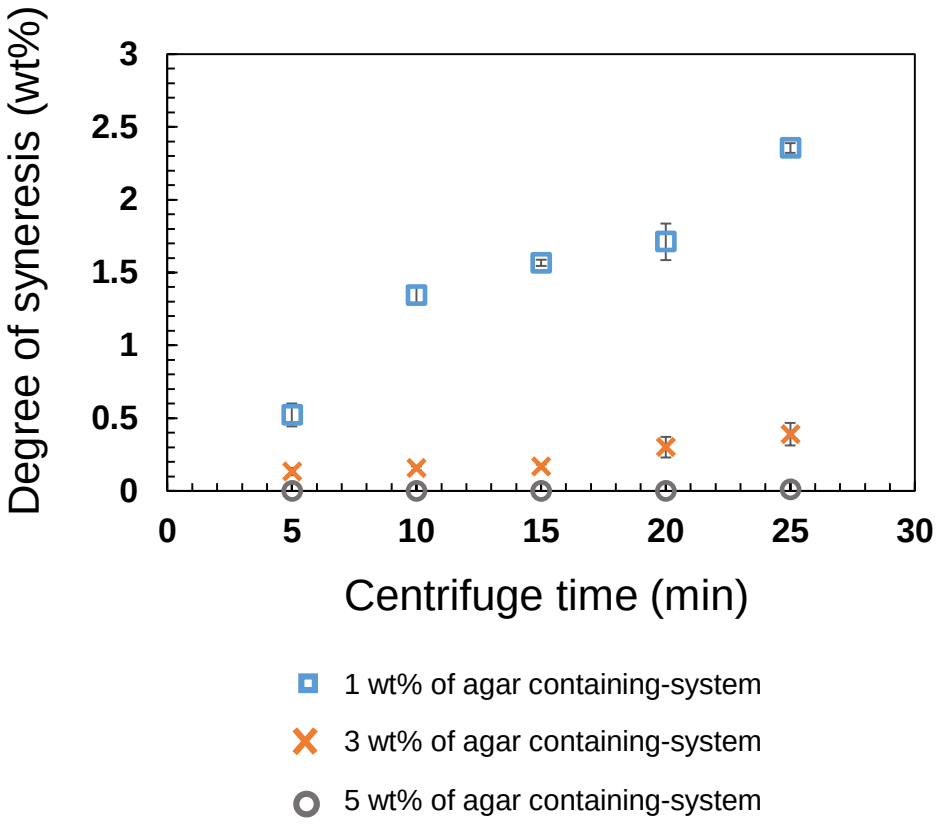

Fig.5.5. Degree of syneresis of ager hydrogels.

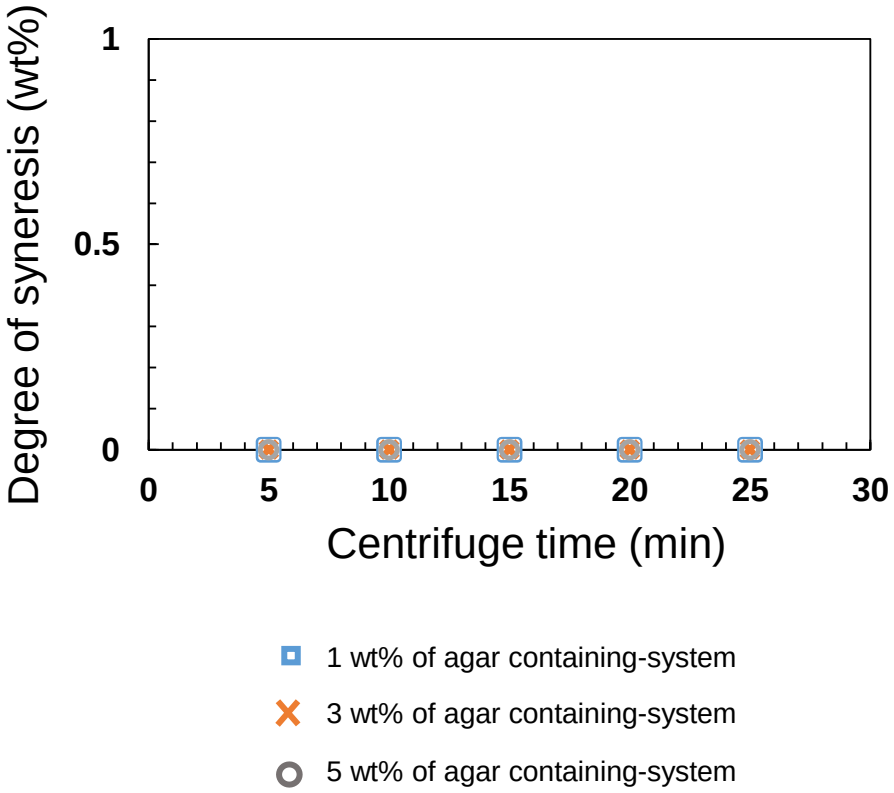

Fig.5.6. Degree of syneresis of ι - carrageenan hydrogels.

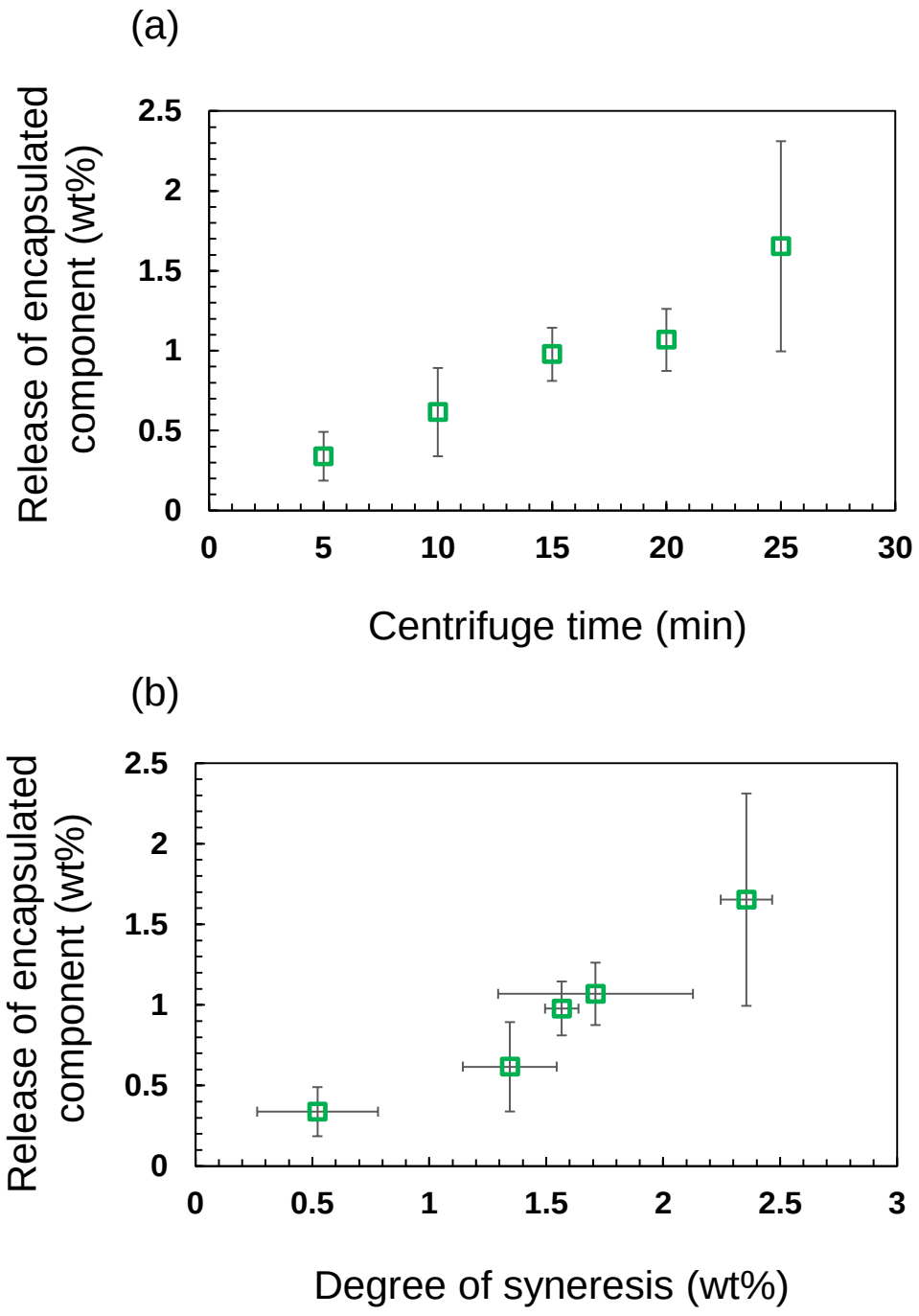

Fig.5.7. (a) Release of methylene blue with syneresis of 1 wt% of agar hydrogel. (b) Correlation of syneresis and release of methylene blue.

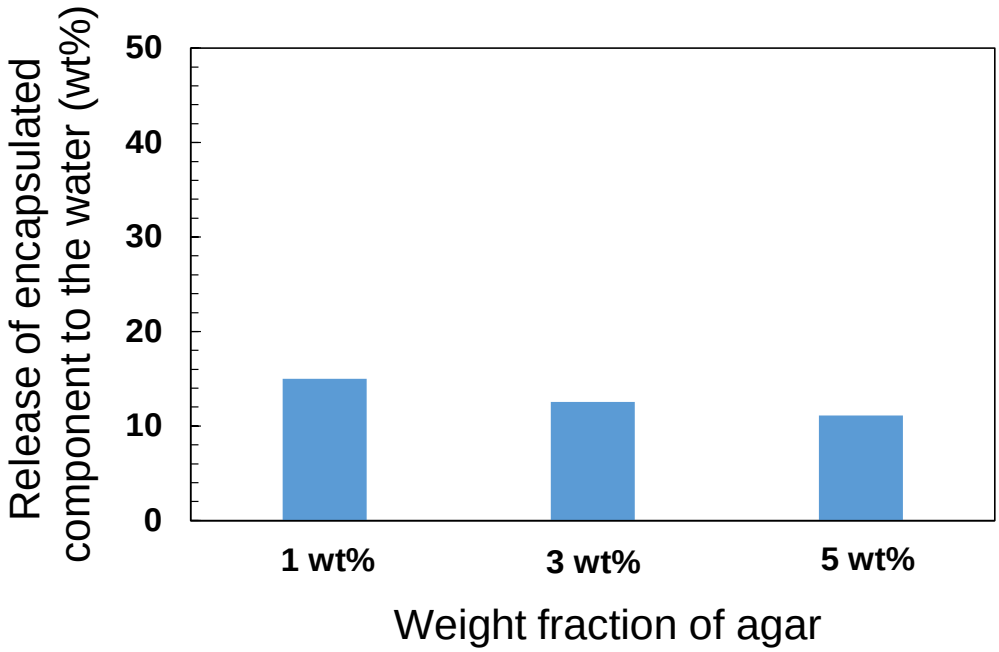

Fig.5.8. Release of methylene blue to the water of agar hydrogel cubes.

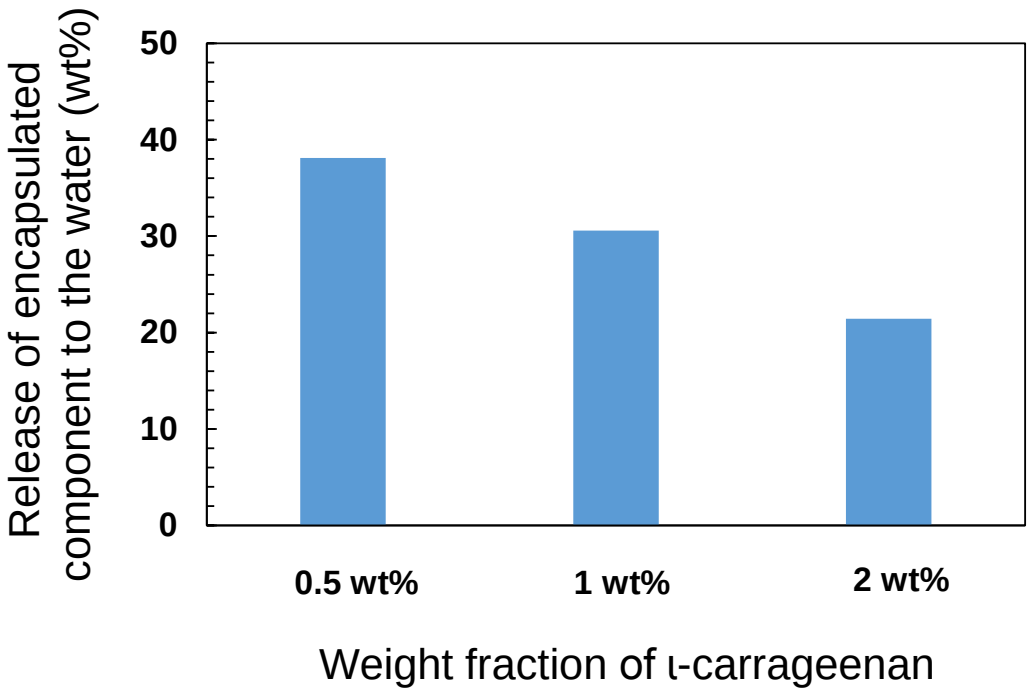

Fig.5.9. Release of methylene blue to the water of ι-carrageenan hydrogel cubes.

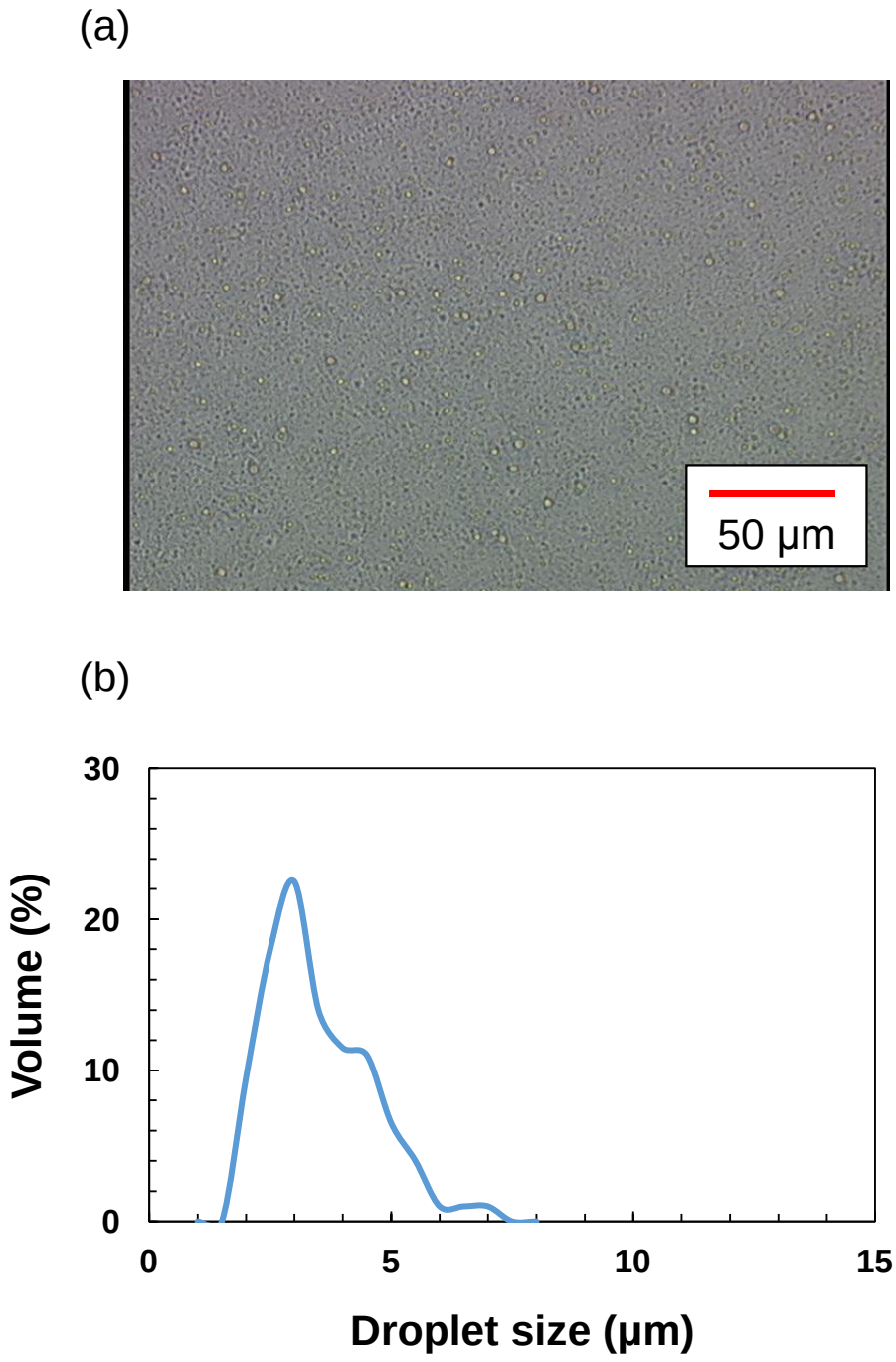

Fig.5.10. (a) Optical micrographs of agar hydrogel microbeads. (b) Size distribution of agar gel microbeads.

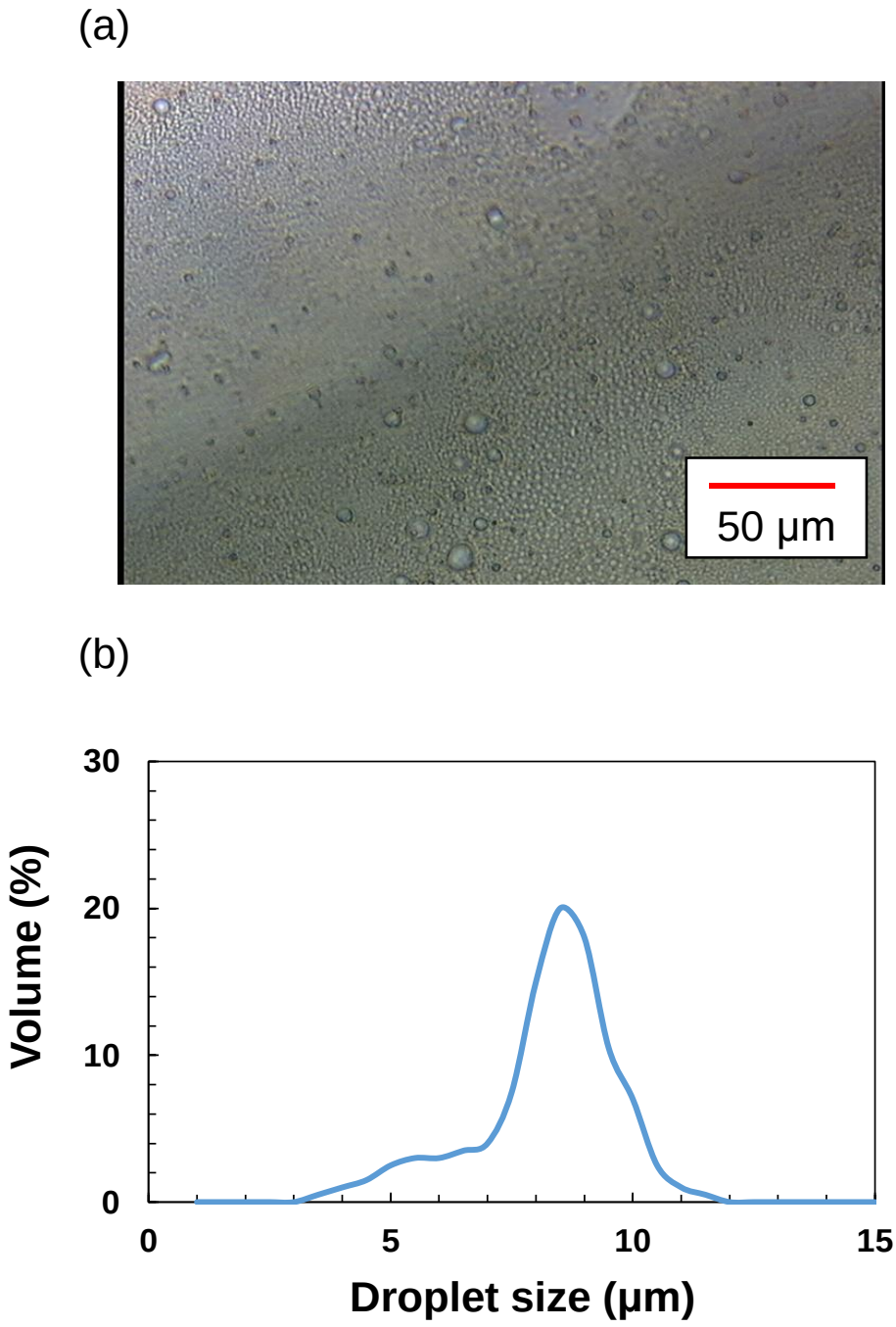

Fig.5.11. (a) Optical micrographs of ι-carrageenan hydrogel microbeads. (b) Size distribution of ι-carrageenan gel microbeads.

Chapter 6

General Conclusions

6.1 Introduction

In this chapter, the results obtained in Chapters 2, 3, 4, and 5 are summarized, and perspectives for further studies are described.

Our food culture and lifestyle have recently diverged, while people that have nutritionally imbalanced foods are getting increased. Interests in keeping and improving their health lead to requirement of functional food products. A large number of studies on foods containing functional ingredient(s) have been intensively performed so far. However study on formulating emulsions loaded with a short-chain fatty acid has not yet been investigated; therefore, this study aimed to formulate W/O and W/O/W emulsions loaded with butyric acid with high physical and storage stabilities. Moreover, the layer-by-layer deposition using electrostatically charged dietary fibers successfully improved stability of for the W/O/W emulsions loaded with butyric acid.

6.2 Summary of Each Chapter

6.2.1 Chapter 1

The human large intestine and its functions, short-chain fatty acids, fundamentals, properties, and stability of emulsions, and emulsification techniques are introduced in Chapter 1. The objectives of this thesis were also described.

6.2.2. Chapter 2

In the Chapter 2, we tried that making of standard of that can calculate appropriate dilution ratio for submicron emulsions in using DLS.

Because a laser beam causes multiple scattering, and it is not possible for the accurate measurement, when W/O emulsion droplets diameter was measured using DLS, it should be diluted. It became clear that W/O emulsion with each degree of disperse phase had dilution magnification having high reproducibility each. The attenuation index at that the measurement results had reproducibility was

7, and it was suggested that reproducibility of results and the attenuation index were correlative.

We drew an approximate curve from these correlations and obtained the following equation.

$$X = 10\, W_d^{1.13}$$

where X is appropriate dilution ratio and W_d is degree of dispersed phase of W/O emulsion. This equation can calculate appropriate dilution ratio each degree of dispersed phase of W/O emulsion. Using this equation, we could measure that droplets size distribution with high reproducibility in each dispersed phase of W/O emulsion.

6.2.3. Chapter 3

In Chapter 3, W/F and W/O emulsions loaded with a short-chain fatty acid were formulated, and their physical and storage stabilities are evaluated. Pre-mixtures, each containing a dispersed aqueous phase loaded with 5 wt% butyric acid and a continuous phase containing a hydrophobic emulsifier, were subjected to temperature-controlled high-pressure homogenization at 100 MPa for one pass to formulate W/F and W/O emulsions. Submicron W/F and W/O emulsions with a Sauter mean diameter ($d_{3,2}$) of <0.5 μm and a monomodal droplet size distribution were obtained at a weight fraction of the dispersed phase (W_d) of 1 to 5 wt%. At W_d of 5 wt%, the W/F emulsions maintained peak distribution after four weeks of storage and melting-solidification cycles. The results also demonstrated formulation of stable submicron W/F emulsions loaded with a short-chain fatty acid, having possible application for nutrient delivery systems to the large bowel.

6.2.4. Chapter 4

In Chapter 4, W/O/W emulsions loaded with a short-chain fatty acid were formulated, and their stability improvement was attempted by layer-by-layer deposition using dietary fibers. The W/O emulsion obtained by the first-step emulsification consisted of an inner water phase containing 5 wt% butyric acid and soybean oil phase containing a hydrophobic emulsifier. The weight fraction of the

inner water phase was 5 wt%. W/O emulsions with a $d_{3,2}$ of 0.4 μm were prepared by high-pressure homogenization. The W/O/W emulsion consisted of W/O emulsion dispersed in an outer water phase containing 0.5 wt% modified lecithin, and the weight fraction of the W/O phase was 20 wt%. The W/O phase was dispersed in the modified lecithin solution to prepare a W/O/W emulsion using rotor-stator homogenization. The $d_{3,2}$ of the resultant W/O/W emulsion droplets was 16.9 μm, and thier ζ-potential was -77.8 mV at pH 5. W/O/W emulsion droplets were coated with chitosan (CHI) and carboxymethyl cellulose (CMC), which is driven by electrostatic interaction. The ζ-potential data indicated successful coating of the droplets. W/O/W emulsion droplets coated with dietary fibers were highly stable over 4 weeks. These results demonstrated that W/O/W emulsions loaded with short-chain fatty acid could be better stabilized with layer-by-layer coating using dietary fibers.

6.2.5. Chapter 5

Chapter 5 prepared hydrogel beads loaded with short-chain fatty acid, and evaluation of syneresis of hydrogels.

In this study, agar and ι-carrageenan gel as hydrogel. And methylene blue was used model as an inner package. Agar gel had high syneresis, however, ι-carrageenan gel did not show syneresis. On the other hand, in the release of methylene blue to the water, ι-carrageenan gel had high release of methylene blue rather than agar gel. These results are caused by structure and electric charge of the gel. Agar and ι-carrageenan gel beads were prepared by rotor-stator homogenization at 5000 rpm for 5 min at 80 ^{o}C. The droplets diameter of agar and ι - carrageenan gel beads were 3.75 μm and 7.57 μm. ι-carrageenan gel had larger droplets than agar gel. This results shows that gel beads loaded with short-chain fatty acid were able to be made by emulsification.

6.3 General Conclusions

- The equation which can calculate an appropriate dilution ratio of W/O emulsion in the

measurement droplet size distribution using DLS was shown.

- Stable submicron W/F and W/O emulsions loaded with a short-chain fatty acid, were formulated, and they have possible applications for nutrient delivery systems to the large intestine.
- W/F emulsions with W_d of 5 wt% or less had high physical and storage stabilities.
- W/O/W emulsions loaded with a short-chain fatty acid were successfully coated by layer-by-layer deposition using oppositely charged dietary fibers.
- The use of layer-by-layer deposition can improve physical and storage stabilities of the W/O/W emulsions loaded with a short-chain fatty acid.
- Syneresis and release characteristics of methylene blue loaded in agar and ι-carrageenan gels. Agar and ι-carrageenan gel beads could prepared using rotor-stator homogenization
- Agar and ι-carrageenan gel microbeads were able to be prepared by rotor-stator homogenization.

6.4 Perspectives

Due to the increased interest in health care, studies on functional foods is getting increased. A wide variety of functional food products have been already commercialized in many countries and regions. Author hope that this study makes use for our healthy promotion.

Further investigations are needed to realize commercialization of nutrient delivery systems loaded with short-chain fatty acids. For example, chemical stability, release kinetics of functional component(s), and in vitro digestion trials should be investigated. It is also necessary for us to consider both emulsions and emulsion-based systems that load short-chain fatty acids. Wang and co-workers (2013) reported that not only preparing O/W emulsion, but also O/W "gel" emulsion. They gelated in O/W emulsion to reduce the stress of the animal when in *vivo* digestion test using experimental animals, however improvement of application as the food and control of digestibility can be hoped by emulsion gelated. For example, W/O/W gel emulsion loaded with short-chain fatty acid may be able to control digestibility and improve storage physical stability, and reduce smell of short-

chain fatty acid.

There are many items which we have to investigate such as release of inner component or digestibility. Through there investigation, the development of the product which can improve our health is expected. It is also expected that the above-stated investigations can contribute to improvement of the human lifestyle.

Reference

Abe, M. (1997). Gel technology. Science forum, Co., Ltd., Abiko, Japan.

Araki, C. (1956). Bull. Chem. Soc. Japan, 29, 543-544

Aserin, A. (2007). Multiple emulsion technology and applications. Hoboken, USA : John Wiley & Sons.

Banerjee. S., Bhattacharya. S., (2011). Compressive textural attributes, opacity and syneresis of gels prepared from gellan, agar and their mixtures. Journal of Food Engineering, 102, 287-292.

Bogart, B, I., Ort, Victoria (2007). Elsevier's Integrated Anatomy and Embryology. Maryland Heights, USA : Mosby

Bortnowska. G., (2015). Multilayer oil-in-water emulsions: formation, characteristics and application as the carriers for lipophilic bioactive food components. Journal of Food and Nutrition Sciences, 65, 157-166.

Chuah, A., Kuroiwa, T., Kobayashi, I., & Nakajima, M. (2009). Effect of chitosan on the stability and properties of modified lecithin stabilized oil-in-water monodisperse emulsion prepared by microchannel emulsification. Food Hydrocolloids. 23, 600-610.

Clausse, D., Gomez, F., Dalmazzone, C., & Noik, C. (2005). A method for the characterization of emulsions, thermogranulometry Application to water-in-crude oil emulsion. Journal of Colloid and Interface Science, 287, 694-703.

Cummings, J. H., Rombeau. J.L., & Sakata. T (1995). Physiological and clinical aspects of short-chain fatty acids. Cambridge, UK : Cambridge University Press.

Elena, M., & Dmitry, G. (2012). Layer-by-layer coated emulsion microparticles as storage and delivery tool. Current Opinion in Colloid and Interface Science, 17, 281-289.

Farahmand, S., Tajerzadeh, H., & Farboud, S. (2006). Formulation and evaluation of a vitamin C multiple emulsion. Pharmaceutical Development and Technology, 11, 255-261.

Greer, J.B., & O'Keefe, S. J., (2011). Microbial induction of immunity, inflammation, and cancer. Frontiers in Physiology, 1, Article 168.

G.T. Macfarlane, G.R. Gibson. (1995). In : "Physiological and clinical aspects of short-chain fatty acids" J.H. Cummings, J.L. Rombeau, T. Sakata eds., Cambridge University Press, Cambridge. 87.

Guerra, A., Etienne-Mesmin, L., Livrelli, V., Denis, S., Blanquet-Diot, S., and Alric, M., (2012). Relevance and challenges in modeling human gastric and small intestinal digestion. Trends in Biotechnology, 30, 591-600.

Hamer. H. M., Jonkers. D., Venema. K., Vanhoutvin. S., Troost. F. J., & Brummer. R. J. (2008). The role of butyrate on colonic function. Alimentary Pharmacology & Therapeutics, 27, 104-119.

Hara, H., (2002). Physiological Effects of Short-Chain Fatty Acid Produced from Prebiotics in the Colon. Journal of Intestinal Microbiology. 16, 35-42. (In Japanese)

Hayashi, K. & Okazaki, A. (1970). Kanten hand book, Kourinn Syoin, Tokyo, Japan. (In Japanese)

Herman. E. Ries, jr. (1961). Monomolecular Films, Scientific American 204, 152-165

Huang, M., Ma, Z., Khor, E., & Lim, L. (2002). Uptake of FITC-chitosan nanoparticles

by A549 cells. Pharmaceutical Research, 19, 1488-1494.

Kanafusa, S., Chu, B, S., & Nakajima, M. (2007). Factors affecting droplet size of sodium caseinate stabilized O/W emulsions containing β-carotene. European Journal of Lipid Science and Technology, 109, 1038-1041.

Kato, H. (2007). A survey on nano sized distribution particle standards. AIST Bullein of Metrology, 6, 185-200

Iwata. N., Neves, M., Watanabe, J., Sato, S., & Ichikawa, S. (2014). Stability control of large oil droplets by layer-by-layer deposition using polyelectrolyte dietary fibers. Colloid and Surfaces A: Physicochemical and Engineering Aspects, 440, 2-9.

Kato, H. (2007) A survey on nano sized distribution particle standards. AIST Bullein of Metrology, 6, 185-200.

Kawakatsu T, Kikuchi Y, Nakajima M (1997). Regular sized cell creation in microchannel emulsification by visual microprocessing method. Journal of the American Oil Chemists' Society 74: 317-321.

Khalid, N., Kobayashi, I., Neves, M., Uemura, K., & Nakajima, M. (2013). Preparation and characterization of water-in-oil emulsions loaded with high concentration of L-ascorbic acid. LWT-Food science and Technology, 51, 448-454.

Khalid, N., Kobayashi, I., Neves, M., Uemura, K., Nakajima, M., & Nabetani, H. (2014). Monodisperse WOW emulsions encapsulating L-ascorbic acid Insights on their formulation using microchannel emulsification and stability studies. Colloid and Surfaces A: Physicochemical and Engineering Aspects, 458, 69-77.

Koiwa, M., & Nakajima, H., Diffusion in materials. Tokyo, Japan ; Uchidarokakuho. (In

Japanese)

Kobayashi, I., Lou, X., Mukataka, S. & Nakajima, M. (2005). Preparation of Monodisperse Water-in-Oil-in-Water Emulsions Using Microfluidization and Straight-Through Microchannel Emulsification. Journal of the American Oil Chemists' Society, 82, 65-71.

Kobayashi I, Mukataka S, Nakajima M (2005). Novel asymmetric through-hole array microfabricated on a silicon plate for formulating monodisperse emulsions. Langmuir 21: 7629-7632.

Kobayashi I, Uemura K, Nakajima M (2007). Formulation of monodisperse emulsions using submicron-channel arrays. Colloid and Surfaces A: Physicochemical and Engineering Aspects, 296, 285-289.

Kobayashi I, Hori Y, Uemura K, Nakajima M. (2010). Production characteristics of large soybean oil droplets by microchannel emulsification using asymmetric through holes. Procedia Food Science 11, 37-48.

Kobayashi I, Neves, M., Wada Y, Uemura K, and Nakajima M. (2012). Large microchannel emulsification device for mass producing uniformly sized droplets on a liter per hour scale. Green Processing and Synthesis, 1, 353-362.

Lee, J., Kim, J., Han, S., Chang, I., Kang, H., Lee, O., Oh, S., & Suh, K. (2004). The stabilization of L-ascorbic acid in aqueous solution and water-in-oil-in-water double emulsion by controlling pH and electrolyte concentration. International Journal of Cosmetic Science, 55, 1-12.

Li, Y., Maux, L., Xiao, H., & McClements, D. J. (2009). Emulsion-based delivery systems

for tributyrin, a potential colon cancer preventative agent. Journal of Agricultural and Food chemistry, 57, 9243-9249.

Lucas, R., comelles, F., Alcántara, D., Maldonado, O. S., Curcuroze, M., Parra , J. L., & Morales, J. C. (2010). Surface-Active Properties of Lipophilic Antioxidants Tyrosol and Hydroxytyrosol Fatty Acid Esters: A Potential Explanation for the Nonlinear Hypothesis of the Antioxidant Activity in Oil-in-Water Emulsions. Journal of Agricultural and Food Chemistry, 58, 8021-8026.

Macfarlane, G.T., Gibson, G.R., In : "Physiological and clinical aspects of short-chain fatty acids" Cummings, J.H., Rombeau, J.L., Sakata, T. eds., (1995). Cambridge University Press, Cambridge, 87.

Mason, T, G., Krall A, H. Gang, H. Bibette J and Weits (1996). Monodisperse Emulsions Propaties and Used. In: Encyclopedia of Emulsion Technology (P. Becher ed.) vol. 4, Marcel Dekker, New York, 299-335.

McClements, D. J. (2004). Food Emulsions: Principles, Practice, and Techniques (2nd ed.). Florida, USA : CRC Press.

McClements, D. J. (2010). Annual review of Food Science and Technology, 1, 241-269.

McClements, D. J., & Li, Y. (2010). Structured emulsion-based delivery systems: Controlling the digestion and release of lipophilic food components. Advances in Colloid and Interface Science, 159, 213-228.

McClements, D. J., & Li, Y. (2010). *in vitro* digestion models for rapid screening of emulsion-based systems. Food & Function Linking the chemistry & physics of food with health & nutrition, 1, 32-59.

Ministry of Health of Japan, Comprehensive Survey of Living Conditions, 2010. (In Japanese)

Morishita, Y., (2000). Probiotics and prebiotics activate the intestinal bacteria for one's health, Journal of Japanese Association for Dietary Fiber Research, 4, 2. (In Japanese)

Nakaya, K., Kohata, T., Doisaki, N., Ushio, H., Ohshima, T., (2006). Effect of oil droplets sizes oil-in-water emulsion on the taste impressions of added tastants. The Journal of Physical Chemistry, 72, 877-883.

Nisinari, K. (2007). *Food Hydrocolloids: Development and Applications*. Tokyo, Japan ; CMC Publishing Co.,Ltd.

Okazawa, T., & Bron, J. (1979). On thermodynamically stable emulsion. Journal of Colloid and Interface Science, 69, 86-96.

Paria, S., Manohar, C., & Khilar, K, C. (2005). Adsorption of anionic and non-ionic surfactants on a cellulosic surface, Colloid and Surface A: Physicochemical and Engineering Aspects, 252, 221-229.

Frith,W. J., Garijo, X., Foster, T. J., and Norton, I. T. (2002). Microstructural origins of the rheology of fluid gels. London, UK., Royal Society of Chemistry.

Pituch, A, JWalkowiak, J., Banaszkiewicz, A. (2013). Butyric acid in functional constipation. Przegląd Gastroenterologiczny, 8, 295–298.

Richardson, J. J., Bjornmalm, M., & Crauso, F. (2015). Technology-driven layer-by-layer assembly of nanofilms. Science. 348, aaa2491-1-aaa2491-11

Saito. M., Yin. L., kobayashi. I., Nakajima. M. (2006). Comparison of stability of bovine

serum albumin-stabilized emulsions prepared by microchannel emulsification and homogenization, Food hydrocolloids, 20, 1020-1028.

Sakata, T., Ichikawa, H., (1997). Physiological Actions of Short-Chain Fatty Acids、Journal of Oleo Science, 46, 10. (In Japanese)

Sato, A., Saeki, Y., Uchida, S., (2009). Human Body Structure and Function 2nd, Ishiyaku Publishers,Inc., Tokyo, Japan. (In Japanese)

Shahidi, F. (2005). Bailey's Industrial Oil and Fat Products, Sixth Edition Wiley & Sons, Inc.

Shima, K., (1998). Research and development for Novel Emulsifiers and New Emusifier Tecchnology. Tokyo, Japan ; CMC Publishing Co.,Ltd.

Souilem, S., Kobayashi, I., Neves, M., Jlailel, L., Isoda, H., Sayadi, S., Nakajima, M. (2014). Interfacial characteristics and microchannel emulsification of oleuropein-contaning triglyceride oil-in-water systems. Food Research International, 62, 467-475.

Trentin, A., DeLamo, S., Guell, C., Lopes, F., & Ferrando, M. (2011). Protein-stabilized emulsions containing beta-carotene produced by premix membrane emulsification. Journal of Food Engineering, 106, 267-274.

Tsung, M., & Harold, G. (2002) “"Palm+stearin"+oleic Lipid biotechnology” New York: CRC Press.

Vladisavljević, G. T., Kobayashi, I., & Nakajima, M (2012) Production of uniform droplets using membrane, microchannel and microfluidic emulsification devices. Microfluidics and Nanofluidics 13, 151-178.

Wang, Z., Neves, M, A., Kobayashi, I., Uemura, K., Nakajima,M., (2013). Preparation, Characterization, and *in Vitro* Gastrointestinal Digestibility of Oil-in-Water Emulsion-Agar Gels. Bioscience, Biotechnology, and Biochemistry. Vol. 77, 3, 467-474.

Yamada, N. (2001). Science of the seaweed application, Seizandou syoten, Co., Ltd., Tokyo, Japan. (In Japanese)

ZetasizerNano ZS User manual, Malvern Instruments Ltd.

URL cites

Link 1. FLORA Co., Ltd. HP

http://flora.link/

Link 2. BeckMan Coulter Co., Ltd. HP.

https://ls.beckmancoulter.co.jp/column/particle/

Link 3. Malvern Instruments Ltd. HP.

http://www.malvern.com/jp/products/measurement-type/particle-size/

Link 4. Otsuka Electronic Co., Ltd. HP.

https://www.otsukael.jp/weblearn/list/category1id/34

Acknowledgments

First of all, I would like to express my profound appreciation and gratitude to Ph.D. supervisor, Professor Mitsutoshi Nakajima (University of Tsukuba) for his excellent guidance and support. I am grateful to him not only for the opportunity given to me study at University of Tsukuba, but also for given me so many opportunities to attend conferences and meetings which broaden my views. My appreciation is to Prof. Sosaku Ichikawa, Prof. Junichi Sugiyama, Prof. Marcos A. Neves and Prof. Isao Kobayashi; dissertation committee members for their helpful advice in the preparation of my Ph.D. thesis.

I am indebted to Prof. Isao Kobayashi for his valuable guidance throughout my work, for his constant and fireless support, his patience in helping me to develop my research and helpful advices and comment in my Ph.D. thesis. His clear explanations and enthusiasm sciences in me.

I feel grateful to Prof. Kunihiko Uemura for all his kindness. Thanks for his advice in my study and laboratory life.

My appreciation is to Prof. Sosaku Ichikawa and Prof. Marcos Antonio das Neves for their kindness and helpful advices in my Ph.D. thesis and thesis presentations.

I feel grateful to Prof. Korekazu Ueyama (Kogakuin University) for all his kindness. Thanks for sending me out to Tsukuba and having given me an opportunity to engage in a study.

My heartfelt gratitude is to the past and present members of the Advanced food Technology lab for their support and help: Dr. Sumiyo Kanafusa, Dr. Yanru Zhang, Dr.

Hiroyuki Kozu, Dr. Nauman Khalid, Dr. Zheng Wang, Ms. Akane Yasunaga, Ms. Ayano Makisita, Ms. Kaoru Abe, Mr. Sota Matsumoto, Mr. Gaofeng Shu, Ms. Ran Li, Mr. Zhao Yiguo, Mr. Wang Yuxin, Mr. Yifeng Jiang, Ms. Lara, Grace, Mr. Muhammad, Arif, and all of laboratory members. My gratitude in depth is to Ms. Chieko Takahashi, Ms. Atsuko Isono, Ms. Yuko Hori, Ms. Yuko Yamamura, Ms Mitsuko Kawamoto, and Ms Etsuko Hamano for their kind support and for constantly ensuring my well-being in the lab.

Finally, I would like to dedicate this dissertation to my family for their unconditional support, love, encouragement, trust and dedication to me.

January, 2017

Yohei YAMANAKA